Fluctuation-induced Phenomena in Non-equilibrium Systems

by

Mohammad F. Maghrebi

Submitted to the Department of Physics
in partial fulfillment of the requirements for the degree of

Doctor of Philosophy in Physics

at the

MASSACHUSETTS INSTITUTE OF TECHNOLOGY

June 2013

Author .....
Department of Physics
May 24, 2013

Certified by .....
Robert L. Jaffe
Professor
Thesis Supervisor

Accepted by .....
John Belcher
Associate Department Head for Education

Fluctuation-induced Phenomena in Non-equilibrium Systems

by

Mohammad F. Maghrebi

Submitted to the Department of Physics
on May 24, 2013, in partial fulfillment of the
requirements for the degree of
Doctor of Philosophy in Physics

Abstract

In this thesis, we investigate the implications of fluctuations in systems away, possibly even far, from equilibrium due to their motion either in or out of thermal equilibrium. This subject encompasses several topics in physics including the dynamical Casimir effect in the presence of moving boundaries, and non-contact friction between objects in relative motion. In both cases, photons are created due to the coupling of the motion and zero-point fluctuations in the vacuum, resulting in dissipation and radiative loss. We introduce a general formalism, equally applicable to lossy and ideal objects, to compute the quantum radiation and dissipation effects solely in terms of the classical scattering matrices. We obtain trace formulas which are general and independent of any approximation scheme where numerous examples, many novel, are discussed in great detail. Specifically, we give an exact treatment of quantum fluctuations in the context of a neutral rotating object, and show that it spontaneously emits photons and drags objects nearby, and compute the associated photon statistics and entropy generation. In the context of non-contact friction, we find a quantum analog of the classical Cherenkov effect for two neutral plates in relative motion, purely due to quantum fluctuations. We present a number of arguments and exact proofs, including a method introduced in the context of quantum field theory in curved space, as well as the scattering approach, to show that a friction force between two plates appears at a threshold velocity set by the speed of light in their medium.

Thesis Supervisor: Mehran Kardar
Title: Professor

Thesis Supervisor: Robert L. Jaffe
Title: Professor

Acknowledgments

Before starting my PhD at MIT in 2008, I had briefly worked on string theory. I decided that I wanted to work in a different, more concrete field for my PhD studies, but I was not sure about the research area that I was most interested in. Now after a few years, my search is still incomplete but I know that my passion lies in physics—not just as a collection of narrowly technical problems but as a connected whole. My *random walk* in research has spanned topics from polymers to quantum field theory, non-equilibrium physics to stochastic phenomena, and quantum fluctuations to black holes. As much as I wanted to, I could not rid myself of the desire to live in a world of *ideas* of which physics is so remarkably rich. I am still in awe of how seemingly abstract ideas can be relevant to the real world.

Five years ago, I had little idea what it takes to earn a doctoral degree, and was far from being a professional researcher. Now, above everything else, I have learned how to conduct research, collaborate, and present my work to an interested audience. I am greatly indebted to my advisers, Prof. Mehran Kardar and Prof. Robert L. Jaffe who have been infinitely caring, responsible, encouraging and open to my ideas. Their exceptionally intuitive approach with an emphasis on clarity has and will mark my career as a physicist. I have looked up to and learned a lot from their teaching and presentation skills.

I have benefitted from discussions and collaborations with various professors, post-docs, and colleagues at MIT and elsewhere. It has been my pleasure to work with Professors Yacov Kantor, Ramin Golestanian, Thorsten Emig, and Noah Graham. I have enjoyed numerous discussions with my colleagues at MIT: Dr. Jamal S. Rahi, Dr. Matthias Krüger, Vladyslav Golyk, John Frank, Dr. Mark Hertzberg, Dr. Homer Reid, and Dr. Hsiang-Ku Lin. More often than not, our lunch breaks ended in heated discussions about physics. I should thank Dr. Mark Mueller who was my sponsor in my first year at MIT, and a friend ever since. He has always been a great company for intellectual conversations about physics and beyond. Finally I would like to thank my committee members, Prof. Edward Farhi and Prof. Raymond Ashoori, who have

been most flexible and helpful.

Five years is a long time, and impossible to survive if not for those who give you a sense of friendship and trust. I would like to thank Arghavan Safavi-Naini, Nima Dehmamy, Tout Wang, Zachary Thomas, Apratim Sahay, Si-Hui Tan, Ali Rajabi, Neda Rohani, Nikolay Perunov, Rotem Gura, Mindaugas Lekaveckas, Ali Hosseini, Soheil Feizi, Arash Adel, Salma Mozaffari, Pegah Hosseinipour, Davoud Ebrahimi, Mahshid Pourmand, Sahar Hakimi, Mohammad-Javad Abdolhosseini, Shaya Famini, Amirreza Aref, Sima Salamat, Abolhassan Vaezi, Hoda Bidkhori, Sarah Paydawosi and many others. Most specially I would like to thank Hoda Hosseini whose support and extreme kindness has been most valuable to me.

I wouldn't be who I am if it were not for my parents. They have been extremely patient, kind, caring, and loving. This thesis is dedicated to my father, Hamid Faghfoor Maghrebi, and my mother, Heshmat Ashnai, as well as my siblings Saeed, Fatemeh, and my younger brother Sajad who has just started to fall in love with physics.

Contents

List of Figures

List of Tables

Chapter 1

Introduction

Quantum fluctuations manifest themselves in a variety of macroscopic effects. A prominent example is Casimir's demonstration that zero-point fluctuations lead to attraction of two perfectly conducting parallel plates [1]. Lifshitz extended this result to include nonzero but uniform temperature, as well as intrinsic properties of realistic materials such as permittivity [2]. Experimental advances in precision measurements of the Casimir force [3, 4] have revived interest in finding frameworks where one can compute these forces both numerically [5, 6] and analytically [7]. A particularly successful approach in applications to different geometries and material properties is based on scattering methods and techniques [8, 9, 10, 11, 12, 13, 14, 15, 16, 17]. In this approach, the quantum-field-theoretic problem is reduced to that of finding the *classical* scattering matrix of each object.

Dissipation and radiative loss are absent in equilibrium, where the objects are at rest and the system (including the environment) is at a uniform temperature, as a consequence of energy conservation and the second law of thermodynamics. Specifically, fluctuation-induced, or Casimir, forces can be written as a derivative of a potential, and are thus conservative. However, out of thermal or dynamical equilibrium, fluctuations alone can lead to radiation and dissipation. In fact, black-body radiation from an object at finite temperature was the starting point of quantum mechanics. We are mainly interested in systems out of dynamical equilibrium: When objects are set in motion, they interact with quantum fluctuations in the background environment

in a time-dependent fashion which pulls out real photons from the vacuum and leads to *quantum radiation.* In fact, neutral boundaries undergoing acceleration or oscillation radiate energy and thus experience a back reaction force, or *quantum friction* [18, 19, 20, 21, 22, 23, 24, 25, 26, 27].

Experiments on dynamical Casimir effect have been out of reach until recently, partly because significant effects can only be observed at high velocities comparable to the speed of light, while achievable mechanical velocities of boundaries are typically much slower. An alternative approach was suggested by modulating optical properties of a resonant cavity [28, 29, 30]. Creation of photons due to the dynamical Casimir effect was first detected in a coplanar waveguide which was terminated by a superconducting quantum electromagnetic device (SQUID) to mimic the moving boundary of a cavity [31, 32]. A rapidly oscillating magnetic field can be applied to change the effective inductance of the SQUID and thus the boundary conditions at the end of the transmission line. The rate of change of the boundary conditions, and thus the effective electrical length, can be made as fast as a substantial fraction of the speed of light making it possible to observe photons generated in a band of GHz frequencies.

Inspection of the literature on the dynamical Casimir effect leads to the following observations: There are a plethora of interesting—sometimes counter-intuitive—phenomena emerging from the motion of a body in an ambient quantum field [33, 34]. These phenomena span a number of subfields in physics (dynamical Casimir effect, general relativity, superfluid and Bose-Einstein condensates among others), and have been treated by a variety of different formalisms. Even the simplest examples appear to require rather complex computations and various approximations. Recent experimental realizations have made precise measurements possible, raising the hope for an explosion of activity similar to the post-precision experiment era of static Casimir forces. This motivates reexamination of theoretical literature on the subject, aiming for simple and, and possibly unifying, frameworks for analysis.

Here, we consider a system that is not in equilibrium due to its motion; it may even be out of thermal equilibrium with the environment, and study quantum and

thermal fluctuations in two complementary directions: We employ a number of *different approaches*, each with its own merits, and apply them to a *single system*, but also develop *a general approach* and discuss it in application to *different systems* in a diverse set of examples. Here is a short list of problems that we tackle in the following:

• We present an exact treatment of quantum fluctuations and associated radiation in the context of a lossy rotating object by utilizing the *Rytov formalism*. This treatment is unique to lossy objects under stationary motion where time translation symmetry is respected.

• By combining scattering theory and *input-output formalism*, we develop a unified scattering approach to dynamical Casimir problems which can be applied to lossy/non-lossy objects under stationary/non-stationary motion. Rotating objects are revisited and the results are reproduced with significantly less labor.

• We discover a quantum analog of Cherenkov effect in the context of two neutral plates in relative motion. We give heuristic arguments and exact proofs with the general approach described above being the shortest, and perhaps the most elegant, one.

In the following, we elaborate on these points in some detail. Our approach builds on a range of previous related work, an inevitably incomplete subset of which is briefly reviewed here. The creation of photons in the context of a one dimensional cavity bounded by moving mirrors was first discussed by Moore [18]. Relativistic results for a single accelerating mirror—modeled by a point subject to Dirichlet boundary conditions— in 1+1 dimension were derived in a seminal paper by Fulling and Davies based on conformal field theory [19]. They showed that the quantum friction force is proportional to the third time derivative of the displacement at small velocities, and has the same form as the relativistic radiative force in classical electrodynamics. Using specific regularization schemes, a perturbative treatment of accelerating (perfectly reflecting) mirrors in 3+1 dimensions showed that the friction force is related to higher time derivatives of the displacement [35].

The relation between quantum dissipation and fluctuations was investigated much later within the linear response theory, or the so-called *fluctuation-dissipation theo-*

rem, by relating force fluctuations for a static object to the frictional force on the moving body [36, 37, 38]. These attempts were partially motivated by finding quantum limits on position measurements in application to gravitational wave detection [39]. This approach has been used to study the dissipative force on a moving sphere in free space [22] and a surface subject to time-dependent perturbation [40].

Among other methods, an effective Hamiltonian has been introduced to compute photon production in cavities [23, 24], and a path-integral formulation was developed to study the dynamic Casimir effect for small deformations in space and time of perfectly reflecting boundaries [41]. We specially note that an input-output formalism relating the incoming and outgoing operators was used to compute, among other things, the frequency and angular spectrum of radiated photons [42].

While a substantial literature is devoted to dynamical Casimir effect in the context of ideal objects with perfect boundary conditions [43, 44, 45, 46, 47, 48], dielectric and dispersive materials have also been studied in some cases [49]. In general, the latter is more complicated since a quantum system is usually defined with a Hamiltonian which is lacking for a lossy system. A path integral formulation is also not trivial as we are dealing with a system out of equilibrium, which requires a rather complicated formalism developed by Schwinger and Keldysh [50, 51]. Interestingly, dispersive objects experience a quantum friction even when they move at a constant velocity: Two parallel plates moving laterally with respect to each other experience a (non-contact) frictional force [52, 53, 54]. Non-contact friction is usually treated within the framework of the Rytov formalism which is grounded in the fluctuation-dissipation theorem for electrodynamics [55]. While a constant translational motion requires at least two bodies (otherwise, trivial due to Lorentz symmetry), a single spinning object can experience friction. In a recent work, rotational friction was studied by formulating the polarization fluctuations of a small spinning particle via the fluctuation-dissipation theorem, and a frictional force was obtained even at zero temperature [56, 57]. This effect is closely related to a classical phenomenon known as superradiance due to Zel'dovich [58]. He argues that a rotating object amplifies certain incident waves, and further conjectures that, when quantum mechanics is

considered, the object should spontaneously emit radiation only for these so-called *superradiating* modes. In a later publication, he and coauthors computed the radiation for a cylinder with a small conductivity by employing an approximate scheme akin to the Born approximation [59]. In the context of general relativity, Penrose process provides a mechanism similar to superradiance to extract energy from a rotating black hole [60], which also leads to quantum spontaneous emission [61]. This radiation, however, is different in nature from Hawking radiation which is due to the existence of event horizons [62]. One can also find similar effects for a superfluid where a rotating object experiences friction even at zero temperature [63]. There are also some proposals for Casimir-like forces in a slowly moving Bose-Einstein condensate [64].

In the first part of this thesis, Chapter 2, we treat vacuum fluctuations in the presence of a lossy object under rotation exactly, except for the assumption of small enough velocities to avoid complications of relativity, and thus go beyond the approximate treatments in Refs. [59, 56]. The object is assumed to be a solid of revolution with its shape and orientation fixed in time, hence stationary motion. The classical scattering amplitude then relates incoming and outgoing waves with the same frequency. By incorporating the Green's function techniques into the Rytov formalism [55], we find a general trace formula for the spontaneous emission by an arbitrary (though rotationally symmetric) spinning object. We reproduce the results in the literature, and find an expression for the radiation by a rotating cylinder. The connection to super-radiance is made explicit and the interplay between loss and spontaneous emission is discussed in great detail. Furthermore, we study the interaction of a rotating body with a *test* object nearby and show that the rotating body drags along nearby objects while making them rotate parallel to its own rotation axis [65].

Then, in Chapter 3, inspired by the success of the scattering-theory methods in (static) Casimir forces [8, 9, 10, 11, 12, 13, 14, 15, 16, 17], we attempt at extending these techniques to a diverse set of dynamical Casimir problems including lossy/non-lossy objects under sationary/non-stationary motion (dispersive objects in relative motion as well as accelerating boundaries). Introducing a second-quantized approach

known as the input-output formalism, we find that the *classical* scattering matrix is naturally incorporated into the formalism. However, dynamical configurations provide new channels where the incoming frequency jumps to different values, hence the scattering matrix should be defined accordingly. A general (trace) formula is derived for the radiation from accelerating boundaries. Applications are provided for objects with different shapes in various dimensions, and undergoing rotational or linear motion. Within this framework, photon generation is discussed in the context of a modulated optical mirror. For dispersive objects, we find general results solely in terms of the scattering matrix. Specifically, we discuss the vacuum friction on a rotating object, and the friction on an atom moving parallel to a surface.

In Chapter 4, we discuss non-contact friction between two surfaces (or semi-infinite plates) moving in parallel [52, 53, 54]. In general, quantum fluctuations induce currents in each object, which then couple to result in the interaction between them. For moving objects, a phase lag between currents leads to a frictional force between them. We present a number of arguments to demonstrate that a quantum analog of Cherenkov effect occurs in this context due to the inherent quantum fluctuations even for neutral objects. Specifically we show that two semi-infinite plates experience friction beyond a threshold velocity which, in their center-of-mass frame, is the phase speed of light within their medium. The loss in mechanical energy is radiated away through the plates before getting fully absorbed in the form of heat. By deriving various correlation functions inside and outside the two plates, we explicitly compute the radiation, and discuss its dependence on the reference frame.

In some sections, computations are performed for a scalar field theory. The generalization to electromagnetism is straightforward in principle, while practical computations are more complicated in the latter.

Finally, in Chapter 5, we discuss some future directions and open problems.

Chapter 2

Spontaneous Emission by Rotating Objects

In this Chapter, we treat the vacuum fluctuations in the presence of a lossy rotating object. By incorporating Green's function techniques into the Rytov formalism [55], we find a general trace formula for the spontaneous emission by an arbitrary spinning object, solely in terms of its scattering matrix. We also compute the statistics of radiated photons and the entropy generation due to radiation. Finally, we study the interaction of a rotating body with a *test* object nearby and show that the rotating body drags along nearby objects while making them rotate parallel to its own rotation axis.

Our starting point is the Rytov formalism [55] which relates fluctuations of the electromagnetic (EM) field to fluctuating *sources* within the material bodies, and in turn to the material's dispersive properties, via the fluctuation-dissipation theorem. For the sake of simplicity and clarity, we start with a toy model based on a scalar field in Sec. 2.1, and postpone the full discussion of electrodynamics to Sec. 2.2.

2.1 A toy model: A *dielectric* object interacting with a scalar field

We consider a scalar field theory which interacts with an object characterized by a response, or *dielectric*, function ϵ. The reponse function is, in principle, a function of both frequency and position, and fully characterizes the object's dispersive properties. The field equation for this model in frequency domain reads

$$\left(\nabla^2 + \frac{\omega^2}{c^2}\epsilon(\omega, \mathbf{x})\right) \Phi(\omega, \mathbf{x}) = 0, \tag{2.1}$$

with ϵ being 1 in the vacuum, and a frequency-dependent function inside the object.

In order to describe quantum (and thermal) fluctuations, one can consider the field as a stochastic entity whose fluctuations are governed by a random *source*. From this perspective, quantum fluctuations are cast into a Langevin-like equation (similar to the random force in the theory Brownian motion). For the electromagnetic field, the Rytov formalsim provides such a stochastic formulation [55]. We introduce a similar approach for the scalar field theory, the central subject of this section. The field equation coupled to a (random) source ρ is given by

$$-\left(\triangle + \frac{\omega^2}{c^2}\,\epsilon(\omega, \mathbf{x})\right) \Phi(\omega, \mathbf{x}) = -\frac{i\omega}{c}\,\rho_\omega(\mathbf{x})\,, \tag{2.2}$$

where the source satisfies a δ-function correlation function in space

$$\langle \rho_\omega(\mathbf{x}) \rho^*_\omega(\mathbf{y}) \rangle = a(\omega)\, \mathrm{Im}\, \epsilon(\omega, \mathbf{x})\, \delta(\mathbf{x} - \mathbf{y}), \tag{2.3}$$

with

$$a(\omega) = 2\hbar \left(n(\omega, T) + \frac{1}{2}\right) = \hbar \coth\left(\frac{\hbar\omega}{2k_B T}\right). \tag{2.4}$$

Note that source fluctuations are related to the imaginary part of the response function in harmony with the fluctuation-dissipation theorem (FDT). At a finite temperature T, the Bose-Einstein distribution function $n(\omega, T) = [\exp(\hbar\omega/k_B T) - 1]^{-1}$

captures thermal fluctuations; the additional 1/2 is due to zero-point quantum fluctuations.

The field is related to the source via the Green's function, G, defined as

$$-\left(\triangle+\frac{\omega^2}{c^2}\epsilon(\omega,\mathbf{x})\right)G(\omega,\mathbf{x},\mathbf{z})=\delta(\mathbf{x}-\mathbf{z}). \tag{2.5}$$

In equilibrium (uniform temperature with static objects), the field correlation function is obtained as

$$\begin{aligned}\langle\Phi(\omega,\mathbf{x})\Phi^*(\omega,\mathbf{y})\rangle &= \frac{\omega^2}{c^2}\int\int_{\text{All space}} d\mathbf{z}\,d\mathbf{w}\,G(\omega,\mathbf{x},\mathbf{z})G^*(\omega,\mathbf{y},\mathbf{w})\,\langle\rho_\omega(\mathbf{z})\rho_\omega^*(\mathbf{w})\rangle \\ &= \frac{\omega^2}{c^2}a(\omega)\int_{\text{All space}} d\mathbf{z}\,G(\omega,\mathbf{x},\mathbf{z})\,\mathrm{Im}\,\epsilon(\omega,\mathbf{z})\,G^*(\omega,\mathbf{y},\mathbf{z}) \\ &= a(\omega)\,\mathrm{Im}\,G(\omega,\mathbf{x},\mathbf{y}).\end{aligned} \tag{2.6}$$

Note that the second line in Eq. (2.6) follows from $\frac{\omega^2}{c^2}\,\mathrm{Im}\,\epsilon = -\,\mathrm{Im}\,G^{-1}$ according to Eq. (2.5). This equation manifests the FDT by relating *field* fluctuations to the imaginary part of the Green's function. However, Eq. (2.6) requires the system to be in equilibrium while Eq. (2.3) is formulated locally and makes no assumption about global properties of the system, namely if it in or out of equilibrium. Therefore, we shall employ Eq. (2.3) to study nonequilibrium systems.

In the following sections we explore the interplay between geometry, motion, and temperature. While our main interest is the consequences of fluctuations in the context of moving objects, we make a detour to study quantum and thermal fluctuations for a static object. Out of thermal equilibrium, the object is at a temperature different from that of the environment. The techniques we develop in the following section are useful when we consider moving objects in or out of thermal equilibrium.

For simplicity, we consider a disk in two-dimensional space, a simple example of a rotationally symmetric object which is the main point of this study specifically in application to rotating objects. The generalization to realistic objects is discussed in the context of electromagnetism.

In the following, we make the convention that $c = 1$ unless stated otherwise.

2.1.1 Field fluctuations for static objects

According to the Rytov formalism, field fluctuations are induced by random sources. The latter fluctuate according to the object's local properties (encoded by the imaginary part of the response function) as well as the local temperature through the Bose-Einstein factor. It is then natural to divide the space into the object and the environment (vacuum), and compute the source fluctuations in each region separately.

Vacuum fluctuations

In this subsection we consider field fluctuations due to random sources only in the vacuum. The scalar field is coupled to fluctuating sources outside the object as

$$-(\triangle + \omega^2 \epsilon(\omega, \mathbf{x}))\Phi(\omega, \mathbf{x}) = \begin{cases} 0, & |\mathbf{x}| < R, \\ -i\omega\rho_\omega(\mathbf{x}), & |\mathbf{x}| > R, \end{cases} \tag{2.7}$$

with R being the radius of the disk. Source fluctuations, according to the Rytov formalism, are determined by

$$\langle \rho_\omega(\mathbf{x}) \rho_\omega^*(\mathbf{y}) \rangle = a_{\text{out}}(\omega)\, \text{Im}\, \epsilon_D(\omega)\, \delta(\mathbf{x} - \mathbf{y}), \tag{2.8}$$

where the points $\mathbf{x}$ and $\mathbf{y}$ are outside the object, a_{out} corresponds to the temperature of the environment, and ϵ_D represents the response functions in the vacuum. It might seem that this function is 1 and $\text{Im}\, \epsilon_D = 0$, hence there are no source fluctuations outside the object. However, even in empty space, these sources should give rise to zero-point fluctuations. Indeed as one has to integrate over infinite volume, the limit of $\text{Im}\, \epsilon_D \to 0$ should be taken with care. The corresponding field correlation function outside the object is given by

$$\langle \Phi(\omega, \mathbf{x}) \Phi^*(\omega, \mathbf{y}) \rangle_{\text{out-fluc}} = \omega^2 a_{\text{out}}(\omega)\, \text{Im}\, \epsilon_D(\omega) \int_{|\mathbf{z}|>R} d\mathbf{z}\, G(\omega, \mathbf{x}, \mathbf{z})\, G^*(\omega, \mathbf{y}, \mathbf{z}). \tag{2.9}$$

Note that the Green's functions are evaluated outside the object. Let (r, ϕ) and (ξ, ψ) be the polar coordinates of $\mathbf{x}$ and $\mathbf{y}$, respectively. The Green's function can be cast as a sum over partial waves in the cylindrical basis as

$$G(\omega, \mathbf{x}, \mathbf{y}) = \sum_{m=-\infty}^{\infty} \frac{i}{8} \left(H_m^{(2)}(\omega r) + S_m(\omega) H_m^{(1)}(\omega r) \right) e^{im\phi} \, H_m^{(1)}(\omega \xi) e^{-im\psi}, \qquad R < r < \xi \,, \tag{2.10}$$

where $H_m^{(1,2)}$ are the Hankel functions of the first and second kind, and $S_m(\omega)$ is the scattering matrix. Furthermore, we have assumed that the point $\mathbf{y}$ is located at a larger radius from the origin without loss of generality. In empty space, $S = 1$, and we recover the free Green's function as

$$G(\omega, \mathbf{x}, \mathbf{y}) = \sum_{m=-\infty}^{\infty} \frac{i}{4} J_m(\omega r) e^{im\phi} \, H_m^{(1)}(\omega \xi) e^{-im\psi}, \qquad r < \xi \,.$$

To compute the integral in Eq. (2.9), one should integrate over $R < |\mathbf{z}| < \infty$; however, we take the limit that $\mathrm{Im}\, \epsilon_D \to 0$, and only a singular contribution, due to the integral over $|\mathbf{z}| \to \infty$, survives. We can then safely choose the domain of integration as $|\mathbf{z}| > r, \xi$. We stress that in the intermediate steps, the argument of the Hankel function should be modified to $\sqrt{\epsilon_D}\, \omega r$ with the limit $\epsilon_D \to 1$ taken in the end. A little algebra yields

$$\langle \Phi(\omega, \mathbf{x}) \Phi^*(\omega, \mathbf{y}) \rangle_{\text{out-fluc}} = \frac{1}{16} a_{\text{out}}(\omega) \sum_{m=-\infty}^{\infty} \left(H_m^{(2)}(\omega r) + S_m(\omega) H_m^{(1)}(\omega r) \right) e^{im\phi} \times \overline{\left(H_m^{(2)}(\omega \xi) + S_m(\omega) H_m^{(1)}(\omega \xi) \right) e^{im\psi}}. \tag{2.11}$$

(The bar indicates complex conjugation.) The correlation function is then a bilinear sum over incoming plus scattered waves. In fact, in the absence of the object, this equation reduces to a bilinear sum over Bessel functions

$$\langle \Phi(\omega, \mathbf{x}) \Phi^*(\omega, \mathbf{y}) \rangle_{\text{empty space}} = \frac{\hbar}{2} \left(n(\omega, T) + \frac{1}{2} \right) \sum_{m=-\infty}^{\infty} J_m(\omega r) J_m(\omega \xi) e^{im(\phi - \psi)}$$

$$= \frac{\hbar}{2}\left(n(\omega,T)+\frac{1}{2}\right) J_0(\omega|\mathbf{x}-\mathbf{y}|)$$
$$= \frac{\hbar}{2}\left(n(\omega,T)+\frac{1}{2}\right) \int_0^{2\pi} \frac{d\alpha}{2\pi}\, e^{i\mathbf{k}\cdot(\mathbf{x}-\mathbf{y})}, \tag{2.12}$$

where $\mathbf{k}$ is the wavevector with $|\mathbf{k}| = \omega$ and $\angle\mathbf{k} = \alpha$. Being a complete basis, the Bessel functions can be recast into another basis such as planar waves in Eq. (2.12). In other words, quantum fluctuations in (empty) space can be written as a uniformly-weighted sum over a complete set of functions. In the presence of the object, vacuum fluctuations are organized into a sum over incoming plus scattered waves as in Eq. (2.11).

Inside fluctuations

Next we turn to study the source fluctuations inside the object:

$$-(\triangle + \omega^2\epsilon(\omega,\mathbf{x}))\Phi(\omega,\mathbf{x}) = \begin{cases} -i\omega\rho_\omega(\mathbf{x}), & |\mathbf{x}| < R, \\ 0, & |\mathbf{x}| > R, \end{cases} \tag{2.13}$$

$$\text{with} \qquad \langle\rho_\omega(\mathbf{x})\rho^*_\omega(\mathbf{y})\rangle = a_{\text{in}}(\omega)\,\text{Im}\,\epsilon(\omega,\mathbf{x})\,\delta(\mathbf{x}-\mathbf{y}), \tag{2.14}$$

where the sources' arguments are inside the object, and $a_{\text{in}}(\omega)$ is defined with respect to the object's temperature. Similar to the previous section, the field correlation function *outside* the object can be computed via Green's functions,

$$\langle\Phi(\omega,\mathbf{x})\Phi^*(\omega,\mathbf{y})\rangle_{\text{in-fluc}} = \omega^2 a_{\text{in}}(\omega)\int_{|\mathbf{z}|<R} d\mathbf{z}\, G(\omega,\mathbf{x},\mathbf{z})\,\text{Im}\,\epsilon(\omega,\mathbf{z})\,G^*(\omega,\mathbf{y},\mathbf{z}), \tag{2.15}$$

where ϵ is a possibly position-dependent response function. However, the Green's function in the last equation involves a point inside and another outside the object, which can be constructed as follows. Note that the two points (inside and outside the object) cannot coincide, and thus the Green's function satisfies a *homogeneous* equation, Eq. (2.1), inside and a free (Helmholtz) equation outside. Hence, we can

expand the Green's function as

$$G(\omega,\mathbf{x},\mathbf{x}') = \sum_{m=-\infty}^{\infty} \frac{i}{8} f_{\omega,m}(r) e^{im\phi} \left(A\, H_m^{(1)}(\omega\xi) + B\, H_m^{(2)}(\omega\xi)\right) e^{-im\psi}, \qquad r < R < \xi, \tag{2.16}$$

where the prefactor is chosen for future convenience, and[1]

$$-\left(\triangle + \omega^2 \epsilon(\omega, r)\right) f_{\omega,m}(r) e^{im\phi} = 0, \tag{2.17}$$

$$-\left(\triangle + \omega^2\right) H_m^{(1,2)}(\omega r) e^{im\phi} = 0. \tag{2.18}$$

The coefficients A and B and the normalization of the function f are determined by matching the Green's functions approaching a point on the boundary from inside and outside the object

$$G(\omega,\mathbf{x},\mathbf{y})|_{|\mathbf{x}|\to R^-} = G(\omega,\mathbf{x},\mathbf{y})|_{|\mathbf{x}|\to R^+}. \tag{2.19}$$

Comparing Eqs. (2.10) and (2.16), we find $(A = 1, B = 0)$

$$G(\omega,\mathbf{x},\mathbf{y}) = \sum_{m=-\infty}^{\infty} \frac{i}{8} f_{\omega,m}(r) e^{im\phi} H_m^{(1)}(\omega\xi) e^{-im\psi}, \qquad r < R < \xi, \tag{2.20}$$

where the function f is normalized by

$$\begin{aligned} &f_{\omega,m}(R) = H_m^{(2)}(\omega R) + S_m(\omega) H_m^{(1)}(\omega R), \\ &\left[\frac{\partial}{\partial r} f_{\omega,m}(r) = \frac{\partial}{\partial r}\left(H_m^{(2)}(\omega r) + S_m(\omega) H_m^{(1)}(\omega r)\right)\right]_{r=R}. \end{aligned} \tag{2.21}$$

In short, the function f solves Eq. (2.17) subject to the continuity boundary conditions in the last equations. We then expand the Green's function in Eq. (2.15) in terms of partial waves from Eq. (2.20). Keeping in mind that $|\mathbf{z}| < r, \xi$, we find

$$\langle \Phi(\omega,\mathbf{x}) \Phi^*(\omega,\mathbf{y}) \rangle_{\text{in-fluc}} = \frac{1}{64} \omega^2 a_{\text{in}}(\omega) \sum_{m=-\infty}^{\infty} H_m^{(1)}(\omega r) e^{-im\phi} \overline{H_m^{(1)}(\omega\xi) e^{-im\psi}} \times$$

[1]For simplicity, we have assumed that the dielectric function is rotationally symmetric. This assumption is not essential for a static object, but is crucial for rotating objects.

$$2\pi \int_0^R d|\mathbf{z}|\, |\mathbf{z}| f_{\omega,m}(|\mathbf{z}|)\, \mathrm{Im}\, \epsilon(\omega, |\mathbf{z}|)\, \overline{f_{\omega,m}(|\mathbf{z}|)}. \tag{2.22}$$

By virtue of the field equation, the integral in the last line of this equation can be converted to an expression on the boundary of the object: The conjugate of the function f satisfies the conjugated wave equation with $\epsilon \to \epsilon^*$. By subtracting off the conjugated from the original equation, one can see that the integrand is equal to a total derivative. The integral then becomes

$$\frac{1}{-2i\omega^2} W\left(f_{\omega,m}(R), \overline{f_{\omega,m}(R)}\right), \tag{2.23}$$

with W being the Wronskian with respect to the radius. The continuity relations of Eq. (2.21) can be exploited to compute the Wronskian

$$W\left(f_{\omega,m}(R), \overline{f_{\omega,m}(R)}\right) = -\frac{4i}{\pi R}\left(1 - |S_m(\omega)|^2\right), \tag{2.24}$$

where we used the identity $W\left(H_m^{(1)}(x), H_m^{(2)}(x)\right) = -4i/\pi x$. Rather remarkably, this equation shows that all the relevant details of the inside solutions f can be encoded in the scattering matrix, i.e. fluctuations inside the object affect the correlation function only through the scattering matrix, S. Combining the previous steps, we arrive at the (outside) correlation function due to the inside source fluctuations,

$$\langle \Phi(\omega, \mathbf{x}) \Phi^*(\omega, \mathbf{x}') \rangle_{\text{in-fluc}} = \frac{1}{16} a_{\text{in}}(\omega) \sum_{m=-\infty}^{\infty} \left(1 - |S_m(\omega)|^2\right) H_m^{(1)}(\omega r) e^{im\phi} \overline{H_m^{(1)}(\omega \xi) e^{im\psi}}. \tag{2.25}$$

The correlation function is a bilinear sum over outgoing (first kind of Hankel) functions; this is reasonable as the sources in the object must produce outgoing waves in the vacuum. The coefficient is, however, more interesting: It depends on the scattering matrix through $1 - |S|^2$, and vanishes for a non-lossy object, i.e. when the scattering matrix is unitary, $|S| = 1$. We revisit this point later when we study radiation out of thermal or dynamical equilibrium.

Thermal radiation

In this section, we employ the results from the previous sections to compute the radiation out of thermal equilibrium when the object is at rest though at a temperature T different from that of the the environment, T_0. But we first show that the equilibrium behavior is consistent with the FDT. At $T = T_0$, the distribution functions $a_{\rm in}(\omega) = a_{\rm out}(\omega) \equiv a(\omega)$ are equal. A sum over Eqs. (2.11) and (2.25) yields

$$\begin{aligned}\langle\Phi(\omega,\mathbf{x})\Phi^*(\omega,\mathbf{y})\rangle &= \langle\Phi(\omega,\mathbf{x})\Phi^*(\omega,\mathbf{y})\rangle_{\text{out-fluc}} + \langle\Phi(\omega,\mathbf{x})\Phi^*(\omega,\mathbf{y})\rangle_{\text{in-fluc}} \\ &= a(\omega)\ \text{Im}\ \sum_{m=-\infty}^{\infty} \frac{i}{8}\left(H_m^{(2)}(\omega r) + S_m(\omega)H_m^{(1)}(\omega r)\right) e^{im\phi}\ H_m^{(1)}(\omega\xi)e^{-im\psi} \\ &= a(\omega)\ \text{Im}\ G(\omega,\mathbf{x},\mathbf{y}), \end{aligned} \tag{2.26}$$

in agreement with the FDT.

Out of thermal equilibrium, the "Poynting" vector quantifies the radiation flux from the object into the environment. In our model for the scalar field, the radial component of the Poynting vector is given by

$$\langle\partial_t\Phi(t,\mathbf{x})\partial_r\Phi(t,\mathbf{x})\rangle = \frac{1}{\pi}\int_0^\infty d\omega\,\omega\,\text{Im}\,\langle\Phi(\omega,\mathbf{x})\partial_r\Phi^*(\omega,\mathbf{x})\rangle. \tag{2.27}$$

The total radiation rate is obtained by integrating over a closed surface enclosing the object. We compute the contribution due to inside and outside source fluctuations separately by inserting the corresponding correlation functions in the last equation. The radiated energy per unit time is then

$$\mathcal{P}_{\text{in-fluc/out-fluc}} = \pm\frac{1}{4\pi}\sum_{m=-\infty}^{\infty}\int_0^\infty d\omega\,\omega a_{\text{in/out}}(\omega)\left(1 - |S_m(\omega)|^2\right), \tag{2.28}$$

with the upper (lower) sign corresponding to inside (outside) fluctuations, where we have used the expression for the Wronskian of Hankel functions. Note that the signs indicate that the flux due to the inside sources is outgoing while the vacuum fluctuations induce an incoming flux. In the absence of loss, i.e. when $|S| = 1$,

there is no flux in either direction since the object lacks an exchange mechanism with the environment. In equilibrium, detailed balance prevails and there is no net radiation. One can also see that the reality of the correlation function in Eq. (2.26) guarantees that the corresponding Poynting vector in Eq. (2.27) vanishes. Out of thermal equilibrium, the total radiation to the environment is given by

$$\mathcal{P} = \sum_{m=-\infty}^{\infty} \int_0^{\infty} \frac{d\omega}{2\pi} \hbar\omega \left(n(\omega, T) - n(\omega, T_0)\right) \left(1 - |S_m(\omega)|^2\right). \tag{2.29}$$

We have expressed the radiation in terms of the Bose-Einstein distribution number $n(\omega, T)$. Clearly the net flux is in a direction opposite to the temperature gradient. The relation in Eq. (2.29) between the thermal emission and the absorptivity, characterized by the deviation of the scattering matrix from unitarity, is *Kirchhoff's law* [66, 67]. In the black-body limit, the dielectric function slightly deviates from 1 with $\mathrm{Im}\,\epsilon \ll 1$ while at high temperatures the thermal radiation is dominated by large frequencies so we can assume $\mathrm{Im}\,\epsilon\,\omega R \gg 1$. Within these limits, one can see that the scattering matrix is almost unitary for $|m| > \omega R$ while it is approximately zero when $|m| < \omega R$. Therefore, the sum over m at a fixed ω gives a factor of $2\omega R$ proportional to the circumference of the disk in harmony with the black-body radiation and Stefan-Boltzmann law [68].

In the following sections, we apply the techniques that we have developed here to rotating objects.

2.1.2 Field fluctuations for moving objects

We first devise a Lagrangian from which Eq. (2.1) follows for a static object, and then, with the guidance of Lorentz invariance, generalize it to a moving object. Schematically, the Lagrangian can be written as[2]

$$\mathcal{L} = \frac{1}{2}\epsilon \left(\partial_t \Phi\right)^2 - \frac{1}{2}(\nabla\Phi)^2$$

[2]The response function may be non-local in time; the Lagrangian merely serves as a guide to obtain the field equation.

$$= \frac{1}{2}\left[(\partial_t\Phi)^2 - (\nabla\Phi)^2\right] + \frac{1}{2}(\epsilon - 1)\,(\partial_t\Phi)^2. \tag{2.30}$$

The second line breaks the Lagrangian into two parts: the first term is merely the free Lagrangian (in empty space) while the second term contributes only within the material, hence defining the interaction of the field with the object. In generalizing to moving objects, the free Lagrangian remains invariant. The interaction, however, should be defined with respect to the rest frame of the object. The latter is cast into a covariant form so that it reduces to the familiar expression in the rest frame

$$\mathcal{L} = \frac{1}{2}(\partial_t\Phi)^2 - \frac{1}{2}(\nabla\Phi)^2 + \frac{1}{2}(\epsilon' - 1)(U^\mu\partial_\mu\Phi)^2\,, \tag{2.31}$$

with U being the four-velocity (or, three-velocity in 2+1 dimensional space-time) of the object. Note that Φ is scalar, i.e. $\Phi'(t', \mathbf{x}') = \Phi(t, \mathbf{x})$ with the (un)primed coordinates defined in the (lab) comoving frame. Also the dielectric function $\epsilon' = \epsilon(\omega', \mathbf{x}')$ is naturally defined in the comoving frame, and should be transformed to the coordinates in the lab frame. Equation (2.31) introduces a *minimal* coupling between the object's motion and the scalar field in the background. For an object in uniform motion, this Lagrangian is obtained by an obvious Lorentz transformation. One might think that this equation should be further elaborated for an accelerating object. However, if the acceleration rate is small compared to the object's internal frequencies (plasma frequency, for example) the motion can be implemented by a local Lorentz transformation, hence Eq. (2.31). The field equation is deduced from the Lagrangian as

$$\left[\triangle - \partial_t^2 - (\epsilon' - 1)(U^\mu\partial_\mu)^2\right]\,\Phi(t, \mathbf{x}) = 0.$$

This is the homogenous field equation in the presence of a moving object. We should also incorporate the coupling to random sources for applications of the Rytov formalism. The source is naturally defined in the comoving frame, thus a similar argument suggests a minimal coupling by adding $\Delta\mathcal{L} = -\rho\, U^\mu\partial_\mu\Phi$ to the Lagrangian. The

governing equation for the scalar field is then

$$-\left[\triangle - \partial_t^2 - (\epsilon' - 1)(U^\mu \partial_\mu)^2\right] \Phi(t, \mathbf{x}) = U^\mu \partial_\mu \rho(t, \mathbf{x}), \tag{2.32}$$

which reduces to Eq. (2.2) for an object at rest. Here, we have *defined* $\rho'(t', \mathbf{x}') \equiv \rho(t, \mathbf{x})$. Source fluctuations are distributed according to Eq. (2.3) but with respect to the comoving frame,

$$\langle \rho'_{\omega'}(\mathbf{x}') \rho'^*_{\omega'}(\mathbf{y}') \rangle = a(\omega') \operatorname{Im} \epsilon(\omega', \mathbf{x}') \, \delta(\mathbf{x}' - \mathbf{y}'), \tag{2.33}$$

with primed quantities defined in the moving frame. The two sets of coordinates are related via

$$\begin{cases} t' = t, \\ r' = r, \\ \phi' = \phi - \Omega t. \end{cases} \tag{2.34}$$

We shall limit ourselves only to objects moving at velocities small compared to the speed of light, in which case, $U \approx (1, \mathbf{v})$ with $\mathbf{v}$ being the local velocity. Rotating at an angular frequency Ω, $\mathbf{v} = \mathbf{\Omega} \times \mathbf{x}$, Eq. (2.32) becomes

$$-\left[\triangle - \partial_t^2 - (\epsilon' - 1)(\partial_t + \Omega \partial_\phi)^2\right] \Phi(t, \mathbf{x}) = (\partial_t + \Omega \partial_\phi) \rho(t, \mathbf{x}). \tag{2.35}$$

Let us expand the random source $\rho(t, \mathbf{x})$ in the lab frame as

$$\rho(t, \mathbf{x}) = \int \frac{d\omega}{2\pi} e^{-i\omega t} \rho_\omega(\mathbf{x}) = \sum_m \int \frac{d\omega}{2\pi} e^{-i\omega t + im\phi} \rho_{\omega,m}(r). \tag{2.36}$$

Similarly, we define $\rho'_{\omega',m'}$ in the comoving frame with ω' and m' being conjugate to the time and angular variables in the same frame. The coordinate transformations in Eq. (2.34) along with the definition $\rho'(t', \mathbf{x}') \equiv \rho(t, \mathbf{x})$ yield $\rho_{\omega,m}(r) = \rho'_{\omega - \Omega m, m}(r)$. Therefore fluctuations in the comoving frame, Eq. (2.33), translate to

$$\langle \rho_{\omega,m}(r) \rho^*_{\omega,m}(\xi) \rangle = a(\omega - \Omega m) \operatorname{Im} \epsilon(\omega - \Omega m, r) \, \frac{r^{-1} \delta(r - \xi)}{2\pi}, \tag{2.37}$$

in the lab frame. This equation is indeed similar to source fluctuations in a static object with ω being replaced by $\omega - \Omega m$. In other words, zero-point fluctuations in the object are centered at a frequency shifted from that of the vacuum.

Having formulated field equations and their corresponding source fluctuations, we compute correlation functions in the next section.

Field correlations

Similar to Sec. 2.1.1, we compute the field correlation functions separately for source fluctuations outside and inside the object. The treatment of the vacuum (outside) fluctuation is entirely identical to the case of static object, Eq. (2.11). Nevertheless the scattering matrix for a rotating object could be different.

For inside source fluctuations, the argument should be modified slightly. Let us define the (new) functions f as solutions to the wave equation inside the object

$$\left[\triangle - \partial_t^2 - (\epsilon' - 1)(\partial_t + \Omega\partial_\phi)^2\right] e^{-i\omega t} e^{im\phi} f_{\omega,m}(r) = 0. \tag{2.38}$$

The Green's function for one point inside and the other outside the object takes a similar form to the static case

$$G(\omega, \mathbf{x}, \mathbf{y}) = \sum_{m=-\infty}^{\infty} \frac{i}{8} f_{\omega,m}(r) e^{im\phi} H_m^{(1)}(\omega\xi) e^{-im\psi}, \qquad r < R < \xi. \tag{2.39}$$

with the function f satisfying continuity relations similar to Eq. (2.21) with $S_m(\omega)$ replaced by $S_{-m}(\omega)$.[3] The field correlation function is then related to source fluctu-

[3]With time reversal invariance, the Green's function, $G(\omega, \mathbf{x}, \mathbf{y})$, is symmetric in its spatial arguments,

$$G(\omega, \mathbf{x}, \mathbf{y}) = G(\omega, \mathbf{y}, \mathbf{x}).$$

For a rotating object, time reversal is no longer a symmetry; however, time reversal followed by reversing the angular velocity forms a symmetry which yields

$$G(\omega, r, \phi, \xi, \psi) = G(\omega, \xi, -\psi, r, -\phi).$$

The negative sign carries through to the sign of the angular momentum m.

ations as

$$\langle\Phi(\omega,\mathbf{x})\Phi^*(\omega,\mathbf{y})\rangle_{\text{in-fluc}} = \frac{1}{64}\sum_{m=-\infty}^{\infty}(\omega-\Omega m)^2\, a_{\text{in}}(\omega-\Omega m)\, H_m^{(1)}(\omega r)e^{im\phi}\overline{H_m^{(1)}(\omega\xi)e^{im\psi}}\times$$
$$2\pi\int_0^R d|\mathbf{z}|\,|\mathbf{z}|f_{\omega,m}(|\mathbf{z}|)\,\text{Im}\,\epsilon(\omega-\Omega m,|\mathbf{z}|)\,\overline{f_{\omega,m}(|\mathbf{z}|)}, \qquad (2.40)$$

where we have used Eq. (2.37). As before, we can exploit the wave equation to convert the integral in the last equation to a boundary term. The correlation function can be then cast in terms of the scattering matrix as

$$\langle\Phi(\omega,\mathbf{x})\Phi^*(\omega,\mathbf{y})\rangle_{\text{in-fluc}} = \sum_{m=-\infty}^{\infty}\frac{a_{\text{in}}(\omega-\Omega m)}{16}\left(1-|S_m(\omega)|^2\right)H_m^{(1)}(\omega r)e^{im\phi}\overline{H_m^{(1)}(\omega\xi)e^{im\psi}}. \qquad (2.41)$$

This equation is similar to the expression for a static object, Eq. (2.25), with the important difference that the distribution a is a function of a shifted frequency defined from the point of view of the rotating frame.

Radiation, spontaneous emission and superradiance

In a Gaussian theory, two-point correlation functions define the complete structure of fluctuations, and can be used to compute force, torque or radiation. Specifically, the energy radiation per unit time is obtained by the integral of $\langle\partial_t\Phi\partial_r\Phi\rangle$ over a surface enclosing the object. For a rotating object, the correlation functions derived in the previous subsection yield

$$\mathcal{P} = \sum_{m=-\infty}^{\infty}\int_0^{\infty}\frac{d\omega}{2\pi}\hbar\omega\left[n_{\text{in}}(\omega-\Omega m)-n_{\text{out}}(\omega)\right]\left(1-|S_m(\omega)|^2\right). \qquad (2.42)$$

Similarly the torque, or the rate of angular momentum radiation, is given by integrating $\langle\partial_t\Phi\partial_\phi\Phi\rangle$ over the surface. We find an expression similar to Eq. (2.42) by replacing $\hbar\omega$ by $\hbar m$,

$$M = \sum_{m=-\infty}^{\infty}\int_0^{\infty}\frac{d\omega}{2\pi}\hbar m\left[n_{\text{in}}(\omega-\Omega m)-n_{\text{out}}(\omega)\right]\left(1-|S_m(\omega)|^2\right). \qquad (2.43)$$

The function $n_{\rm in}$ is singular at $\omega = \Omega m$; however, at this frequency $\mathrm{Im}\,\epsilon(\omega - \Omega m) = \mathrm{Im}\,\epsilon(0) = 0$ which results in no loss. Therefore, $1 - |S|^2$ is zero at $\omega = \Omega m$ removing the singularity and rendering above expressions well-defined.

Let us consider the limit of zero temperature so that thermal radiation can be neglected. In this limit, $n(\omega) = \Theta(-\omega)$, that is the distribution function vanishes for positive frequency but becomes 1 for negative frequencies. This distribution defines a *vacuum* state in which all positive-energy states are empty, and, roughly speaking, all negative energy states are occupied. Now the distribution function pertaining to inside fluctuations is defined with respect to a frequency shifted by a multiple of rotation frequency and thus can find negative values even when ω is positive. The difference of the Bose-Einstein distributions contributes in a frequency window of $[0, \Omega m]$. Therefore, even at zero temperature, a rotating object emits photons and loses energy; the number of photons emitted at frequency $\omega(> 0)$ and partial wave m is given by

$$\frac{d\mathcal{N}_m(\omega)}{d\omega} = \Theta(\Omega m - \omega)\left(|S_m(\omega)|^2 - 1\right). \tag{2.44}$$

The corresponding energy or angular momentum radiation is obtained by integrating over photon number multiplied by $\hbar\omega$ or $\hbar m$ respectively. It follows from Eq. (2.44) that a (physically acceptable) positive outflux of photons requires a *super-unitary* scattering matrix, $|S_m(\omega)| > 1$. Indeed Zel'dovich argued that classical waves should amplify upon scattering from a rotating object exactly for frequencies in a range $0 < \omega < \Omega m$, a phenomenon which is called superradiance [58]. While spontaneous emission by a rotating object is a purely quantum effect, super-radiance can be understood entirely within classical mechanics: A system is lossy if the imaginary part of its response function is positive (negative) for positive (negative) frequencies. For a rotating object, $\mathrm{Im}\,\epsilon(\omega')$ has the same sign as $\omega' = \omega - \Omega m$, the frequency defined in the comoving frame; however, for (positive) ω smaller than Ωm, the argument of the dielectric function is negative and thus the object amplifies the corresponding incident waves, hence superradiance. In fact, incoming waves in the superradiating regime extract energy form a rotating object and slow it down.

Superradiance and spontaneous emission are intimately related. When the object is at rest, it absorbs energy by getting excited to a higher level, and de-excites by emitting a photon. For a rotating body, this picture breaks down, that is the object can emit a photon while being excited to a higher level: The energy of the emitted photon is $\hbar\omega > 0$ in the lab frame; however, a rotating observer sees the same particle at a shifted frequency $\omega' = \omega - \Omega m$. In the superradiant regime where $\omega < \Omega m$, the frequency is negative in the comoving frame, hence the object has gained (positive) energy. This gain should be interpreted as heat generated inside the body. The energy conservation still holds because the energy of the emitted photon as well as heat are extracted from the rotational energy of the object. This observation is also at the heart of the superradiance phenomenon when incoming waves are enhanced upon scattering from a rotating object. The above argument shows that spontaneous emission conserves the energy and thus is (energetically) possible. In fact, as the object spontaneously emits photons (and heats up), it also slows down unless kept in steady motion by an external agent; see the discussion below Eq. (2.44). In the context of general relativity, the Penrose process provides a similar mechanism to extract energy from a rotating black hole [60], which also leads to spontaneous emission [61].

We define E and E' as the energy of the object in the lab frame and the rotating frame, respectively. The two are related by $E' = E - \Omega L$ where L is the angular momentum of the object. Hence, the heat generated per unit time, $\mathcal{Q} \equiv dE'/dt$, is given by

$$\mathcal{Q} \equiv \frac{dE'}{dt} = \frac{dE}{dt} - \Omega\frac{dL}{dt} = \Omega M - \mathcal{P}. \tag{2.45}$$

In order to maintain a steady rotation, one should exert a constant torque M. The work done is equal to the radiated energy plus heat, $\Omega M = \mathcal{P} + \mathcal{Q}$. Note that the object loses energy to the environment, $dE/dt = -\mathcal{P} < 0$, as well as angular momentum, $dL/dt = -M < 0$. The rate of the energy gain in the object's rest frame can be obtained from Eqs. (2.42) and (2.43) as

$$\mathcal{Q} = \sum_{m=-\infty}^{\infty} \int_0^{\infty} \frac{d\omega}{2\pi}\, \hbar(\Omega m - \omega)\, \frac{d\mathcal{N}_m(\omega)}{d\omega}. \tag{2.46}$$

At zero temperature, the photon number production, Eq. (2.44), has nonzero support only for $0 < \omega < \Omega m$ and thus the heat generation is manifestly positive. In brief, the object heats up while it loses energy (E decreases) if not connected to an infinite thermal bath. This suggests that the heat capacity from the point of view of the lab frame is negative; however, thermodynamic quantities are well-defined in the comoving frame where the energy, E', increases, hence the heat capacity is indeed positive.

We have argued that spontaneous emission is energetically possible consistent with the energy conservation. This process also generates heat inside the object and photons in the environment, hence the entropy is increasing. Notice that the line of argument can be reversed: A phenomenon which satisfies requirements of energy conservation and is thermodynamically favored due to entropy production should occur. This observation completes the link between superradiance and spontaneous emission, see also Refs. [58, 69]. In Sec. 2.1.4, we study the statistics of radiated photons in some detail. In particular, we compute the entropy generation due to the creation of photons.

Radiation: rotating disk

In this section, we study quantum radiation by a rotating disk of radius R described by a spatially uniform but frequency-dependent dielectric function $\epsilon(\omega)$. We find solutions to the field equation inside and outside the object, and match them on the boundary to compute the scattering amplitude. When linear velocities are small, Eq. (2.35) for the field equation (with the source term in the RHS set to zero) yields

$$\left[\triangle - \partial_t^2 - (\epsilon' - 1)\left(\partial_t + \Omega\partial_\phi\right)^2\right]\Phi(t, \mathbf{x}) = 0. \tag{2.47}$$

A solution characterized by frequency ω and the angular momentum m, i.e. of the form $\Phi = f(r)e^{-i\omega t}e^{im\phi}$, casts this equation to

$$\left[\frac{1}{r}\partial_r r\partial_r - \frac{m^2}{r^2} + \tilde{\omega}_m^2\right] f(r) = 0. \tag{2.48}$$

Here, we have defined a new m-dependent (possibly complex) frequency $\tilde{\omega}_m$ as

$$\tilde{\omega}_m^2 = (\epsilon' - 1)\,(\omega - \Omega m)^2 + \omega^2, \tag{2.49}$$

which is a constant for a fixed ω and m, and position-independent $\epsilon' = \epsilon(\omega') = \epsilon(\omega - \Omega m)$. Therefore, the equation that governs the field dynamics inside the object is a Helmholtz equation whose regular solutions are Bessel-J functions, with the frequency replaced by $\tilde{\omega}_m$. Note that both the order and the argument of the Bessel functions depend on m, the latter through $\tilde{\omega}_m$. We define a scattering ansatz as

$$\Phi(\omega, \mathbf{x}) = \begin{cases} V_m(\omega)\, J_m(\tilde{\omega}_m r) e^{im\phi}, & r < R, \\ H_m^{(2)}(\omega r) e^{im\phi} + S_m(\omega) H_m^{(1)}(\omega r) e^{im\phi}, & r > R, \end{cases} \tag{2.50}$$

with the outside solutions being a linear combination of incoming and (with the scattering matrix as the amplitude) outgoing waves. The scattering matrix can be easily obtained by matching boundary conditions,

$$S_m(\omega) = -\frac{\partial_R J_m(\tilde{\omega}_m R) H_m^{(2)}(\omega R) - J_m(\tilde{\omega}_m R) \partial_R H_m^{(2)}(\omega R)}{\partial_R J_m(\tilde{\omega}_m R) H_m^{(1)}(\omega R) - J_m(\tilde{\omega}_m R) \partial_R H_m^{(1)}(\omega R)}. \tag{2.51}$$

When ϵ is real, i.e. for a loss-less material, the denominator is merely the complex conjugate of the numerator, and the scattering is unitary. Conversely, if ϵ has an imaginary part the scattering matrix is non-unitary. For a lossy object at rest, $\operatorname{Im} \tilde{\omega}_m = |\omega| \operatorname{Im} \sqrt{\epsilon} > 0$ (for positive frequency) and $|S|^2 < 1$. For a spinning object, $\operatorname{Im} \tilde{\omega}_m \propto \operatorname{Im} \epsilon' \propto \operatorname{sgn}(\omega - \Omega m)$, hence the scattering matrix is sub-unitary for $\omega > \Omega m$ but super-unitary, $|S|^2 > 1$, in the superradiating range $\omega < \Omega m$.

One can now compute the radiation from the S-matrix. Assuming that the object's linear velocity is small, the radiation is strongest at frequencies comparable to Ω, thus the first partial wave $m = 1$ suffices, and the Bessel-J functions can be expanded. The scattering matrix deviates form unitarity by (restoring units of c)

$$|S_1(\omega)|^2 - 1 \approx -\frac{\pi}{8} \frac{\omega^2 (\omega - \Omega)^2 R^4}{c^4} \operatorname{Im} \epsilon(\omega - \Omega). \tag{2.52}$$

This expression is manifestly negative for $\omega > \Omega$ but positive when $\omega < \Omega$ for any causal ϵ. One can then compute various quantities of interest such as torque, heat generation, and radiation. Energy radiation per unit time is given by Eq. (2.42) as

$$\mathcal{P} \approx \frac{\hbar R^4}{16c^4} \int_0^\Omega d\omega\, \omega^3 (\omega - \Omega)^2 |\operatorname{Im} \epsilon(\omega - \Omega)|. \tag{2.53}$$

For a specific dielectric function, the radiation can be computed explicitly.

2.1.3 Higher dimensions, non-scalar field theories and Trace formulas

The above results can be readily generalized to higher dimensions. For a cylinder extended along the third dimension, quantum radiation is given by

$$\mathcal{P} = \int_0^\infty \frac{d\omega}{2\pi} \hbar\omega \sum_{m=-\infty}^{\infty} \int_{-\omega}^{\omega} \frac{L dk_z}{2\pi} \left[n_{\text{in}}\left(\omega - \Omega m\right) - n_{\text{out}}(\omega) \right] \left(1 - |S_{mk_z}(\omega)|^2\right), \tag{2.54}$$

where L is the length of the cylinder, and k_z is the wavevector along the z direction. Note that $|k_z|$ is bounded by ω (we have set $c = 1$) corresponding to propagating waves as opposed to evanescent waves which affect short distances from the cylinder but do not contribute to the radiation at infinity.

If the rotating object is not translationally symmetric in the z direction (while rotationally symmetric), the scattering matrix is no longer diagonal in k_z. An expression analogous to Eq. (2.54) becomes more complicated, nevertheless, the S-matrix can always be written in a diagonal basis. Indeed one can write a general Trace formula for the quantum radiation which is independent of a particular basis,

$$\mathcal{P} = \int_0^\infty \frac{d\omega}{2\pi} \hbar\omega \operatorname{Tr}\left[\left(n_{\text{in}}\left(\omega - \Omega \hat{l}_z\right) - n_{\text{out}}(\omega) \right) \left(1 - \mathbb{S}\mathbb{S}^\dagger\right) \right], \tag{2.55}$$

where we trace over all the propagating modes. In this equation, $\hat{l}_z = \frac{1}{i}\frac{\partial}{\partial\phi}$ is the angular momentum operator (in units of $\hbar$) projecting out the rotational index m. The scattering matrix $\mathbb{S}$ is written in a general basis-free notation. Equation (2.55)

is not specific to scalar fields or translationally symmetric objects but also holds for arbitrary shapes (though rotationally symmetric) and electromagnetism—the latter requires tracing over polarizations too. We present a general derivation of Eq. (2.55) in Sec. 2.2 in the context of electrodynamics.

2.1.4 Photon statistics and entropy generation

Heretofore, we have studied in some detail the radiation from an object out of thermal or dynamical equilibrium with the environment, where it is shown that the object emits photons. In this section, we turn to a different aspect of this problem, namely the statistics of radiated photons.

We first note that the field correlation function receives contributions from photons as well as zero-point and, at finite temperature, thermal fluctuations, and can be broken up as

$$\langle \Phi\Phi \rangle = \langle \Phi\Phi \rangle_{\text{non-rad}} + \langle \Phi\Phi \rangle_{\text{rad}}. \tag{2.56}$$

The first term on the RHS is the non-radiative term given by

$$\langle \Phi(\omega, \mathbf{x})\Phi^*(\omega, \mathbf{y}) \rangle_{\text{non-rad}} = \hbar \coth\left(\frac{\hbar\omega}{2k_B T}\right) \operatorname{Im} G(\omega, \mathbf{x}, \mathbf{y}). \tag{2.57}$$

This term is purely real, and does not contribute to radiation. For a disk rotating at a rate Ω possibly at a finite temperature T, the radiation term can be deduced from the total correlation function (see Sec. 2.1.2), and using the above definition we find

$$\langle \Phi(\omega, \mathbf{x})\Phi^*(\omega, \mathbf{y}) \rangle_{\text{rad}} = \frac{\hbar}{8} \sum_{m=-\infty}^{\infty} n(\omega - \Omega m, T) \left(1 - |S_m(\omega)|^2\right) H_m^{(1)}(\omega r) e^{im\phi} \overline{H_m^{(1)}(\omega \xi) e^{im\psi}}. \tag{2.58}$$

The radiation is entirely outgoing be expected. In the remainder of this section, we focus on the ensemble of radiated photons.

Radiation can be quantified by the photon current, or the number of photons radiated per unit time. Different frequencies and partial waves are statistically independent, thus we consider the current of a single mode of frequency ω and angular

momentum m,

$$I_{\omega,m} = \frac{1}{i}\int r d\phi \left[\Phi^*_m(\omega,\mathbf{x})\,\partial_r\Phi_m(\omega,\mathbf{x}) - \text{c.c.}\right], \tag{2.59}$$

where the field is expanded over partial waves as $\Phi(\omega,\mathbf{x}) = \sum_m \Phi_m(\omega,\mathbf{x})$. When averaged over the radiation ensemble, this expression reproduces Eq. (2.44) for a rotating object at $T = 0$, or, more generally at a finite T,

$$\mathcal{N}_m(\omega) = \langle I_{\omega,m}\rangle = n(\omega - \Omega m, T)\left(1 - |S_m(\omega)|^2\right). \tag{2.60}$$

Furthermore, we want to know higher statistical moments in which case we have to compute the correlation function of currents themselves. Since fluctuations are Gaussian-distributed, current correlation functions can be reduced to a product of two-point functions of fields according to Wick's theorem.

We compute the fluctuations of the current at the radiation zone far away from the object. Keeping in mind that the radiation field in Eq. (2.58) is strictly outgoing, the radial derivative acting on Φ gives a factor of $i\omega$. Therefore, far from the object, the current defined in Eq. (2.59) can be cast as

$$I_{\omega,m} = \lim_{r\to\infty} 4\pi\omega r\ \Phi^*_m(\omega,\mathbf{x})\,\Phi_m(\omega,\mathbf{x}); \tag{2.61}$$

this expression is useful in evaluating n-point correlation functions.

We can also define the probability distribution function $P(n)$ with n being the number of photons per mode emitted in a time duration t. We drop the subscript indices as the statistics can be computed independently for each mode. Remarkably, the probability distribution is given in terms of current correlators by the Glauber-Kelley-Kleiner formula [70, 71],

$$P(n) = \frac{1}{n!}\langle I^n e^{-I}\rangle_{\text{rad}}. \tag{2.62}$$

We introduce a generating function $F(\eta)$ as

$$e^{F(\eta)} = \langle e^{\eta I}\rangle. \tag{2.63}$$

The probability distribution can be computed from the generating function as

$$P(n) = \lim_{\eta \to -1} \frac{1}{n!} \frac{d^n}{d\eta^n} e^{F(\eta)}. \tag{2.64}$$

Taylor-expanding F over η yields

$$F(\eta) = \sum_{p=1}^{\infty} \frac{\kappa_p \eta^p}{p!}. \tag{2.65}$$

From Eq. (2.63), it is then clear that the cumulants κ_p are given by

$$\kappa_p = \langle I^p \rangle_c, \tag{2.66}$$

with the subscript c indicating that the *connected* component of the n-point function should be computed. For a single object discussed above, Eq. (2.61) is a bilinear term in the field Φ and its conjugate. Diagrammatically, we can represent this term as a vertex with an incoming and an outgoing line corresponding to Φ^* and Φ respectively. A little thought shows that the connected correlation function in Eq. (2.66) yields

$$\kappa_p = (p-1)! \mathcal{N}^p, \tag{2.67}$$

with $\mathcal{N} = \langle I \rangle$ is the average current per mode. The generating function is then

$$F(\eta) = -\log(1 - \eta\mathcal{N}), \qquad \text{or,} \qquad e^{F(\eta)} = \frac{1}{1 - \eta\mathcal{N}}. \tag{2.68}$$

These equations indicate that the counting distribution is solely determined from the mean value of the radiation. This strong version of Kirchhoff's law is due to Bekenstein and Schiffer [72]; see also Ref. [73]. F can also be interpreted as a one-loop effective action in a background defined by ηI. Adopting this point of view, Eqs. (2.66) and (2.68) follow immediately. The probability distribution is easily deduced from Eqs. (2.64) and (2.68) as

$$P(n) = \frac{\mathcal{N}^n}{(\mathcal{N}+1)^{n+1}}. \tag{2.69}$$

This equation completely determines photon number statistics [72]. Having the full statistics, we can compute the entropy of radiated photons as

$$\begin{aligned}\frac{S}{k_B} &= -\sum_{n=0}^{\infty} P(n)\log P(n) \\ &= (\mathcal{N}+1)\log(\mathcal{N}+1) - \mathcal{N}\log\mathcal{N}. \end{aligned} \tag{2.70}$$

In fact, this equation describes the entropy of a bosonic system out of equilibrium [74]. If the occupation number $\mathcal{N}$ obeys the Bose-Einstein distribution, Eq. (2.70) indeed produces the entropy of a gas of thermal bosons. Quantum or thermal radiation from a single object consists of photons across the whole spectrum. Therefore, we should sum over all frequencies and quantum numbers

$$\sum_{\omega,m} \quad \to \quad t\int \frac{d\omega}{2\pi}\sum_{m},$$

where t is the time interval under consideration. The entropy from Eq. (2.70) is then linearly increasing over time giving rise to a constant entropy generation (restoring ω and m) as

$$\mathcal{S} \equiv \frac{dS}{dt} = k_B \sum_m \int_0^{\infty} \frac{d\omega}{2\pi} \left(\mathcal{N}_m(\omega)+1\right)\log(\mathcal{N}_m(\omega)+1) - \mathcal{N}_m(\omega)\log\mathcal{N}_m(\omega). \tag{2.71}$$

In the black-body limit (for a perfectly absorbing object at rest), we recover the entropy associated with Planckian radiation. For a finite-size object (comparable with thermal wavelength), the spectrum approaches that of the grey-body radiation where one should include the dependence on absorptivity $r \equiv 1 - |S|^2$. Equation (2.71) then depends on temperature, object's length scale, and material properties in a complicated way. On the other hand, the object loses energy thus contributes negatively to entropy generation as $\mathcal{S}_{\text{object}} = -\mathcal{P}/T$ with $\mathcal{P}$ being the (mean) energy radiation. The total entropy increase per mode is then

$$\frac{\mathcal{S}_{\text{total}}}{k_B} = \left(\frac{r}{e^x-1}+1\right)\log\left(\frac{r}{e^x-1}+1\right) - \frac{r}{e^x-1}\log\frac{r}{e^x-1} - \frac{xr}{e^x-1}, \tag{2.72}$$

where $x = \hbar\omega/k_BT$ and r is the absorptivity of the corresponding mode. It can be shown that this expression is positive for all $0 \leq r \leq 1$ as expected.

We are mainly interested in a rotating object at zero temperature with the radiation given by Eq. (2.44). Defining $\sigma \equiv |S|^2$, the entropy generation due to radiation from a rotating object is given by

$$\mathcal{S} = k_B \sum_{m=1}^{\infty} \int_0^{\Omega m} \frac{d\omega}{2\pi} \left[\sigma_m(\omega) \log \sigma_m(\omega) - (\sigma_m(\omega) - 1) \log(\sigma_m(\omega) - 1)\right]. \tag{2.73}$$

Similarly to thermal radiation, there is another contribution to entropy due to the object itself. In this case, however, the latter is also increasing in time since the object heats up. Hence, as we have argued in Sec. 2.1.2, a rotating object tends to emit radiation for purely thermodynamic reasons.

Before concluding this section, we note that Eq. (2.73) can also be written as a Trace formula similar to the expression (2.55) for the energy radiation which should be valid in higher dimensions and other field theories including electrodynamics.

2.1.5 Test object: torque and tangential force

In this section, we consider a second, or a *test*, object in the vicinity of the rotating body, and study the interaction between the two. This problem goes beyond the Casimir-Polder force [75] between two polarizable objects since the radiation field exerts pressure on the nearby object. As we argue below, the latter is the dominant contribution to the force when the two objects are far apart. Let the objects be two disks of radii R and a separated by a distance d. We shall assume that $d \gg R, a$ and the test object is at rest. Our starting point is Eq. (2.56) where the correlation function is broken into non-radiative and radiative parts—the former is related to the imaginary part of the Green's function via Eq. (2.57), while the latter is given by Eq. (2.58).

We consider the scattering of the radiation field from the test object. It is useful to expand the radiation field around this object in order to compute the scattering. Hence, we introduce *translation matrices* relating wave functions around two different

origins,

$$H_m^{(1)}(\omega r_1)e^{im\phi_1} = \sum_{n=-\infty}^{\infty} H_{n-m}^{(1)}(\omega d)J_n(\omega r_2)e^{in\phi_2}, \tag{2.74}$$

with (r_2, ϕ_2) being the coordinates with respect to the center of the second object. Upon scattering off the test object, the amplitude of the outgoing waves is given by the object's S-matrix designated as $\mathfrak{S}$,

$$J_m(\omega r)e^{im\phi} = \frac{1}{2}\left(H_m^{(2)}(x) + H_m^{(1)}(x)\right)e^{im\phi} \quad \rightarrow \quad \frac{1}{2}\left(H_m^{(2)}(\omega r) + \mathfrak{S}_m(\omega)H_m^{(1)}(\omega r)\right)e^{im\phi}. \tag{2.75}$$

We can then write the scattering off of the second object as

$$\langle\Phi(\omega,\mathbf{x})\Phi^*(\omega,\mathbf{y})\rangle_{\text{scat}} = \frac{\hbar}{32}\sum_{m=1}^{\infty} n(\Omega m-\omega,T)\left(1-|S_m(\omega)|^2\right)\times \frac{\left(\sum_{n=-\infty}^{\infty} H_{n-m}^{(1)}(\omega d)\left(H_n^{(2)}(\omega r)+\mathfrak{S}_n(\omega)H_n^{(1)}(\omega r)\right)e^{in\phi}\right)\times}{\left(\sum_{p=-\infty}^{\infty} H_{p-m}^{(1)}(\omega d)\left(H_p^{(2)}(\omega\xi)+\mathfrak{S}_p(\omega)H_p^{(1)}(\omega\xi)\right)e^{ip\psi}\right)}. \tag{2.76}$$

Separation distance being large, single reflection should be a good approximation.

Next we compute the torque exerted on the test object by the radiation field of the rotating body. Note that we have neglected the non-radiative term in Eq. (2.56) because it is given by the imaginary part of the Green's function which can be reduced to a potential energy. The two objects being symmetric, the energy function is indifferent to a rotation of the disk and thus makes no contribution to the torque. The radiation field, on the other hand, exerts a torque which is the integral of $\langle\partial_\phi\Phi\partial_r\Phi\rangle$ over a closed contour around the test object. Note that $\partial_\phi \rightarrow in$ and ∂_r combine into the Wronskian of Bessel H functions of the first and second kind. A little algebra yields, in the-first-reflection approximation,

$$M_{2\leftarrow 1} = \frac{\hbar}{8\pi}\sum_{m>0,n} n\int_0^\infty d\omega\, n(\omega-\Omega m,T)\left(1-|S_m(\omega)|^2\right)\left|H_{n-m}^{(1)}(\omega d)\right|^2\left(1-|\mathfrak{S}_n(\omega)|^2\right). \tag{2.77}$$

The subscript indicates that the torque is exerted due to the radiation field of the first on the second object. For a slowly rotating object at zero temperature, we should include only $m = 1$. Further, $n = 1$ is dominant at large separation. We then find the torque at $T = 0$ as

$$M_{2\leftarrow 1} = \frac{\hbar}{8\pi}\int_0^\Omega d\omega \left(|S_1(\omega)|^2 - 1\right)\left|H_0^{(1)}(\omega d)\right|^2 \left(1 - |\mathfrak{S}_1(\omega)|^2\right). \tag{2.78}$$

At close separations, one should include higher-order reflections. In the opposite extreme of large separations, $\Omega d/c \gg 1$, the torque falls off as the inverse distance as

$$M_{2\leftarrow 1} \sim \frac{\hbar c}{4\pi^2 d}\int_0^\Omega d\omega \frac{1}{\omega}\left(|S_1(\omega)|^2 - 1\right)\left(1 - |\mathfrak{S}_1(\omega)|^2\right), \tag{2.79}$$

where we have restored the units of c. Note that a finite torque requires the test object to be lossy, i.e. $|\mathfrak{S}_1(\omega)| < 1$.

One can also compute the force exerted on the test object. Let the two objects be separated along the x axis. Geometrically, they are symmetric with respect to the axis connecting them, nevertheless, a *tangential* force arises in the perpendicular direction along the y axis due to the radiation field. The force can be computed from the expectation value of the stress tensor

$$T_{ij} = \partial_i\Phi\partial_j\Phi + \frac{1}{2}\delta_{ij}\left((\partial_t\Phi)^2 - (\nabla\Phi)^2\right). \tag{2.80}$$

To compute the force parallel to the y axis, one should integrate the expectation value of the stress tensor over a closed contour around the test object:

$$\begin{aligned} F_y &= r\int_0^{2\pi} d\phi \left\langle T_{ij}\right\rangle \hat{r}_i\hat{y}_j \\ &= r\int_0^{2\pi} d\phi \left\langle \frac{1}{2}\sin\phi\left((\partial_t\Phi)^2 + (\partial_r\Phi)^2 - \frac{1}{r^2}(\partial_\phi\Phi)^2\right) + \cos\phi\frac{1}{r}\partial_r\Phi\partial_\phi\Phi\right\rangle. \end{aligned} \tag{2.81}$$

Again, non-radiative terms do not contribute on the basis of symmetry. We can compute the tangential force explicitly; however, the algebra is rather long and the result is not very illuminating for our toy model of scalar fields. We postpone the

discussion of the force to Sec. 2.2.3 in the context of electromagnetism.

2.2 Electrodynamics

In this section, we generalize the methods and techniques that we have developed in application to a scalar field to electromagnetism. The vector character of the latter complicates mathematical expressions, but the underlying concepts are identical to Sec. 2.1, with the techniques straightforwardly extended to electrodynamics. We start from electromagnetic fluctuations and the corresponding correlation functions in the context of static objects, and generalize them to spinning objects. Throughout this section, we consider objects of arbitrary shape (rotationally symmetric in the case of spinning bodies) in a general basis of partial waves in three dimensions. We derive general trace formulas for the quantum and thermal radiation from a single object. We shall also explicitly keep the dependence on c.

2.2.1 Static objects

Quantum fluctuations of the electromagnetic field can be formulated in a number of ways. In a lossy medium such as a dielectric object, there are subtle complications requiring a careful treatment [76, 77, 78]. A convenient starting point for our purposes is the Rytov formalism [55] which relates quantum fluctuations of the fields to those of the sources and currents. For a dielectric object, Maxwell equations in the presence of sources are

$$\begin{cases} \nabla \times \mathbf{E} = i\frac{\omega}{c}\mathbf{B}, \\ \nabla \times \mathbf{B} = -i\,\epsilon(\omega)\,\frac{\omega}{c}\mathbf{E} - i\frac{\omega}{c}\mathbf{K}, \end{cases} \tag{2.82}$$

or equivalently

$$\left(\nabla \times \nabla \times - \frac{\omega^2}{c^2}\epsilon(\omega)\mathbb{I}\right)\mathbf{E} = \frac{\omega^2}{c^2}\mathbf{K}. \tag{2.83}$$

Then, according the Rytov formalism, source fluctuations are related to the imaginary part of the local dielectric function by

$$\langle \mathbf{K}(\omega, \mathbf{x}) \otimes \mathbf{K}^*(\omega, \mathbf{y}) \rangle = a(\omega) \operatorname{Im} \epsilon(\omega, \mathbf{x}) \delta(\mathbf{x} - \mathbf{y}) \mathbb{I}, \tag{2.84}$$

where the distributions a and n are defined as before. Current fluctuations are independent at different points (hence the delta function in space), and also independent for different spatial components denoted by the 3×3 unit matrix $\mathbb{I}$. The corresponding fluctuations of the electromagnetic (EM) field can be described in terms of the sources from Eq. (2.83) via the EM Green's function, $\mathbf{E} = \frac{\omega^2}{c^2} \int \mathbb{G}\mathbf{K}$. We are mainly interested in the EM field fluctuations outside the object from which we can compute the quantum radiation. As we have discussed in the previous section, field fluctuations receive contributions both from the fluctuating sources within the object and from fluctuations (zero-point and at finite temperature, thermal) in the vacuum outside the object. In the following, we first consider source fluctuations outside the object.

The dyadic EM Green's function is defined as

$$\left(\nabla \times \nabla \times - \frac{\omega^2}{c^2} \epsilon(\omega) \mathbb{I}\right) \mathbb{G}(\omega, \mathbf{x}, \mathbf{z}) = \mathbb{I}\, \delta(\mathbf{x} - \mathbf{z}). \tag{2.85}$$

In an appropriate coordinate system (ξ_1, ξ_2, ξ_3), the free Green's function (in empty space) can be broken up along the coordinate ξ_1 as [79, 12]

$$\mathbb{G}(\omega, \mathbf{x}, \mathbf{z}) = i \begin{cases} \sum_\alpha \mathbf{E}^{\text{out}}_{\bar{\alpha}}(\omega, \mathbf{x}) \otimes \mathbf{E}^{\text{reg}}_{\alpha}(\omega, \mathbf{z}) & \xi_1(\mathbf{x}) > \xi_1(\mathbf{z}), \\ \sum_\alpha \mathbf{E}^{\text{reg}}_{\alpha}(\omega, \mathbf{x}) \otimes \mathbf{E}^{\text{out}}_{\bar{\alpha}}(\omega, \mathbf{z}) & \xi_1(\mathbf{x}) < \xi_1(\mathbf{z}), \end{cases} \tag{2.86}$$

where $\mathbf{E}^{\text{out}}$ is the outgoing electric field normalized such that the corresponding energy flux is ω—equivalently, the corresponding current is unity. Also $\mathbf{E}^{\text{reg}}$ defines a solution to the EM field regular everywhere in space. The index α runs over partial waves, and $\bar{\alpha}$ indicates the partial wave which is related to α by time reversal. In the presence of an external object, the free Green's function should be modified to incorporate the

scattering from the object (with $\xi_1(\mathbf{x}) < \xi_1(\mathbf{z})$)

$$\mathbb{G}(\omega, \mathbf{x}, \mathbf{z}) = \frac{i}{2} \sum_{\alpha} \left(\mathbf{E}_{\alpha}^{\text{in}}(\omega, \mathbf{x}) + S_{\alpha}(\omega) \mathbf{E}_{\alpha}^{\text{out}}(\omega, \mathbf{x}) \right) \otimes \mathbf{E}_{\bar{\alpha}}^{\text{out}}(\omega, \mathbf{z}), \tag{2.87}$$

where $S_\alpha(\omega)$ is the scattering matrix as a function of the frequency ω and partial wave α. Note that we have assumed that the scattering matrix is diagonal in partial waves[4]. In general, one should sum over all β such that $S_{\beta\alpha} \neq 0$ with the rest of the derivation closely following the remainder of this section. The incoming wave $\mathbf{E}^{\text{in}}$ is normalized to ensure that the corresponding energy flux is negative ω. When the object is not present, $S_\alpha(\omega) = 1$, and the last equation reduces to the free Green's function with $\mathbf{E}_\alpha^{\text{reg}} = (\mathbf{E}_\alpha^{\text{in}} + \mathbf{E}_\alpha^{\text{out}})/2$. We stress that the Green's function in Eq. (2.87) is defined with both points outside the object.

The EM field correlation function due to the outside source fluctuations is then given by

$$\begin{aligned} \langle \mathbf{E}(\omega, \mathbf{x}) \otimes \mathbf{E}^*(\omega, \mathbf{y}) \rangle_{\text{out-fluc}} &= \frac{\omega^4}{c^4} \int d\mathbf{z} \langle \mathbb{G}(\omega, \mathbf{x}, \mathbf{z}) \mathbf{K}(\omega, \mathbf{z}) \otimes \mathbb{G}^*(\omega, \mathbf{y}, \mathbf{z}) \mathbf{K}^*(\omega, \mathbf{z}) \rangle \\ &= a_{\text{out}}(\omega) \frac{\omega^4}{c^4} \operatorname{Im} \epsilon_D \int_{\text{out}} d\mathbf{z}\, \mathbb{G}(\omega, \mathbf{x}, \mathbf{z}) \cdot \mathbb{G}^*(\omega, \mathbf{y}, \mathbf{z}), \end{aligned} \tag{2.88}$$

where the dot product should be understood as the contraction of the second subindex of the two dyadic functions. The last line in this equation is obtained according to Eq. (2.84) where a_{out} corresponds to the distribution function at the environment temperature and ϵ_D is the "dielectric function" of the vacuum dust. The latter can be set to one only in the end as explained in the previous section: The integral over infinite space brings down a factor of $1/\operatorname{Im} \epsilon_D$ [67], while the integration over any finite region vanishes as we take the limit $\operatorname{Im} \epsilon_D \to 0$. Therefore we can choose the domain of integration over $\mathbf{z}$ such that $\xi_1(\mathbf{z}) > \xi_1(\mathbf{x}), \xi_1(\mathbf{y})$. This allows us to use the

[4]We choose an appropriate coordinate system where Maxwell equations are separable, and take ξ_1 to be constant on the object's surface.

partial wave expansion of the Green's function in Eq. (2.87) to find

$$\begin{aligned}
&\langle \mathbf{E}(\omega,\mathbf{x}) \otimes \mathbf{E}^*(\omega,\mathbf{y})\rangle_{\text{out-fluc}} = \\
&\frac{\omega^4}{4c^4}\, a_{\text{out}}(\omega) \sum_{\alpha,\beta} \left(\mathbf{E}^{\text{in}}_{\alpha}(\omega,\mathbf{x}) + S_\alpha(\omega)\mathbf{E}^{\text{out}}_{\alpha}(\omega,\mathbf{x})\right) \otimes \left(\mathbf{E}^{\text{in}*}_{\beta}(\omega,\mathbf{y}) + S^*_\beta \mathbf{E}^{\text{out}*}_{\beta}(\omega,\mathbf{y})\right) \times \\
&(\operatorname{Im}\epsilon_D) \int_{\text{out}} d\mathbf{z}\, \mathbf{E}^{\text{out}}_{\tilde{\alpha}}(\omega,\mathbf{z}) \cdot \mathbf{E}^{\text{out}*}_{\tilde{\beta}}(\omega,\mathbf{z}). \qquad (2.89)
\end{aligned}$$

Here and in subsequent parts, we frequently compute volume integrals similar to the last line of this equation, which can be cast as

$$\begin{aligned}
&(\operatorname{Im}\epsilon_D) \int_{\text{out}} d\mathbf{z}\, \mathbf{E}^{\text{out}}_{\tilde{\alpha}}(\omega,\mathbf{z}) \cdot \mathbf{E}^{\text{out}*}_{\tilde{\beta}}(\omega,\mathbf{z}) \\
=&\frac{1}{2i} \int_{\text{out}} d\mathbf{z} \left[\epsilon_D\, \mathbf{E}^{\text{out}}_{\tilde{\alpha}}(\omega,\mathbf{z}) \cdot \mathbf{E}^{\text{out}*}_{\tilde{\beta}}(\omega,\mathbf{z}) - \mathbf{E}^{\text{out}}_{\tilde{\alpha}}(\omega,\mathbf{z}) \cdot \epsilon^*_D\, \mathbf{E}^{\text{out}*}_{\tilde{\beta}}(\omega,\mathbf{z})\right] \\
=&\frac{c^2}{2i\omega^2} \int_{\text{out}} d\mathbf{z} \left[(\nabla \times \nabla \times \mathbf{E}^{\text{out}}_{\tilde{\alpha}}(\omega,\mathbf{z})) \cdot \mathbf{E}^{\text{out}*}_{\tilde{\beta}}(\omega,\mathbf{z}) - \mathbf{E}^{\text{out}}_{\tilde{\alpha}}(\omega,\mathbf{z}) \cdot \nabla \times \nabla \times \mathbf{E}^{\text{out}*}_{\tilde{\beta}}(\omega,\mathbf{z})\right],
\end{aligned}$$

where in the last line we have used the homogenous version of Eq. (2.83) with the RHS set to zero. The volume integration can be then recast as a surface integral with two boundaries, one at the infinity and another at a finite distance from the object. The infinitesimal imaginary part of the dielectric function guarantees that outgoing functions are exponentially decaying at large distances and thus the surface integral at infinity does not contribute. We then obtain

$$\begin{aligned}
&\operatorname{Im}\epsilon_D \int_{\text{out}} d\mathbf{z}\, \mathbf{E}^{\text{out}}_{\tilde{\alpha}}(\omega,\mathbf{z}) \cdot \mathbf{E}^{\text{out}*}_{\tilde{\beta}}(\omega,\mathbf{z}) \\
=&\frac{ic^2}{2\omega^2} \oint d\mathbf{\Sigma} \cdot \left[(\nabla \times \mathbf{E}^{\text{out}}_{\tilde{\alpha}}(\omega,\mathbf{z})) \times \mathbf{E}^{\text{out}*}_{\tilde{\beta}}(\omega,\mathbf{z}) + \mathbf{E}^{\text{out}}_{\tilde{\alpha}}(\omega,\mathbf{z}) \times \nabla \times \mathbf{E}^{\text{out}*}_{\tilde{\beta}}(\omega,\mathbf{z})\right]. \qquad (2.90)
\end{aligned}$$

A vector form of the Green's theorem can be used to prove, consistent with our

normalization, that (see Appendix A)

$$\frac{i}{2}\oint d\boldsymbol{\Sigma}\cdot\Big[(\nabla\times\mathbf{E}_\alpha^{\text{out/in}}(\omega,\mathbf{z}))\times\mathbf{E}_\beta^{\text{out/in}*}(\omega,\mathbf{z})+\mathbf{E}_\alpha^{\text{out/in}}(\omega,\mathbf{z})\times\nabla\times\mathbf{E}_\beta^{\text{out/in}*}(\omega,\mathbf{z})\Big]$$
$$=\pm\delta_{\alpha\beta}\,, \tag{2.91}$$
$$\oint d\boldsymbol{\Sigma}\cdot\Big[(\nabla\times\mathbf{E}_\alpha^{\text{out/in}}(\omega,\mathbf{z}))\times\mathbf{E}_\beta^{\text{in/out}*}(\omega,\mathbf{z})+\mathbf{E}_\alpha^{\text{out/in}}(\omega,\mathbf{z})\times\nabla\times\mathbf{E}_\beta^{\text{in/out}*}(\omega,\mathbf{z})\Big]$$
$$=0. \tag{2.92}$$

Therefore, the correlation function of the EM fields takes the form

$$\langle\mathbf{E}(\omega,\mathbf{x})\otimes\mathbf{E}^*(\omega,\mathbf{y})\rangle_{\text{out-fluc}}=a_{\text{out}}(\omega)\frac{\omega^2}{4c^2}\sum_\alpha\left(\mathbf{E}_\alpha^{\text{in}}(\omega,\mathbf{x})+S_\alpha(\omega)\mathbf{E}_\alpha^{\text{out}}(\omega,\mathbf{x})\right)\otimes$$
$$\left(\mathbf{E}_\alpha^{\text{in}*}(\omega,\mathbf{y})+S_\alpha^*(\omega)\mathbf{E}_\alpha^{\text{out}*}(\omega,\mathbf{y})\right). \tag{2.93}$$

The radiation due to the outside fluctuations can be computed by integrating over the Poynting vector, $\mathbf{S}=c\,\mathbf{E}\times\mathbf{B}$, of the corresponding correlation function,

$$\begin{aligned}\mathcal{P}_{\text{out-fluc}}&=\int_0^\infty\frac{d\omega}{2\pi}\oint d\boldsymbol{\Sigma}\cdot\frac{ic^2}{\omega}\langle(\nabla\times\mathbf{E})\times\mathbf{E}^*+\mathbf{E}\times\nabla\times\mathbf{E}^*\rangle_{\text{out-fluc}}\\&=\int_0^\infty\frac{d\omega}{2\pi}\sum_\alpha(-1+|S_\alpha(\omega)|^2)\,a_{\text{out}}(\omega)\frac{i\omega}{4}\times\\&\qquad\oint d\boldsymbol{\Sigma}\cdot\left[(\nabla\times\mathbf{E}_\alpha^{\text{out}})\times\mathbf{E}_\alpha^{\text{out}*}+\mathbf{E}_\alpha^{\text{out}}\times\nabla\times\mathbf{E}_\alpha^{\text{out}*}\right]\\&=\frac{1}{4\pi}\int_0^\infty d\omega\,\omega\,a_{\text{out}}(\omega)\sum_\alpha(-1+|S_\alpha(\omega)|^2),\end{aligned} \tag{2.94}$$

where we used Eqs. (2.91) and (2.92) .

The field correlation function induced by the inside fluctuations can be computed similarly. In this case, however, we need the Green's function with one point inside the object. Following an argument similar to the scalar case, we note that as the two points do not coincide, the Green's function satisfies a *homogeneous* equation inside with respect to the *smaller* coordinate while it satisfies the free EM equation outside the object in the *larger* coordinate. Hence, we can expand the Green's function as

(with $\xi_1(\mathbf{z}) < \xi_1(\mathbf{x})$)

$$\mathbb{G}(\omega, \mathbf{x}, \mathbf{z}) = \frac{i}{2} \sum_{\alpha} \left(A\, \mathbf{E}^{\text{out}}_{\tilde{\alpha}}(\omega, \mathbf{x}) + B\, \mathbf{E}^{\text{in}}_{\tilde{\alpha}}(\omega, \mathbf{x}) \right) \otimes \mathbf{F}_{\alpha}(\omega, \mathbf{z}), \tag{2.95}$$

where the prefactor $i/2$ is chosen for convenience, A and B are constants to be determined, and $\mathbf{F}_{\alpha}$ is defined as a solution to the EM equation inside the object

$$\left(\nabla \times \nabla \times - \frac{\omega^2}{c^2} \epsilon(\omega, \mathbf{x}) \mathbb{I} \right) \mathbf{F}_{\alpha}(\omega, \mathbf{x}) = 0. \tag{2.96}$$

We can determine the coefficients A and B and the normalization of $\mathbf{F}$ by matching the Green's functions approaching a point on the boundary from inside and outside the object

$$\mathbb{G}(\omega, \mathbf{x}, \mathbf{y})|_{\mathbf{y} \to \Sigma^-} = \mathbb{G}(\omega, \mathbf{x}, \mathbf{y})|_{\mathbf{y} \to \Sigma^+}, \quad \xi_1(\mathbf{x}) > \xi_1(\mathbf{y}), \tag{2.97}$$

where Σ represents the boundary. Comparing the two Green's functions given by Eqs. (2.87) and (2.95), we find ($A = 1, B = 0$)

$$\mathbb{G}(\omega, \mathbf{x}, \mathbf{z}) = \frac{i}{2} \sum_{\alpha} \mathbf{E}^{\text{out}}_{\tilde{\alpha}}(\omega, \mathbf{x}) \otimes \mathbf{F}_{\alpha}(\omega, \mathbf{z}), \tag{2.98}$$

where $\mathbf{F}$ is normalized by the continuity of the Green's function which requires parallel components of electric and magnetic (the latter because $\mu = 1$) fields to match at the boundary

$$\begin{aligned} \mathbf{F}_{\alpha}(\omega, \mathbf{z})_{\parallel} &= \left(\mathbf{E}^{\text{in}}_{\alpha}(\omega, \mathbf{z}) + S_{\alpha}(\omega) \mathbf{E}^{\text{out}}_{\alpha}(\omega, \mathbf{z}) \right)_{\parallel}, \\ \left(\nabla \times \mathbf{F}_{\alpha}(\omega, \mathbf{z}) \right)_{\parallel} &= \left(\nabla \times \mathbf{E}^{\text{in}}_{\alpha}(\omega, \mathbf{z}) + S_{\alpha}(\omega) \nabla \times \mathbf{E}^{\text{out}}_{\alpha}(\omega, \mathbf{z}) \right)_{\parallel}. \end{aligned} \tag{2.99}$$

The correlation function due to the inside fluctuations is then given by

$$\begin{aligned} &\langle \mathbf{E}(\omega, \mathbf{x}) \otimes \mathbf{E}^*(\omega, \mathbf{y}) \rangle_{\text{in-fluc}} \\ =& a_{\text{in}}(\omega) \frac{\omega^4}{4c^4} \sum_{\alpha, \beta} \mathbf{E}^{\text{out}}_{\tilde{\alpha}}(\omega, \mathbf{x}) \otimes \mathbf{E}^{\text{out}*}_{\tilde{\beta}}(\omega, \mathbf{y}) \int_{\text{in}} d\mathbf{z}\, \mathbf{F}_{\alpha}(\mathbf{z}) \cdot \text{Im}\, \epsilon(\omega, \mathbf{z})\, \mathbf{F}^*_{\beta}(\mathbf{z}), \end{aligned} \tag{2.100}$$

where a is the distribution function defined at the object's temperature. Again exploiting the wave equation for $\mathbf{F}$, the volume integral can be cast as a surface term

$$\begin{aligned}&\int_{\text{in}} d\mathbf{z}\, \mathbf{F}_\alpha(\mathbf{z}) \cdot \text{Im}\, \epsilon(\omega, \mathbf{z})\, \mathbf{F}^*_\beta(\omega, \mathbf{z}) \\ =&\frac{c^2}{2i\omega^2} \oint d\boldsymbol{\Sigma} \cdot \left[(\nabla \times \mathbf{F}_\alpha(\omega, \mathbf{z})) \times \mathbf{F}^*_\beta(\omega, \mathbf{z}) + \mathbf{F}_\alpha(\omega, \mathbf{z}) \times \nabla \times \mathbf{F}^*_\beta(\omega, \mathbf{z}) \right]. \end{aligned} \tag{2.101}$$

The continuity equations can be used to evaluate the surface integral

$$\int_{\text{in}} d\mathbf{z}\, \mathbf{F}_\alpha(\omega, \mathbf{z}) \cdot \text{Im}\, \epsilon(\omega, \mathbf{z})\, \mathbf{F}^*_\beta(\omega, \mathbf{z}) = \frac{c^2}{\omega^2} \delta_{\alpha\beta} \left(1 - |S_\alpha(\omega)|^2 \right). \tag{2.102}$$

The field correlation function then becomes[5]

$$\langle \mathbf{E}(\omega, \mathbf{x}) \otimes \mathbf{E}^*(\omega, \mathbf{y}) \rangle_{\text{in-fluc}} = a_{\text{in}}(\omega) \frac{\omega^2}{4c^2} \sum_\alpha \left(1 - |S_\alpha(\omega)|^2 \right) \mathbf{E}^{\text{out}}_\alpha(\omega, \mathbf{x}) \otimes \mathbf{E}^{\text{out}*}_\alpha(\omega, \mathbf{y}). \tag{2.103}$$

The radiation power due to the inside fluctuations can be computed from the corresponding correlation function as

$$\mathcal{P}_{\text{in-fluc}} = \frac{1}{4\pi} \int_0^\infty d\omega\, \omega\, a_{\text{in}}(\omega) \sum_\alpha (1 - |S_\alpha(\omega)|^2). \tag{2.104}$$

The total radiation per unit time is given by

$$\begin{aligned}\mathcal{P} &= \frac{1}{4\pi} \int_0^\infty d\omega\, \omega\, \left(a_{\text{in}}(\omega) - a_{\text{out}}(\omega) \right) \sum_\alpha \left(1 - |S_\alpha(\omega)|^2 \right) \\ &= \int_0^\infty \frac{d\omega}{2\pi} \hbar\omega\, \left(n(\omega, T) - n(\omega, T_0) \right) \sum_\alpha \left(1 - |S_\alpha(\omega)|^2 \right), \end{aligned} \tag{2.105}$$

where in the last line the radiation is expressed in terms of the Bose-Einstein distribution function. In brief, we have derived the Kirchhoff's law in the context of electrodynamics [66, 67], and the partial waves also include electromagnetic polarizations. Notice that Eq. (2.105) is independent of the coordinate system and the shape

[5]We have changed $\alpha \to \bar{\alpha}$; note that $|S_{\bar{\alpha}}| = |S_\alpha|$ due to time reversal symmetry.

of the object. In a general basis that the scattering matrix is not diagonal, the sum over α is replaced by a double sum over incoming and outgoing modes as

$$\begin{aligned}&\sum_{\alpha,\beta}\left(\delta_{\beta\alpha}-|S_{\beta\alpha}(\omega)|^2\right)\\&=\mathrm{Tr}\left(\mathbb{I}-\mathbb{S}^\dagger(\omega)\mathbb{S}(\omega)\right),\end{aligned}\tag{2.106}$$

which is cast as a manifestly invariant (trace) formula in the last line.

2.2.2 Moving objects

For bodies in uniform motion, the equations in the previous (sub)section are applied in the rest frame of the object and then transformed to describe the EM-field fluctuations in the appropriate laboratory frame. With all contributions of the field correlation functions in a single frame, one can then compute various physical quantities of interest, such as forces, or energy transfer from one object to another, or to the vacuum. For nonuniform motion, we assume that the same equations apply locally to the instantaneous rest frame of the body [80]. This assumption should be valid as long as the rate of acceleration is less than typical internal frequencies characterizing the object, which are normally quite large. The EM wave equation for a moving medium can be inferred from a Lagrangian. A dielectric object is described by

$$\mathcal{L}=\frac{1}{2}\epsilon'\,\mathbf{E}'^2-\frac{1}{2}\mathbf{B}'^2,\tag{2.107}$$

where $\mathbf{E}'$ and $\mathbf{B}'$ are the EM fields in the comoving frame related to the EM fields in the lab frame as

$$\mathbf{E}'=\mathbf{E}+\frac{\mathbf{v}}{c}\times\mathbf{B},\quad \mathbf{B}'=\mathbf{B}-\frac{\mathbf{v}}{c}\times\mathbf{E},\tag{2.108}$$

to the lowest order in velocity. Note that $\epsilon'=\epsilon(\omega',\mathbf{x}')$ is the dielectric function defined in the moving frame similarly defined in Sec. 2.1. The Lagrangian can be cast as

$$\mathcal{L}=\mathcal{L}_0+\frac{1}{2}(\epsilon'-1)\,\mathbf{E}'^2,$$

where $\mathcal{L}_0 = \frac{1}{2}\mathbf{E}'^2 - \frac{1}{2}\mathbf{B}'^2$ is the free Lagrangian. Notice that $\mathcal{L}_0$ is invariant under the transformation in Eq. (2.108) to the first order in v/c, *i.e.* $\mathcal{L}_0 = \frac{1}{2}\mathbf{E}^2 - \frac{1}{2}\mathbf{B}^2 + \mathcal{O}(v^2/c^2)$, while the second term is related to the EM field in the lab frame by Eq. (2.108). The modified Maxwell equations are then obtained from the Lagrangian as

$$\left[\nabla \times \nabla \times -\frac{\omega^2}{c^2}\mathbb{I} - \frac{\omega^2}{c^2}\tilde{\mathbb{D}}(\epsilon' - 1)\mathbb{D}\right]\mathbf{E} = 0, \tag{2.109}$$

where

$$\mathbb{D} = \mathbb{I} + \frac{1}{i\omega}\mathbf{v} \times \nabla \times, \quad \tilde{\mathbb{D}} = \mathbb{I} + \frac{1}{i\omega}\nabla \times \mathbf{v} \times . \tag{2.110}$$

The coupling with the (fluctuating) currents can be formulated by adding to the Lagrangian

$$\Delta\mathcal{L} = \mathbf{K}' \cdot \mathbf{E}', \tag{2.111}$$

where $\mathbf{K}'$ is defined in the moving frame. This equation follows from the assumption that a local current density is coupled to the electric field in the instantaneous rest frame of the corresponding point in the moving object; see the discussion in Sec. 2.1.2. The inhomogeneous EM equation in the presence of random currents follows from the Lagrangian as

$$\left[\nabla \times \nabla \times -\frac{\omega^2}{c^2}\mathbb{I} - \frac{\omega^2}{c^2}\tilde{\mathbb{D}}(\epsilon' - 1)\mathbb{D}\right]\mathbf{E} = \frac{\omega^2}{c^2}\tilde{\mathbb{D}}\mathbf{K}'. \tag{2.112}$$

Again we should compute field correlation functions due to the outside and inside current fluctuations separately. The former can be easily deduced from Eq. (2.93) simply by inserting the scattering matrix for a rotating object,

$$\begin{aligned}\langle \mathbf{E}(\omega, \mathbf{x}) \otimes \mathbf{E}^*(\omega, \mathbf{y})\rangle_{\text{out-fluc}} =& a_{\text{out}}(\omega)\frac{\omega^2}{4c^2}\sum_{\alpha_m}\left(\mathbf{E}^{\text{in}}_{\alpha_m}(\omega, \mathbf{x}) + S_{\alpha_m}\mathbf{E}^{\text{out}}_{\alpha_m}(\omega, \mathbf{x})\right) \otimes \\ & \left(\mathbf{E}^{\text{in}*}_{\alpha_m}(\omega, \mathbf{y}) + S^*_{\alpha_m}\mathbf{E}^{\text{out}*}_{\alpha_m}(\omega, \mathbf{y})\right), \end{aligned} \tag{2.113}$$

where the partial-wave index α_m includes m, the eigenvalue of the angular momentum along the z-direction (in units of $\hbar$).

The inside fluctuations, on the other hand, are defined with respect to the rest frame of the object,

$$\langle \mathbf{K}'(\omega', \mathbf{x}') \otimes \mathbf{K}'^{*}(\omega', \mathbf{y}') \rangle = a_{\text{in}}(\omega') \operatorname{Im} \epsilon(\omega', \mathbf{x}') \delta(\mathbf{x}' - \mathbf{y}') \mathbb{I}. \tag{2.114}$$

Consider $\mathbf{K}'_{\omega' m'}(t', \mathbf{x}')$, a fluctuation of the current characterized by the angular momentum m' and frequency ω' in the rotating frame. For the sake of convenience, we define $\mathbf{K}(t, \mathbf{x}) \equiv \mathbf{K}'(t', \mathbf{x}')$ which captures current fluctuations in the lab-frame coordinates. Note that the two sets of reference frame are related by Eq. (2.34) and supplemented by $z = z'$ along the symmetry axis of the object. One can then see that the partial wave m is invariant with respect to the reference frame while the frequency is shifted as

$$\omega' = \omega - \Omega m.$$

This modifies the spectral density of source fluctuations simply by replacing the frequency in ϵ and a by $\omega - \Omega m$. Therefore, the inside source fluctuations from the point of view of the lab–frame observer are given by

$$\langle \mathbf{K}_m(\omega, \mathbf{x}) \otimes \mathbf{K}^*_m(\omega, \mathbf{y}) \rangle = a_T(\omega - \Omega m) \operatorname{Im} \epsilon(\omega - \Omega m, r, z) \frac{\delta(r_{\mathbf{x}} - r_{\mathbf{y}}) \delta(z_{\mathbf{x}} - z_{\mathbf{y}})}{2\pi r} \mathbb{I}. \tag{2.115}$$

Henceforth, we shall use the same notation $\mathbb{G}$ for the Green's function in the presence of a moving object corresponding to Eq. (2.109). The EM field correlation function is given by

$$\langle \mathbf{E}(\omega, \mathbf{x}) \otimes \mathbf{E}^*(\omega, \mathbf{y}) \rangle_{\text{in-fluc}} = \frac{\omega^4}{c^4} \int_{\text{in}} d\mathbf{z} \, \langle \mathbb{G}(\omega, \mathbf{x}, \mathbf{z}) \tilde{\mathbb{D}} \mathbf{K}(\omega, \mathbf{z}) \cdot \mathbb{G}^*(\omega, \mathbf{y}, \mathbf{z}) \tilde{\mathbb{D}}^* \mathbf{K}^*(\omega, \mathbf{z}) \rangle. \tag{2.116}$$

We can expand the Green's function similar to the previous section as

$$\mathbb{G}(\omega, \mathbf{x}, \mathbf{z}) = \frac{i}{2} \sum_{\alpha_m} \mathbf{E}^{\text{out}}_{\bar{\alpha}_m}(\omega, \mathbf{x}) \otimes \mathbf{F}_{\alpha_m}(\omega, \mathbf{z}), \tag{2.117}$$

where $\mathbf{F}$ is a solution to the *modified* EM equation inside the dielectric object

$$\left[\nabla\times\nabla\times-\frac{\omega^2}{c^2}\mathbb{I}-\frac{\omega^2}{c^2}\tilde{\mathbb{D}}(\epsilon'-1)\mathbb{D}\right]\mathbf{F}=0, \tag{2.118}$$

and satisfies boundary conditions similar to Eq. (2.99), albeit with the scattering matrices for a rotating object[6]

$$\begin{aligned}\mathbf{F}_{\alpha_m}(\omega,\mathbf{z})_\parallel&=\left(\mathbf{E}^{\text{in}}_{\alpha_m}(\omega,\mathbf{z})+S_{\bar{\alpha}_m}\mathbf{E}^{\text{out}}_{\alpha_m}(\omega,\mathbf{z})\right)_\parallel,\\(\nabla\times\mathbf{F}_{\alpha_m}(\omega,\mathbf{z}))_\parallel&=\left(\nabla\times\mathbf{E}^{\text{in}}_{\alpha_m}(\omega,\mathbf{z})+S_{\bar{\alpha}_m}\nabla\times\mathbf{E}^{\text{out}}_{\alpha_m}(\omega,\mathbf{z})\right)_\parallel.\end{aligned} \tag{2.119}$$

The correlation function of the EM fields is then given by

$$\begin{aligned}\langle\mathbf{E}(\omega,\mathbf{x})\otimes\mathbf{E}^*(\omega,\mathbf{y})\rangle_{\text{in-fluc}}=&\frac{\omega^4}{4c^4}\sum_{\alpha_m,\beta_m}a_{\text{in}}(\omega-\Omega m)\,\mathbf{E}^{\text{out}}_{\bar{\alpha}_m}(\omega,\mathbf{x})\otimes\mathbf{E}^{\text{out}*}_{\bar{\beta}_m}(\omega,\mathbf{y})\times\\&\int_{\text{in}}d\mathbf{z}\,\mathbb{D}\,\mathbf{F}_{\alpha_m}(\omega,\mathbf{z})\cdot\,\text{Im}\,\epsilon(\omega-\Omega m,\mathbf{z})\,\mathbb{D}^*\mathbf{F}^*_{\beta_m}(\omega,\mathbf{z}).\end{aligned} \tag{2.120}$$

The volume integral can be computed similar to that of the previous subsection. We write the second line of the last equation as

$$\begin{aligned}&\frac{1}{2i}\int_{\text{in}}d\mathbf{z}\left[(\epsilon'-1)\mathbb{D}\,\mathbf{F}_{\alpha_m}(\omega,\mathbf{z})\cdot\mathbb{D}^*\mathbf{F}^*_{\beta_m}(\omega,\mathbf{z})-\mathbb{D}\,\mathbf{F}_{\alpha_m}(\omega,\mathbf{z})\cdot(\epsilon'^*-1)\,\mathbb{D}^*\mathbf{F}^*_{\beta_m}(\omega,\mathbf{z})\right]\\=&\frac{1}{2i}\int_{\text{in}}d\mathbf{z}\left[\left(\tilde{\mathbb{D}}(\epsilon'-1)\mathbb{D}\,\mathbf{F}_{\alpha_m}(\omega,\mathbf{z})\right)\cdot\mathbf{F}^*_{\beta_m}(\omega,\mathbf{z})-\mathbf{F}_{\alpha_m}(\omega,\mathbf{z})\cdot\tilde{\mathbb{D}}^*(\epsilon'^*-1)\,\mathbb{D}^*\mathbf{F}^*_{\beta_m}(\omega,\mathbf{z})\right]\\=&\frac{c^2}{2i\omega^2}\int_{\text{in}}d\mathbf{z}\left[(\nabla\times\nabla\times\mathbf{F}_{\alpha_m}(\omega,\mathbf{z}))\cdot\mathbf{F}^*_{\beta_m}(\omega,\mathbf{z})-\mathbf{F}_{\alpha_m}(\omega,\mathbf{z})\cdot\nabla\times\nabla\times\mathbf{F}^*_{\beta_m}(\omega,\mathbf{z})\right]\\=&\frac{c^2}{2i\omega^2}\oint d\boldsymbol{\Sigma}\cdot\left[(\nabla\times\mathbf{F}_{\alpha_m}(\omega,\mathbf{z}))\times\mathbf{F}^*_{\beta_m}(\omega,\mathbf{z})+\mathbf{F}_{\alpha_m}(\omega,\mathbf{z})\times\nabla\times\mathbf{F}^*_{\beta_m}(\omega,\mathbf{z})\right],\end{aligned} \tag{2.121}$$

[6]Note that the scattering matrix is given for $\bar{\alpha}$. This is because the Green's function in the presence of a moving object is no longer symmetric with respect to its spatial arguments but satisfies a rather different symmetry; see the discussion in Sec. 2.1.2. If Eq. (2.87) defines the Green's function with $\xi_1(\mathbf{x})<\xi_1(\mathbf{z})$, then

$$\mathbb{G}(\omega,\mathbf{z},\mathbf{x})=\frac{i}{2}\sum_\alpha\mathbf{E}^{\text{out}}_{\bar{\alpha}}(\omega,\mathbf{z})\otimes\left(\mathbf{E}^{\text{in}}_{\alpha}(\omega,\mathbf{x})+S_{\bar{\alpha}}\mathbf{E}^{\text{out}}_{\alpha}(\omega,\mathbf{x})\right).$$

where in the step from the second to the third line, we have used Eq. (2.109). Using the continuity relations, the last line gives

$$\int_{\text{in}} d\mathbf{z}\, \mathbb{D}\, \mathbf{F}_{\alpha_m}(\omega, \mathbf{z}) \cdot \text{Im}\, \epsilon(\omega - \Omega m, \mathbf{z})\, \mathbb{D}^* \mathbf{F}^*_{\beta_m}(\omega, \mathbf{z}) = \frac{c^2}{\omega^2} \delta_{\alpha_m \beta_m} \left(1 - |S_{\bar{\alpha}_m}|^2\right), \quad (2.122)$$

which is the analog of Eq. (2.102) for moving objects. The EM field correlation function corresponding to the inside fluctuations is then obtained as

$$\langle \mathbf{E}(\omega, \mathbf{x}) \otimes \mathbf{E}^*(\omega, \mathbf{y}) \rangle_{\text{in-fluc}} = \frac{\omega^2}{4c^2} \sum_{\alpha_m} a_{\text{in}}(\omega - \Omega m) \left(1 - |S_{\alpha_m}|^2\right) \mathbf{E}^{\text{out}}_{\alpha_m}(\omega, \mathbf{x}) \otimes \mathbf{E}^{\text{out}*}_{\alpha_m}(\omega, \mathbf{y}), \quad (2.123)$$

The total radiation per unit time can be obtained by integrating over the Poynting vector as

$$\begin{aligned} \mathcal{P} &= \frac{1}{4\pi} \int_0^\infty d\omega\, \omega \sum_{\alpha_m} \left(a_{\text{in}}(\omega - \Omega m) - a_{\text{out}}(\omega)\right) \left(1 - |S_{\alpha_m}(\omega)|^2\right) \\ &= \int_0^\infty \frac{d\omega}{2\pi} \hbar\omega \sum_{\alpha_m} \left(n(\omega - \Omega m, T) - n(\omega, T_0)\right) \left(1 - |S_{\alpha_m}(\omega)|^2\right). \end{aligned} \quad (2.124)$$

At zero temperature everywhere, $n(\omega - \Omega m, 0) - n(\omega, 0) = -\Theta(\Omega m - \omega)$, and the quantum radiation happens in the superradiating regime; see the discussion in Sec. 2.1.2. Again we note that our derivation leading to Eq. (2.124) is not specific to a coordinate system and shape as long as the object is a solid of revolution with the angular momentum m being a good quantum number. In a general basis where the scattering matrix is not diagonal (except in m), we have

$$\begin{aligned} \mathcal{P} &= \int_0^\infty \frac{d\omega}{2\pi} \hbar\omega \sum_{\alpha_m, \beta_m} \left(n(\omega - \Omega m, T) - n(\omega, T_0)\right) \left(\delta_{\beta_m \alpha_m} - |S_{\beta_m \alpha_m}(\omega)|^2\right) \\ &= \int_0^\infty \frac{d\omega}{2\pi} \hbar\omega\, \text{Tr} \left[\left(n(\omega - \Omega \hat{l}_z, T) - n(\omega, T_0) \right) \left(\mathbb{I} - \mathbb{S}^\dagger(\omega) \mathbb{S}(\omega) \right) \right], \end{aligned} \quad (2.125)$$

where $\hat{l}_z$ is the angular momentum operator. This equation casts the quantum (and thermal) radiation from a rotating object into a Trace formula applicable to any shape

with rotational symmetry.

Vacuum friction on a rotating object

For a rotating object, we have to solve a complicated equation, Eq. (2.118), but in the lowest order we can neglect the explicit dependence on velocity and set $\mathbb{D} \approx \tilde{\mathbb{D}} \approx \mathbb{I}$, changing the argument of the dielectric function as $\epsilon(\omega) \to \epsilon(\omega - \Omega m)$. Finally, at zero temperature, only frequencies within the range $[0, \Omega]$ contribute.

Sphere— EM Scattering from a sphere is most conveniently described in a basis (l, m, P) where l corresponds to the total angular momentum, m is the angular momentum along the z axis, and P is the polarization. In the approximations made here, the lowest partial wave, $l = 1$, gives the leading order, while larger ls are suppressed by higher powers of the (linear) velocity divided by the speed of light. We assume a non-magnetic object, thus the electric polarization gives the leading contribution to scattering matrix as

$$S_{1mE}(\omega) = 1 + i\frac{4\omega^3}{3c^3}\,\alpha(\omega - \Omega m), \tag{2.126}$$

where $\alpha(\omega)$ is the polarizability of a small spherical object depending solely on the dielectric function $\epsilon(\omega)$. Note that, at zero temperature, only $m = 1$ (and not $m = 0, -1$) contributes to the radiation. The rate of energy radiation to the vacuum is obtained as

$$\begin{aligned}\mathcal{P} &\approx \int_0^\Omega \frac{d\omega}{2\pi}\,\hbar\omega\left(|S_{11E}|^2 - 1\right) \\ &\approx \frac{4\hbar}{3\pi c^3}\int_0^\Omega d\omega\,\omega^4\,\left(-\operatorname{Im}\alpha(\omega - \Omega)\right),\end{aligned} \tag{2.127}$$

where we have kept only the leading term in powers of frequency. For a dielectric sphere of radius R, the polarizability is $\alpha(\omega) = R^3(\epsilon(\omega) - 1)/(\epsilon(\omega) + 2)$; the radiation is then given by [56, 57]

$$\mathcal{P} \approx \frac{4\hbar R^3}{3\pi c^3}\int_0^\Omega d\omega\,\omega^4\left|\operatorname{Im}\frac{\epsilon(\omega - \Omega) - 1}{\epsilon(\omega - \Omega) + 2}\right|. \tag{2.128}$$

Cylinder— For a cylinder, the scattering matrices are more complicated due to mixing between the two polarizations. A complete basis for cylindrical waves is (m, k_z, P) with k_z being the wavevector parallel to the z axis. In the limit of a thin cylinder where $\Omega R/c, \epsilon\Omega R/c \ll 1$, the first partial wave, $m = 1$, gives the leading contribution while k_z should be integrated over all propagating waves. The corresponding scattering matrices are

$$\begin{aligned} S_{1k_zMM}(\omega) &= 1 + \frac{i\pi}{2}\frac{\epsilon(\omega-\Omega)-1}{\epsilon(\omega-\Omega)+1}\frac{\omega^2}{c^2}R^2, \\ S_{1k_zEE}(\omega) &= 1 + \frac{i\pi}{2}\frac{\epsilon(\omega-\Omega)-1}{\epsilon(\omega-\Omega)+1}k_z^2R^2, \\ S_{1k_zEM}(\omega) = S_{1k_zME}(\omega) &= \frac{i\pi}{2}\frac{\epsilon(\omega-\Omega)-1}{\epsilon(\omega-\Omega)+1}\frac{\omega k_z}{c}R^2, \end{aligned} \tag{2.129}$$

where the argument of the dielectric function is $\omega - \Omega$ corresponding to $m = 1$. The energy radiation per unit time is obtained as [65]

$$\begin{aligned} \mathcal{P} &\approx \int_0^\Omega \frac{d\omega}{2\pi}\hbar\omega \int_{-\omega/c}^{\omega/c}\frac{Ldk_z}{2\pi}\sum_{P,P'\in\{M,E\}}\left[|S_{1k_zPP'}(\omega)|^2 - \delta_{PP'}\right] \\ &\approx \frac{2\hbar LR^2}{3\pi c^3}\int_0^\Omega d\omega\,\omega^4\left|\operatorname{Im}\frac{\epsilon(\omega-\Omega)-1}{\epsilon(\omega-\Omega)+1}\right|, \end{aligned} \tag{2.130}$$

where we have neglected terms of the order of R^4. If the cylinder has a small conductivity described by the dielectric function $\epsilon = 1 + i4\pi\sigma/\omega$ with $\sigma \ll \Omega$, Eq. (2.130) yields

$$\mathcal{P} = \frac{8\hbar LR^2\Omega^4\sigma}{c^3}\log\frac{\Omega}{\sigma}, \tag{2.131}$$

in agreement with the results of Ref. [59].

To get an estimate for the magnitude of radiation effects, we consider a rapidly spinning nanotube of radius R and length L, and assume that $\Omega R/c$ is small. We then find that the rotation slows down by an order of magnitude over a time scale of $\tau \sim (I/\hbar)\,(c^3/LR^2\Omega^3)$. The moment of inertia of a nanotube can be as small as 10^{-33} in SI units [81] (compare with $\hbar \approx 10^{-34}$). So even at small velocities, τ can be of the order of a few hours.

2.2.3 A test object in the presence of a rotating body

In this section, we study the interaction of the radiation field from a rotating body with a test object at rest, and assume that both objects are dielectric spheres. The overall EM field correlation function is given by the sum of Eqs. (2.113) and (2.123) as

$$\langle \mathbf{E} \otimes \mathbf{E}^* \rangle = \langle \mathbf{E} \otimes \mathbf{E}^* \rangle_{\text{in-fluc}} + \langle \mathbf{E} \otimes \mathbf{E}^* \rangle_{\text{out-fluc}}. \tag{2.132}$$

In the following, we consider the limit of zero temperature both in the object and the environment. The generalization to finite temperature is straightforward. Similar to Sec. 2.1, the correlation function in Eq. (2.132) can be recast as

$$\langle \mathbf{E} \otimes \mathbf{E}^* \rangle = \langle \mathbf{E} \otimes \mathbf{E}^* \rangle_{\text{non-rad}} + \langle \mathbf{E} \otimes \mathbf{E}^* \rangle_{\text{rad}}\,, \tag{2.133}$$

where we have broken up the correlation function into radiative (due to propagating photons) and non-radiative (due to zero-point fluctuations) parts. The latter is given by

$$\langle \mathbf{E}(\omega, \mathbf{x}) \otimes \mathbf{E}^*(\omega, \mathbf{y}) \rangle_{\text{non-rad}} = \hbar\, \text{sgn}(\omega)\, \text{Im}\, \mathbb{G}(\omega, \mathbf{x}, \mathbf{y}), \tag{2.134}$$

where $\mathbb{G}$ is the Green's function in the presence of a rotating object. This equation is reminiscent of the FDT in equilibrium; the term in the RHS is purely real and thus does not contribute to the radiation, but leads to a Casimir-like force between the rotating body and nearby objects. The radiative term in the correlation function can be obtained from Eqs. (2.132) and (2.133) as

$$\langle \mathbf{E}(\omega, \mathbf{x}) \otimes \mathbf{E}^*(\omega, \mathbf{y}) \rangle_{\text{rad}} \approx \frac{\hbar\omega^2}{2c^2} \sum_{\alpha_m} \Theta(\Omega m - \omega) \left(|S_{\alpha_m}|^2 - 1 \right) \mathbf{E}^{\text{out}}_{\alpha_m}(\omega, \mathbf{x}) \otimes \mathbf{E}^{\text{out}*}_{\alpha_m}(\omega, \mathbf{y})\,, \tag{2.135}$$

and contributes to the Poynting vector in the superradiating regime $0 < \omega < \Omega m$.

To find the interaction with a *test* object, we only consider the radiative term in the correlation function for two reasons. First radiation pressure exerts a force falling

off more slowly with the separation distance compared to the non-radiative part. Furthermore, non-radiative fluctuations give rise to a potential energy depending only on the separation distance akin to the Casimir energy. The test object being spherical, the corresponding tangential force or torque due to the corresponding term in Eq. (2.133) is identical to zero.

The radiation from a (non-magnetic) rotating sphere is dominated by the lowest (electric) partial wave ($l = 1, m = 1, P = E$) in which case Eq. (2.135) yields

$$\langle \mathbf{E}(\omega, \mathbf{x}) \otimes \mathbf{E}^*(\omega, \mathbf{y}) \rangle_{\text{rad}} = \frac{\hbar \omega^2}{2c^2} \Theta(\Omega - \omega) \left(|S_{11E}|^2 - 1 \right) \mathbf{E}^{\text{out}}_{11E}(\omega, \mathbf{x}) \otimes \mathbf{E}^{\text{out}*}_{11E}(\omega, \mathbf{y}). \tag{2.136}$$

The partial waves in Eq. (2.135) are defined in spherical basis as

$$\begin{aligned} \mathbf{E}^{\text{out}}_{lmM}(\omega, \mathbf{x}) &= \frac{\sqrt{\omega/c}}{\sqrt{l(l+1)}} \nabla \times h_l^{(1)} \left(\frac{\omega r}{c} \right) Y_{lm}(\theta, \phi) \mathbf{x}, \\ \mathbf{E}^{\text{out}}_{lmE}(\omega, \mathbf{x}) &= -i \frac{\sqrt{c/\omega}}{\sqrt{l(l+1)}} \nabla \times \nabla \times h_l^{(1)} \left(\frac{\omega r}{c} \right) Y_{lm}(\theta, \phi) \mathbf{x}, \end{aligned} \tag{2.137}$$

where Y_{lm} is usual spherical harmonic function. The normalization is chosen to ensure the conditions in Eqs. (2.91) and (2.92).

In order to find the scattering from the second object, we expand the EM field around its origin located at a separation d on the x axis. To the lowest order in frequency, we have

$$\mathbf{E}^{\text{out}}_{11E}(\omega, \mathbf{x}) = \mathcal{U}_{11E,11E} \mathbf{E}^{\text{reg}}_{11E}(\omega, \tilde{\mathbf{x}}) + \mathcal{U}_{10M,11E} \mathbf{E}^{\text{reg}}_{10M}(\omega, \tilde{\mathbf{x}}) + \cdots, \tag{2.138}$$

where $\tilde{\mathbf{x}}$ is defined with respect to the new origin. The *regular* functions are defined by replacing the spherical Hankel function $h_l^{(1)}$ in Eq. (3.50) by the spherical Bessel function j_l. The *translation* matrices are given by [12]

$$\mathcal{U}_{11E,11E} = h_0^{(1)} \left(\frac{\omega d}{c} \right), \qquad \mathcal{U}_{10M,11E} = \frac{\sqrt{2} \omega d}{4c} h_0^{(1)} \left(\frac{\omega d}{c} \right). \tag{2.139}$$

Next we consider the scattering from the test object:

$$\mathbf{E}^{\rm reg}_{lmP}(\omega,\tilde{\mathbf{x}}) \quad \to \quad \frac{1}{2}\left(\mathbf{E}^{\rm in}_{lmP}(\omega,\tilde{\mathbf{x}}) + \mathfrak{S}_{lmP}\mathbf{E}^{\rm out}_{lmP}(\omega,\tilde{\mathbf{x}})\right), \tag{2.140}$$

where $\mathfrak{S}_{lmP}$ is the corresponding scattering matrix. We then find the EM field correlation function upon one scattering from the test object as

$$\begin{aligned}\langle \mathbf{E}(\omega,\tilde{\mathbf{x}}) \otimes \mathbf{E}^*(\omega,\tilde{\mathbf{y}})\rangle_{\rm rad} &= \frac{\hbar\omega^2}{8c^2}\,\Theta(\Omega-\omega)\left(|S_{11E}|^2-1\right)\times \\ &\left[\mathcal{U}_{11E,11E}\left(\mathbf{E}^{\rm in}_{11E}(\omega,\tilde{\mathbf{x}}) + \mathfrak{S}_{11E}\mathbf{E}^{\rm out}_{11E}(\omega,\tilde{\mathbf{x}})\right) + \mathcal{U}_{10M,11E}\left(\mathbf{E}^{\rm in}_{10M}(\omega,\tilde{\mathbf{x}}) + \mathfrak{S}_{10M}\mathbf{E}^{\rm out}_{10M}(\omega,\tilde{\mathbf{x}})\right)\right] \\ &\otimes \overline{\left[\mathcal{U}_{11E,11E}\left(\mathbf{E}^{\rm in}_{11E}(\omega,\tilde{\mathbf{y}}) + \mathfrak{S}_{11E}\mathbf{E}^{\rm out}_{11E}(\omega,\tilde{\mathbf{y}})\right) + \mathcal{U}_{10M,11E}\left(\mathbf{E}^{\rm in}_{10M}(\omega,\tilde{\mathbf{y}}) + \mathfrak{S}_{10M}\mathbf{E}^{\rm out}_{10M}(\omega,\tilde{\mathbf{y}})\right)\right]}.\end{aligned} \tag{2.141}$$

Having the correlation functions, we can compute physical quantities of interest. In computing the torque, the partial waves $(1,1,E)$ and $(1,0,M)$ decouple; however, the latter does not contribute since its angular momentum along the z axis is zero. We then find that the torque falls off as $1/d^2$ with the separation distance as

$$\begin{aligned} M &\sim \frac{\hbar}{8\pi}\int_0^\Omega d\omega\left(|S_{11E}|^2-1\right)|\mathcal{U}_{11E,11E}|^2\left(1-|\mathfrak{S}_{11E}|^2\right), \\ &= \frac{\hbar c^2}{8\pi d^2}\int_0^\Omega d\omega\,\frac{1}{\omega^2}(|S_{11E}|^2-1)(1-|\mathfrak{S}_{11E}|^2). \end{aligned} \tag{2.142}$$

Computing the force is more complicated since the two partial waves mix, and one has to find their overlap via the Maxwell stress tensor

$$T_{ij}(\omega) = E_i(\omega)E_j^*(\omega) + B_i(\omega)B_j^*(\omega) - \frac{1}{2}\left(\mathbf{E}^2+\mathbf{B}^2\right)\delta_{ij}. \tag{2.143}$$

The y-component of the force, perpendicular the x axis connecting the two objects, and the z axis along the rotation, is obtained as

$$F_y = \int\frac{d\omega}{2\pi}\int r^2 d\Omega_{\hat{r}}\,\langle T_{ij}\rangle\,\hat{r}_i\hat{y}_j, \tag{2.144}$$

with $\Omega_{\hat{r}}$ being the solid angle corresponding to the unit vector $\hat{r}$ from the origin of

the test object. A lengthy, though straightforward, calculation leads to

$$F_y = \frac{\hbar}{4\pi c^2}\int_0^\Omega d\omega\,\omega^2\left(|S_{11E}|^2-1\right)\mathcal{U}_{10M,11E}\mathcal{U}_{11E,11E}\,\mathcal{T}_{10M,11E}\,\mathrm{Re}\left(-1+\overline{\mathfrak{S}_{10M}}\mathfrak{S}_{11E}\right), \tag{2.145}$$

where $\mathcal{T}_{10M,11E}$ characterizes the stress tensor sandwiched between the two partial waves, whose dependence on frequency is given by

$$\mathcal{T}_{10M,11E} = -\frac{\pi c}{2\sqrt{2}\omega}. \tag{2.146}$$

For a non-magnetic object, we can safely assume $\mathfrak{S}_{10M} \approx 1$ since its frequency dependence can be neglected compared to $\mathfrak{S}_{11E}$, hence

$$F_y = \frac{\hbar}{32\pi d}\int_0^\Omega d\omega\left(|S_{11E}|^2-1\right)(1-\mathrm{Re}\,\mathfrak{S}_{11E}). \tag{2.147}$$

Notice that the force falls off as the inverse separation distance while the usual Casimir force decays much faster.

Chapter 3

A Scattering Approach to the Dynamical Casimir Effect

Quantum zero-point fluctuations manifest themselves in a variety of macroscopic effects. A prominent example is Casimir's demonstration that these fluctuations lead to attraction of two perfectly conducting parallel plates [1]. Experimental advances in precision measurements of the Casimir force [3, 4] have revived interest in finding frameworks where one can compute these forces both numerically [82, 83] and analytically. A particularly successful approach in applications to different geometries and material properties is based on scattering methods and techniques [8, 9, 10, 11, 12, 13, 14]. In this approach, the quantum-field-theoretic problem is reduced to that of finding the *classical* scattering matrix of each object.

Another manifestation of fluctuations appears in the so-called dynamical Casimir effect: when objects are set in motion, they interact with the fluctuations of the background vacuum in a time-dependent fashion which excites photons and emits radiation. In fact, accelerating boundaries radiate energy and thus experience friction. An early example of this phenomenon was discussed by Moore for a one dimensional cavity [18]. A relativistic analysis of an accelerating mirror in 1+1 dimension in Ref. [19] employs techniques from conformal field theory. A perturbative study of the latter confirmed and generalized its results to higher dimensions [35]. Among other methods, the fluctuation-dissipation theorem has been used to compute the

frictional force on a moving sphere in free space [22], a Hamiltonian formalism has been applied to the problem of photon production in cavities [23, 24], and a (Euclidean) path-integral formulation is introduced to study the "vacuum" friction for a rough plate moving laterally [41]. We specially note that an input-output formalism relating the incoming and outgoing operators is used to compute, among other things, the frequency and angular spectrum of radiated photons [42]. While a substantial literature is devoted to objects with perfect boundary conditions, dielectric and dispersive materials have also been studied in some cases [49]. In fact, dispersive objects exhibit similar effects even when they move at a constant velocity. For example, two parallel plates moving laterally with respect to each other experience a (non-contact) frictional force [52, 53]. Even a single object experiences friction if put in constant rotation [56, 65], a phenomenon most intimately related to *superradiance* first discovered by Zel'dovich [58]. (Translational motion of a single object is trivial due to the Lorentz symmetry.) The latter examples, consisting of dispersive objects moving at a constant rate, are usually treated within the framework of the fluctuation-dissipation theorem or the closely related Rytov formalism [55].

Inspection of the literature on the dynamical Casimir effect leads to the following observations: There are a plethora of interesting—sometimes counter-intuitive—phenomena emerging from the motion of a body in an ambient quantum field [33, 34]. These phenomena span a number of subfields in physics, and have been treated by a variety of different formalisms. Even the simplest examples appear to require rather complex computations. Only recently experimental realizations—using a SQUID to mimic the moving boundary of a cavity (transmission line) [31, 32]—have made precise measurements possible, raising the hope for an explosion of activity similar to the post-precision experiment era of static Casimir forces. This motivates reexamination of theoretical literature on the subject, aiming for a simple and unifying framework for analysis.

In this work, we follow two goals. First, inspired by the success of the scattering-theory methods in (static) Casimir forces, we attempt at extending these techniques to dynamical Casimir problems. We find that the *classical* scattering matrix is naturally

incorporated into the formalism. However, dynamical configurations provide new channels where the incoming frequency jumps to different values, hence the scattering matrix should be defined accordingly. Second, we aim for a universal framework which brings the diverse set of problems in dynamical Casimir under the same rubric. Most notably, we treat accelerating boundaries, modulated optical setups and moving dispersive objects—usually tackled with different techniques, as explained above—on the same footing.

In this paper, computations are performed for a scalar field theory. The generalization to electromagnetism is straightforward in principle, while practical computations are more complicated in the latter. We find scalar field theory convenient to set the framework for more realistic applications.

The paper is organized as follows: In Sec. 3.1, starting from a second-quantized formalism, we derive general formulas for the energy radiation due to the dynamical Casimir effect. In Sec. 3.2, we consider lossless objects undergoing non-uniform motion or optical modulation, and provide a variety of examples to showcase the power of the scattering approach. Specifically, we find that an (asymmetric) spinning object slows down, and further contrast linear and angular motion. In Sec. 3.3, we consider dispersive objects moving at a constant rate. We also generalize to the case of multiple objects in relative motion where we study, among other things, an "atom" moving parallel to a dispersive surface.

3.1 Formalism

We start with input-output relations as described in Ref. [66]. The underlying formalism has been developed to quantize the electromagnetic field in a lossy or amplifying medium [76, 77, 78]. (A similar method is also used to study the dynamical Casimir effect; see, for example, Refs. [43, 42]. However the more general formalism in Ref. [66] allows further extensions specially to dispersive objects.) Within this formalism the operators $\hat{a}^{\text{in}}$ and $\hat{a}^{\text{out}}$ represent annihilation operators of the incoming or outgoing waves, respectively, in the vacuum (outside the object). These operators are then

related by [66]

$$\hat{a}_\beta^{\text{out}} = \sum_\alpha S_{\beta\alpha}\,\hat{a}_\alpha^{\text{in}} + \sum_\alpha U_{\beta\alpha}\,\hat{b}_\alpha\,, \tag{3.1}$$

where $\hat{b}$ is the operator corresponding to the absorption within the object, and α and β are quantum numbers. In this equation, S is the object's scattering matrix while U describes its lossy character—the latter is related to the scattering matrix as shown later. This method treats field theory in the second quantized picture where quantum (annihilation or creation) operators are introduced. Equation (3.1) then relates quantum operators via the *classical* scattering matrix. This proves to be useful in applications to the dynamical Casimir effect.

Equation (3.1) has its roots in the classical wave equation. To see this, we first define "in" and "out" wave functions. The incoming wave can be expanded as

$$\Phi^{\text{in}}(\mathbf{x}) = \sum_\alpha c_\alpha^{\text{in}} \Phi_\alpha^{\text{in}}(\mathbf{x}), \tag{3.2}$$

where c_α^{in} is the amplitude of the corresponding wave function Φ_α^{in}. The latter function should be normalized so that the number of incoming quanta per unit time is (negative) unity,

$$\frac{1}{2i}\oint \mathrm{d}\boldsymbol{\Sigma}\cdot\left[\Phi_\alpha^{\text{in}*}\,\nabla\Phi_\beta^{\text{in}} - \nabla\Phi_\alpha^{\text{in}*}\,\Phi_\beta^{\text{in}}\right] = -\delta_{\alpha\beta}, \tag{3.3}$$

with the integral defined over a closed surface enclosing the object. The reason for this choice is that we shall associate the wave function with a quantum operator which satisfies the canonical commutation relations, and the normalization should be defined consistently. Similarly the outgoing wave functions are normalized as

$$\frac{1}{2i}\oint \mathrm{d}\boldsymbol{\Sigma}\cdot\left[\Phi_\alpha^{\text{out}*}\,\nabla\Phi_\beta^{\text{out}} - \nabla\Phi_\alpha^{\text{out}*}\,\Phi_\beta^{\text{out}}\right] = \delta_{\alpha\beta}. \tag{3.4}$$

In Eqs. (3.3) and (3.4), we have assumed that the frequency of the corresponding wavefunctions is positive. For negative frequencies, the above equations describe outgoing and incoming wavefunctions, respectively, since the energy flux changes

sign. We also designate the solutions to the wave equation inside the object as $\Phi^{\rm obj}$. Now suppose that there are sources in two regions in space: at infinity where they generate the incoming wave, $\Phi^{\rm in}$ in Eq. (3.2); and within the object where they induce a field $\Phi^{\rm obj} = \sum_\alpha d_\alpha \Phi^{\rm obj}_\alpha$—the normalization of these functions does not affect the scattering matrix and thus is not discussed here. The incoming wave is scattered by the object while the object itself radiates due to the induced field. The resulting outgoing wave, $\Phi^{\rm out} = \sum_\alpha c^{\rm out}_\alpha \Phi^{\rm out}_\alpha$, is determined by

$$c^{\rm out}_\beta = \sum_\alpha S_{\beta\alpha} c^{\rm in}_\alpha + \sum_\alpha U_{\beta\alpha} d_\alpha, \tag{3.5}$$

where the first term is merely the scattering of the incoming waves, and the second term captures the radiation of the object itself. The above analysis is based on a classical wave equation. Equation (3.1) extends the last equation to a relation between quantum operators, i.e. the complex-valued coefficients in Eq. (3.5) become quantum operators in Eq. (3.1) through $c^{\rm in/out} \to \hat{a}^{\rm in/out}$ and $d \to \hat{b}$ (see also the discussion in Ref. [84] on the relation between wave mechanics and the classical limit). From this point on, we shall drop the hat symbol from quantum operators.

For objects in motion, scattering can also change the frequency of the incoming wave. We make the dependence on frequency explicit while reserving α for other quantum numbers; the sum in Eq. (3.1) is replaced by

$$\sum_\alpha \int_{-\infty}^{\infty} \frac{{\rm d}\omega}{2\pi}.$$

Most importantly, the scattering matrix may mix positive and negative frequencies, in which case an outgoing operator of positive frequency is related to an incoming operator of negative frequency via Eq. (3.1). Note that an operator $a_{\omega\alpha}$ with negative ω should be interpreted as a creation operator; more precisely, $a_{\omega\alpha} = a^\dagger_{-\omega\bar{\alpha}}$ where $\bar{\alpha}$ is related to α by time reversal.

We assume that the environment is at a temperature $T_{\rm env}$ while the object is at a (possibly different) temperature T. The distribution of the incoming modes (before

scattering) is solely characterized by $T_{\rm env}$,

$$\langle a^{\rm in\dagger}_{\omega'\beta} a^{\rm in}_{\omega\alpha}\rangle = {\rm sgn}(\omega) n(\omega, T_{\rm env})\, \delta(\omega-\omega')\, \delta_{\alpha\beta}\,, \tag{3.6}$$

where $n(\omega,T) = \frac{1}{\exp(\hbar\omega/kT)-1}$ is the Bose-Einstein factor. Note that this equation holds for both positive and negative values of frequency; an operator $a_{\omega\alpha}$ ($a^\dagger_{\omega\alpha}$) defined at a negative frequency, ω, is interpreted as a creation (annihilation) operator of a positive-frequency mode.

On the other hand, the occupation number for the operators b, localized on the object, is determined by T, the object's temperature. But we should keep in mind that the object could be moving, so the frequency defined from the point of view of a reference system (co)moving with the object is different from that of an observer in the vacuum, or the *lab*, frame. For a partial wave (ω,α) in the lab frame, we define $\tilde\omega_\alpha$ as the frequency according to the comoving reference frame. The occupation number is then[1]

$$\langle b^\dagger_{\omega'\beta} b_{\omega\alpha}\rangle = {\rm sgn}(\tilde\omega_\alpha) n(\tilde\omega_\alpha, T)\, \frac{\partial\tilde\omega_\alpha}{\partial\omega}\, \delta(\omega-\omega')\, \delta_{\alpha\beta}\,. \tag{3.7}$$

From the distribution of the incoming and localized operators, Eqs. (3.6) and (3.7), we can evaluate the distribution for an outgoing mode (ω',β),

$$\begin{aligned}\langle a^{\rm out\dagger}_{\omega'\beta} a^{\rm out}_{\omega'\beta}\rangle &= \int_{-\infty}^{\infty}\frac{{\rm d}\omega}{2\pi}\, {\rm sgn}(\omega) n(\omega, T_{\rm env}) \sum_\alpha |S_{\omega'\beta,\omega\alpha}|^2 \\ &+ \sum_\alpha \int_{-\infty}^{\infty}\frac{{\rm d}\tilde\omega_\alpha}{2\pi}\, {\rm sgn}(\tilde\omega_\alpha) n(\tilde\omega_\alpha, T)\, |U_{\omega'\beta,\omega\alpha}|^2\,. \end{aligned}\tag{3.8}$$

To find the flux of field quanta to the environment, one should compute the difference of outgoing and incoming flux. To study Eq. (3.8) in some detail, we consider two different situations.

Accelerating objects—First we assume that the object is non-lossy so that the second term on the RHS of Eqs. (3.1) and (3.8) is absent. For the sake of simplicity,

[1]The change of basis from the frequency in the moving frame to that of the lab frame gives rise to the Jacobian. The partial derivative is positive on physical grounds.

we choose to work at zero temperature[2], i.e. $T_{\text{env}} = 0$; the generalization to finite temperatures is straightforward. From Eq. (3.8), we find

$$\langle a^{\text{out}\dagger}_{\omega'\beta} a^{\text{out}}_{\omega'\beta} \rangle = \int_{-\infty}^{0} \frac{\mathrm{d}\omega}{2\pi} \sum_{\alpha} |S_{\omega'\beta,\omega\alpha}|^2 . \tag{3.9}$$

We have used the fact that the Bose-Einstein distribution at $T = 0$ is different from zero only for negative frequencies. Loosely speaking, this means that, in the vacuum state, all single-particle states with negative energy are occupied while those of positive energy are empty. The rate of energy radiation is obtained as an integral over the outgoing flux in Eq. (3.9) multiplied by the quanta energy

$$P = \int_{0}^{\infty} \frac{\mathrm{d}\omega'}{2\pi} \hbar\omega' \int_{-\infty}^{0} \frac{\mathrm{d}\omega}{2\pi} \sum_{\alpha,\beta} |S_{\omega'\beta,\omega\alpha}|^2 . \tag{3.10}$$

The choice of basis α is a matter of convenience, as in a basis-independent notation Eq. (3.10) is cast as

$$P = \int_{0}^{\infty} \frac{\mathrm{d}\omega'}{2\pi} \hbar\omega' \int_{-\infty}^{0} \frac{\mathrm{d}\omega}{2\pi} \mathrm{Tr} \left(\mathbb{S}_{\omega',\omega} \mathbb{S}^{\dagger}_{\omega',\omega} \right) , \tag{3.11}$$

where $\mathbb{S}$ is the basis-free scattering matrix. A similar expression is derived in Ref. [43] for the radiation from a vibrating cavity. These equations provide a simple and compact formulation which serve as the starting point for studying accelerating boundaries and modulated optical devices in Sec. 3.2.

Stationary motion—Next we consider objects in stationary, linear or rotational, motion. Although the objects are moving, the boundaries do not change their shape or orientation. One such example is two infinite plates moving parallel to their surface. Despite the motion, the relative configuration of the two plates does not change in time.

This type of dynamical problem is not explicitly time dependent, nevertheless the relative motion leads to dissipative effects. In other words, such systems respect time

[2]In the absence of loss, the object's temperature does not play a role.

translation but break time-reversal symmetry, and thus allow for dissipation. Because of the stationary character of the setup, however, the scattering matrix $\mathbb{S}$ as well as the matrix $\mathbb{U}$ are diagonal in frequency, and we indicate this by a single frequency dependence as $S_{\beta\alpha}(\omega)$ and $U_{\beta\alpha}(\omega)$.

For a lossy object, the scattering matrix cannot be unitary as part of the incoming wave is lost inside the object. Interestingly, unitarity alone, sufficiently constrains the matrix $\mathbb{U}$ for our purposes [66]. There is a large body of literature on quantization in an absorbing (or amplifying) medium, covering a variety of approaches. The method of input-output relations [76, 77, 66] starts by formulating canonical commutation relations for the incoming and outgoing operators,

$$[a^{\text{out/in}}_{\omega\alpha}, a^{\text{out/in}\dagger}_{\omega'\beta}] = \text{sgn}(\omega)\delta(\omega-\omega')\,\delta_{\alpha\beta}. \tag{3.12}$$

We extend this method to moving systems by demanding that the operators b (localized on the object) satisfy the commutation relations in the rest frame of the object,

$$[b_{\omega\alpha}, b^{\dagger}_{\omega'\beta}] = \text{sgn}(\tilde{\omega}_\alpha)\frac{\partial\tilde{\omega}_\alpha}{\partial\omega}\delta(\omega-\omega')\,\delta_{\alpha\beta}, \tag{3.13}$$

with $\tilde{\omega}_\alpha$ defined above. This set of relations along with Eq. (3.1) lead to

$$\text{sgn}(\omega)\,(1-\sum_\alpha |S_{\beta\alpha}(\omega)|^2) = \sum_\alpha \text{sgn}(\tilde{\omega}_\alpha)\frac{\partial\tilde{\omega}_\alpha}{\partial\omega}\,|U_{\beta\alpha}(\omega)|^2\,. \tag{3.14}$$

In the comoving frame, the object is momentarily at rest, and thus the frequency according to this frame does not change, i.e. $\tilde{\omega}_\alpha = \tilde{\omega}_\beta$ if $U_{\beta\alpha} \neq 0$. Therefore, Eq. (3.14) can be recast as

$$\text{sgn}(\omega)\,(1-\sum_\alpha |S_{\beta\alpha}(\omega)|^2) = \text{sgn}(\tilde{\omega}_\beta)\frac{\partial\tilde{\omega}_\beta}{\partial\omega}\sum_\alpha |U_{\beta\alpha}(\omega)|^2\,, \tag{3.15}$$

or in a matrix notation,

$$\text{sgn}(\omega)\,(\mathbb{I}-\mathbb{S}\mathbb{S}^\dagger)_{\beta\beta} = \text{sgn}(\tilde{\omega}_\beta)\frac{\partial\tilde{\omega}_\beta}{\partial\omega}(\mathbb{U}\mathbb{U}^\dagger)_{\beta\beta}\,, \tag{3.16}$$

which constrains the matrix $\mathbb{U}$ in terms of the scattering matrix, $\mathbb{S}$. In the limit of static objects, one recovers the (basis-free) relation [66]

$$\mathbb{I} - \mathbb{S}\mathbb{S}^\dagger = \mathbb{U}\mathbb{U}^\dagger. \tag{3.17}$$

This equation is interpreted by Beenakker as a "fluctuation-dissipation" relation with the LHS giving the dissipation due to the classical scattering from a lossy material, and the RHS accounting for field fluctuations due to spontaneous absorption or emission (in an amplifying medium) of field quanta.

Equation (3.15) for a moving object can be inserted in Eq. (3.8) to obtain the flux due to the outgoing quanta. We are interested in the total flux,

$$\frac{d\mathcal{N}}{\mathrm{d}\omega} = \sum_\beta \langle a^{\mathrm{out}\dagger}_{\omega\beta} a^{\mathrm{out}}_{\omega\beta}\rangle - \langle a^{\mathrm{in}\dagger}_{\omega\beta} a^{\mathrm{in}}_{\omega\beta}\rangle. \tag{3.18}$$

The total radiation is obtained as the latter quantity multiplied by $\hbar\omega$ integrated over frequency. Using Eqs. (3.8) and (3.15), one obtains the radiated energy per unit time as

$$\mathcal{P} = \int_0^\infty \frac{\mathrm{d}\omega}{2\pi}\,\hbar\omega \sum_{\alpha,\beta} (n(\tilde{\omega}_\alpha, T) - n(\omega, T_{\mathrm{env}}))\left(\delta_{\beta\alpha} - |S_{\beta\alpha}(\omega)|^2\right). \tag{3.19}$$

In the absence of motion ($\tilde{\omega}_\alpha = \omega$), this equation correctly reproduces the thermal radiation from an object out of equilibrium from the environment [66, 67]. Interestingly, the moving object radiates energy even when the temperature is zero both in the object and the environment. In this limit, the energy radiation takes the form

$$\mathcal{P} = \int_0^\infty \frac{\mathrm{d}\omega}{2\pi}\,\hbar\omega \sum_{\alpha,\beta} \Theta(-\tilde{\omega}_\alpha)\,\left(|S_{\beta\alpha}(\omega)|^2 - \delta_{\beta\alpha}\right), \tag{3.20}$$

where Θ is the Heaviside step function. Therefore, spontaneous emission takes place for a process whose frequency ω is positive in the lab frame while, from the point of view of the moving observer, the corresponding frequency $\tilde{\omega}_\alpha$ is negative. This mixing between negative and positive frequencies is at the heart of the dynamical Casimir

effect [34].

In Sec. 3.3, we employ Eq. (3.20) to find the spontaneous emission due to a rotating object. Furthermore, we study the configuration of multiple objects in relative motion where we generalize the results presented in this section. In the process, we find that Eqs. (3.16) and (3.17) need to be modified for evanescent waves.

In summary, Eqs. (3.10) and (3.20) express the energy radiation for an accelerating lossless body and a lossy moving object, respectively. In both cases, the radiated energy density is related to the off-diagonal part of the scattering matrix in $|S|^2$. Hence, they have a characteristic "Fermi-Golden-Rule" structure. In fact, to the lowest order, one can think of the off-diagonal S-matrix as a *potential* due to the boundary condition or the object's material, akin to the Fermi Golden Rule.

In the following sections, we provide a variety of examples where we discuss applications of the general formulas presented above.

3.2 Lossless accelerating objects

In this section, we consider lossless objects with different shapes in various dimensions undergoing rotational or translational motion or oscillation. In the process, we reproduce some existing results in the literature, and also present many novel applications. Equation (3.10) is the central formula according to which we compute and discuss these results.

3.2.1 A Dirichlet point in 1+1d

The prototype of dynamical Casimir phenomena is the motion of a point-like *mirror* in one dimension [19, 35]. For simplicity, we assume that the ambient vacuum consists of a scalar field, Φ, subject to Dirichlet boundary conditions on the mirror

$$\Phi(t, q(t)) = 0, \tag{3.21}$$

where $q(t)$ is the trajectory of the mirror in time. We use a perturbative scheme [35] where we expand Eq. (3.21) for small $q(t)$ to obtain

$$\Phi(t,0) + q(t)\partial_z\Phi(t,0) + \cdots = 0\,. \tag{3.22}$$

The scattering solution can be formally expanded in powers of q,

$$\Phi = \Phi_0 + \Phi_1 + \cdots\,. \tag{3.23}$$

The boundary condition, to the first order, takes the form

$$\Phi_1(t,0) = -q(t)\partial_z\Phi_0(t,0). \tag{3.24}$$

The incoming and outgoing modes are defined as

$$\Phi_\omega^{\text{in/out}} = \sqrt{\frac{c}{|\omega|}}\exp[-i\omega(t \pm z/c)]. \tag{3.25}$$

Note that the normalization is chosen in accordance with Eqs. (3.3) and (3.4). In the zeroth order, i.e. for a static mirror, we have

$$\Phi_0 = \Phi_\omega^{\text{in}} - \Phi_\omega^{\text{out}}\,. \tag{3.26}$$

We can compute Φ_1 by solving the free field equation ($\Box\,\Phi = 0$) in the vacuum subject to its time-dependent value at the origin ($z = 0$) as given by Eq. (3.24). We leave the details to Appendix B.1; the scattering matrix (from either side of the point) is obtained as

$$S_{\omega+\Omega,\omega} = -\frac{2i\,\tilde{q}(\Omega)}{c}\sqrt{|(\omega+\Omega)\,\omega|}\,, \tag{3.27}$$

where $\tilde{q}(\Omega)$ is the Fourier transform of $q(t)$. (Note that, here and in the following, we only write the off-diagonal correction to the scattering matrix.) One can then compute the radiation according to Eq. (3.10). For a Fourier mode Ω, the integral in the latter equation contributes in the window of $0 < -\omega < \Omega$. Putting all the pieces

together, and multiplying by a factor of two accounting for the scattering from both sides, we find

$$\begin{aligned} P &= \frac{8\hbar}{c^2}\int_0^\infty \frac{\mathrm{d}\Omega}{2\pi}|\tilde{q}(\Omega)|^2 \int_{-\Omega}^0 \frac{\mathrm{d}\omega}{2\pi}\,(\omega+\Omega)^2\,|\omega| \\ &= \frac{\hbar}{3\pi c^2}\int_0^\infty \frac{\mathrm{d}\Omega}{2\pi}|\tilde{q}(\Omega)|^2\Omega^4 \\ &= \frac{\hbar}{6\pi c^2}\int \mathrm{d}t\,\dddot{q}^2. \end{aligned} \tag{3.28}$$

In the last line, the radiation is expressed as an integral over time. From Eq. (3.28), one can infer the dissipative component of the force

$$f(t) = \frac{\hbar}{6\pi c^2}\dddot{q}, \tag{3.29}$$

in complete agreement with Ref. [35].

3.2.2 Modulated reflectivity in 1+1d

For moving bodies, the dynamical Casimir radiation is difficult to detect experimentally since it requires the objects to move at very high frequencies. An alternative approach is suggested by modulating optical properties of a resonant cavity [28, 29, 30]. In fact, any *linear* time-dependent process can lead to similar dynamical Casimir effects. Modulated reflectivity, for example, generates photons and gives rise to radiation [85, 33]. The latter can be studied within the same framework that we developed for non-lossy objects[3]. In this section, we consider a point particle in one spatial dimension, but, unlike the model in the previous (sub)section, a linear coupling of (time-dependent) strength ϵ is introduced at the position of the particle. The field equation then reads

$$\left(\frac{1}{c^2}\partial_t^2 - \partial_z^2\right)\Phi(t,z) + \epsilon(t)\delta(z)\Phi(t,0) = 0. \tag{3.30}$$

[3]In treating the dynamical Casimir effect in the absence of loss, we did not assume that the objects are actually moving.

We recover a perfectly reflecting object for $\epsilon \to \infty$. An imperfect mirror undergoing arbitrary motion is studied in Ref. [86]. Note that in our model the particle is at rest at the origin while the coupling is modulated. The S-matrix can be computed by techniques similar to quantum mechanical scattering in a one-dimensional delta potential. For simplicity, we take $\epsilon(t) = \epsilon_0 + \epsilon_\Omega \cos(\Omega t)$ with $\epsilon_0 \gg \epsilon_\Omega$. We note that there are new scattering channels with incoming waves from one side transmitted to the other side of the object. A scattering ansatz with incoming waves from the RHS is given by

$$\Phi \approx \begin{cases} \Phi_\omega^{R\,\mathrm{in}} + r\Phi_\omega^{R\,\mathrm{out}} + r_\pm \Phi_{\omega\pm\Omega}^{R\,\mathrm{out}}, & z > 0, \\ t\Phi_\omega^{L\,\mathrm{out}} + t_\pm \Phi_{\omega\pm\Omega}^{L\,\mathrm{out}}, & z < 0, \end{cases} \tag{3.31}$$

where summation is made over both signs, and the wavefunctions denoted by $R(L)$ are defined on the right (left) side. Obviously, the two sets of definitions are related by reversing the sign of the coordinate z. In the above ansatz, we have exploited the smallness of the oscillatory part of ϵ by truncating the sum at the lowest harmonics. One can obtain the scattering amplitudes by matching the functions on the two sides of the mirror while setting the difference in their first derivative to $\epsilon\Phi(t,0)$. We find

$$r_\pm = t_\pm = \frac{i\epsilon_\Omega \sqrt{|\omega(\omega \pm \Omega)|}/c}{(\epsilon_0 - 2i\omega/c)(\epsilon_0 - 2i(\omega \pm \Omega)/c)}. \tag{3.32}$$

This equation can be further simplified by assuming $\epsilon_0 \gg \Omega/c$. In this limit, the energy radiation (per unit time) is, according to Eq. (3.10),

$$\mathcal{P} = \frac{\hbar \Omega^4 \epsilon_\Omega^2}{6\pi c^2 \epsilon_0^4}. \tag{3.33}$$

For a general $\epsilon(t)$ slowly varying around a mean value of ϵ_0, the total energy radiation is given by

$$P = \frac{\hbar}{3\pi c^2 \epsilon_0^4} \int \mathrm{d}t\, \ddot{\epsilon}(t)^2. \tag{3.34}$$

3.2.3 A Dirichlet line in 2+1d

Now consider a line extended along the x axis in two spatial dimensions. In this geometry, the incoming and outgoing waves are described by

$$\Phi^{\text{in/out}}_{\omega k_x} = \frac{1}{\sqrt{k_\perp}} \exp(-i\omega t + ik_x x \mp ik_\perp z)\,, \tag{3.35}$$

for $\omega > 0$ (and defined conversely for $\omega < 0$) where k_x is the wavevector along the line, and $k_\perp$ is the perpendicular component, $k_\perp(\omega, k_x) = \sqrt{\omega^2/c^2 - k_x^2}$. We assume that the line undergoes a rigid but time-dependent motion, $q(t)$, normal to the x axis. One then finds

$$S_{\omega+\Omega k_x, \omega k_x} = -2i\,\tilde{q}(\Omega)\sqrt{k_\perp(\omega, k_x)\,k_\perp(\omega+\Omega, k_x)}\,; \tag{3.36}$$

see Appendix B.1. The scattering matrix is diagonal in k_x due to translational symmetry along the x-axis. Note that Eq. (3.36) is computed only for propagating modes—evanescent waves fall off rapidly with the distance from the surface and do not contribute to radiation at infinity. The sum over all partial waves in Eq. (3.10) becomes $\int \frac{L\mathrm{d}k_x}{2\pi}$ with L being the extent of the line; the integration is over propagating waves only, i.e. $c|k_x| < |\omega|$ and $c|k_x| < \omega + \Omega$. Finally, an integration over the frequency, ω, gives

$$P = \frac{\hbar L}{128c^3}\int_0^\infty \frac{\mathrm{d}\Omega}{2\pi}\,|\tilde{q}(\Omega)|^2\Omega^5. \tag{3.37}$$

In order to write this equation in the time domain, we extend the integral to $(-\infty, \infty)$ and recast the integrand as $\Omega\,|\tilde{q}(\Omega)|^2\,\mathrm{Im}\,\chi(\Omega)$. The function χ is the (normalized) response function whose imaginary part is proportional to the energy dissipation to the environment, $\mathrm{Im}\,\chi(\Omega) = \frac{1}{2}\Omega^4\mathrm{sgn}(\Omega)$. Because of causality, the full response function can be obtained via Kramers-Kronig relations. In the time domain, we find

this function as

$$\chi(t) = \frac{24}{\pi}\Theta(t)\,\mathrm{P}\,\frac{1}{t^5}\,, \tag{3.38}$$

with P being the principal part. In this context, the response function relates the force to the object's displacement. So the force acting on the object at time t is given by

$$f(t) = \frac{3\hbar L}{16\pi c^3}\int_{-\infty}^{t} \mathrm{d}t'\,\mathrm{P}\,\frac{1}{(t-t')^5}\,q(t')\,. \tag{3.39}$$

The force is manifestly causal, i.e. it depends on q at earlier times. However, Eq. (3.39) is possibly divergent near the upper bound of the integral unless a short-time cutoff is introduced to replace this bound by $t-\tau$. This does not affect the dissipative component of the force but regularizes the inertial force which sensitively depends on the large-frequency physics. In fact, in deriving Eq. (3.39), we have used the small-frequency behavior of the response function, so this equation should be valid only for large times. Interestingly, the force does not vanish even when the object no longer moves. We find that the force, long after the object comes to a full stop, falls as

$$f(t) = \frac{3\hbar L}{16c^3t^5}\int \mathrm{d}t'\,q(t') = \frac{3\hbar L}{16c^3t^5}\,\tilde{q}(0)\,, \tag{3.40}$$

where the integral is over the displacement of the object for the duration of the motion (which is assumed to be much smaller than t), and $\tilde{q}(0)$ is the integrated displacement.

3.2.4 A Dirichlet segment in a waveguide in 2+1d

Next we consider a finite segment of size L along the x-axis confined between two infinite Dirichlet lines (a *waveguide*) in two spatial dimensions; see Fig. 3-1. Dirichlet boundary conditions are assumed on all surfaces. The segment undergoes a rigid motion $q(t)$ parallel to the infinite lines. The only difference compared to the previous (sub)section is that the modes along the x-axis are quantized. Therefore the integral over k_x is replaced by a sum over n where $k_n = \frac{n\pi}{L}$. The radiation takes the form (cf.

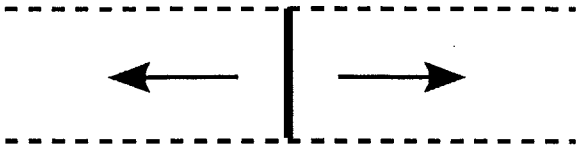

Figure 3-1: A segment in a waveguide. The arrows indicate the direction along which the segment oscillates. Below a certain frequency, $\omega_{\min} = 2\omega_0$, the motion is frictionless.

Eq. (3.37))

$$P = \frac{\hbar}{128c^2}\int_0^\infty \frac{\mathrm{d}\Omega}{2\pi}|\tilde{q}(\Omega)|^2\Omega^4\, g\left(\Omega L/c\right), \tag{3.41}$$

where the function g is defined as

$$g(\nu) = \frac{512}{\pi}\sum_{n=1}^{\lfloor \nu/2\pi\rfloor}\int_{\frac{\pi n}{\nu}}^{1-\frac{\pi n}{\nu}} \mathrm{d}z\,(1-z)\sqrt{(z^2-\frac{\pi^2n^2}{\nu^2})((1-z)^2-\frac{\pi^2n^2}{\nu^2})}\,. \tag{3.42}$$

For large L, $g(\nu) \to \nu$, and we recover the results of the previous (sub)section. However, this function vanishes below $\nu = 2\pi$; a low-frequency motion does not dissipate energy since propagating waves inside a waveguide have no support in the range $(-\omega_0, \omega_0)$ with ω_0 being the lowest eigenmode of the waveguide, hence $\omega_{\min} = 2\omega_0 = 2\pi c/L$. Close to this frequency, the function g vanishes quadratically,

$$g(\nu) \sim \frac{8}{\pi^2}(\nu - 2\pi)^2, \qquad \nu \gtrsim 2\pi. \tag{3.43}$$

Similar to the previous (sub)section, one can use Kramers-Kronig relations to obtain the response function. Specifically, we are interested in the long-time limit after the object comes to a full stop. The dependence on large t can be inferred from the short-frequency response (Eq. (3.43)) as

$$f(t) = -\frac{\hbar}{2\pi c L\, t^3}\,\mathrm{Re}\left(e^{-i2\omega_0 t}\,\tilde{q}(2\omega_0)\right), \tag{3.44}$$

with $\omega_0 = \pi c/L$ as defined before. Note that the force now falls as $1/t^3$ while its amplitude undergoes periodic oscillations at frequency $2\omega_0$, twice the lowest natural

frequency of the waveguide.

3.2.5 A Dirichlet plate in 3+1d

In this section, we consider a (two-dimensional) plate in three dimensions subject to the same (Dirichlet) boundary conditions. Again we assume that the plate undergoes a rigid motion $q(t)$ normal to its surface, and find the scattering matrix as

$$S_{\omega+\Omega\mathbf{k}_\parallel,\omega\mathbf{k}_\parallel} = -2i\,\tilde{q}(\Omega)\sqrt{k_\perp(\omega,\mathbf{k}_\parallel)\,k_\perp(\omega+\Omega,\mathbf{k}_\parallel)}\,; \tag{3.45}$$

see Appendix B.1. In order to compute the radiation, one should integrate over propagating modes only (both for incoming and outgoing waves), i.e. $c|\mathbf{k}_\parallel| < |\omega|$ and $c|\mathbf{k}_\parallel| < \omega + \Omega$. Equation (3.10) then gives

$$\begin{aligned} P &= \frac{\hbar L^2}{180\pi^2 c^4}\int_0^\infty \frac{\mathrm{d}\Omega}{2\pi}|\tilde{q}(\Omega)|^2\Omega^6 \\ &= \frac{\hbar L^2}{360\pi^2 c^4}\int \mathrm{d}t\,\dddot{q}^2, \end{aligned} \tag{3.46}$$

where L^2 is the area of the plate. The resulting (dissipative component of the) force is then

$$f(t) = -\frac{\hbar L^2}{360\pi^2 c^4}\,q^{(5)}, \tag{3.47}$$

again in agreement with Ref. [35].

We also note the difference between odd and even dimensions. In 2 dimensions, the force displays long-time tails, while in 1 and 3 dimensions it is an (almost) instantaneous function of the displacement.

3.2.6 A Dirichlet corrugated plate in 3+1d

We can generalize the results in the previous (sub)section by considering a corrugated plate. For corrugations of wavevector $\mathbf{q}$, the scattering matrix is given by (cf.

Eq. (3.45))

$$S_{\omega+\Omega\mathbf{k}_\parallel+\mathbf{q},\omega\mathbf{k}_\parallel} = -2i\,\tilde{q}(\Omega,\mathbf{q})\sqrt{k_\perp(\omega,\mathbf{k}_\parallel)\,k_\perp(\omega+\Omega,\mathbf{k}_\parallel+\mathbf{q})}\,. \tag{3.48}$$

where q, the displacement from the $x-y$ plane, is a function of both ω and $\mathbf{q}$; see Appendix B.1. The condition for propagating waves is modified as $c|\mathbf{k}_\parallel| < |\omega|$ and $c|\mathbf{k}_\parallel+\mathbf{q}| < \omega+\Omega$. The radiation formula should be modified accordingly to ensure that only the propagating modes are integrated. While this integral can be computed explicitly, we use a trick as follows: For $\Omega > c|\mathbf{q}|$, we Lorentz-transform to a frame in which the scattering matrix is diagonal in the wavevector $\mathbf{k}_\parallel$; the velocity of this frame is $\mathbf{v} = \frac{c^2\mathbf{q}}{\Omega}$. The scattering matrix, the integral measure, as well as the condition for propagating waves are invariant under such a transformation. But the frequency ($\hbar\omega'$ in Eq. (3.10)) picks up a factor of $\gamma(\mathbf{v}) = 1/\sqrt{1-\mathbf{v}^2/c^2}$, while the lower bound of the integral over ω changes from $-\Omega$ to $-\gamma(\mathbf{v})(\Omega-\mathbf{v}\cdot\mathbf{q}) = -\Omega/\gamma(\mathbf{v})$ which, through comparison with the first line of Eq. (3.46), contributes a factor of $1/\gamma^6$. Hence, the radiated energy density in Ω and $\mathbf{q}$ becomes

$$P(\Omega,\mathbf{q}) = \frac{\hbar}{360\pi^2c^4}|\tilde{q}(\Omega,\mathbf{q})|^2\Omega(\Omega^2-c^2\mathbf{q}^2)^{5/2}, \tag{3.49}$$

consistent with Ref. [41]. Note that the difference of a factor of two in comparison with Eq. (3.46) is in harmony with the setup in Ref. [41] where the plate occupies a half-space. Similar results can be obtained for Neumann boundary conditions [87].

3.2.7 A Dirichlet sphere in 3+1d

In this section, we consider a sphere subject to Dirichlet boundary conditions linearly oscillating in three dimensions. The oscillation amplitude, $q(t)$, is small compared to the radius of the sphere, R. We choose the z axis parallel to the motion and passing through the center of the sphere. The incoming and outgoing waves for a spherical

geometry are defined as

$$\Phi_{\omega lm}^{\text{in/out}} = \sqrt{\frac{|\omega|}{c}} e^{-i\omega t} h_l^{(1,2)}\left(\frac{\omega r}{c}\right) Y_{lm}(\theta,\phi), \tag{3.50}$$

where $h_l^{(1,2)}$ are spherical Hankel functions, and Y_{lm} is the usual spherical harmonic function. Due to azimuthal symmetry, the scattering matrix is diagonal in the index m but possibly mixes different ls. The scattering from an oscillating sphere can be computed by using Green's theorem; see Appendix B.2 for more details. We find the (off-diagonal) scattering matrix as

$$S_{\omega+\Omega l'm,\,\omega lm} = \frac{2i\tilde{q}(\Omega)}{c} d_{ll'm} \sqrt{|(\omega+\Omega)\,\omega|}\, F_l\left(\frac{\omega R}{c}\right) F_{l'}\left(\frac{(\omega+\Omega)R}{c}\right), \tag{3.51}$$

where $d_{ll'm}$ as defined in Appendix B.2 is nonzero only for $l' = l \pm 1$, and the function F is defined as

$$F_l(x) = \frac{1}{x h_l^{(1)}(x)}. \tag{3.52}$$

Using Eq. (3.10), the radiated energy density is given by

$$P(\Omega) = \frac{8\hbar|\tilde{q}(\Omega)|^2}{3c^2} \int_{-\Omega}^{0} \frac{\mathrm{d}\omega}{2\pi} (\omega+\Omega)^2 \omega \sum_{l=0}^{\infty} (l+1) \left| F_l\left(\frac{\omega R}{c}\right) F_{l+1}\left(\frac{(\omega+\Omega)R}{c}\right)\right|^2. \tag{3.53}$$

We consider two different limits:

a) $\Omega R/c \ll 1$. For a slowly oscillating object, we need only consider the lowest partial wave, i.e. the $l = 0$ term in Eq. (3.53). One then finds the radiated energy density in frequency as

$$P(\Omega) = \frac{\hbar\,\Omega^6 R^2}{30\pi c^4} |\tilde{q}(\Omega)|^2. \tag{3.54}$$

b) $\Omega R/c \gg 1$. In this case, one should include all partial waves up to $l_{\max} \approx \Omega R/c \gg 1$. Below we closely follow the line of argument in Ref. [22]. For large l, we

have

$$|F_l(x)| \approx (1 - l^2/x^2)^{1/4}, \qquad 1 \ll l < x. \tag{3.55}$$

The sum over all partial waves can then be recast as an integral over l yielding (through the change of variables $\sigma = l/(\Omega R/c)$ and $x = |\omega|/\Omega$)

$$\begin{aligned} P(\Omega) &= \frac{4\hbar R^2 \Omega^6 |\tilde{q}(\Omega)|^2}{3\pi c^4} \int_0^{1/2} \mathrm{d}\sigma\sigma \int_\sigma^{1-\sigma} \mathrm{d}x\,(1-x)x^2 \left[1 - \frac{\sigma^2}{x^2}\right]^{1/2} \left[1 - \frac{\sigma^2}{(1-x)^2}\right]^{1/2} \\ &= \frac{\hbar \Omega^6 R^2}{270\pi c^4} |\tilde{q}(\Omega)|^2 . \end{aligned} \tag{3.56}$$

This equation reproduces the contribution of the TE modes to the electromagnetic version of a perfectly reflecting sphere; see Eq. (4.20) in Ref. [22].[4] Indeed one finds a similar correspondence for a perfectly reflecting plate, that is the radiation due to the TE modes is equal to that of the Dirichlet plate [42].

Finally we note that the radiation due to the oscillatory motion can be computed for a variety of other geometries such as cylinders, ellipsoids, etc.

3.2.8 A spinning object in 2+1d

Heretofore, we studied examples where the object is accelerated by an external force. In this section, we consider an object rotating at a constant angular velocity Ω. We further assume that the object is not rotationally symmetric, as illustrated in Fig. 3-2. As usual, we assume a scalar field subject to Dirichlet boundary conditions on the object's surface, and limit ourselves to 2+1 dimensions.

Since the orientation changes with time, waves impinging on the object are partially scattered at a shifted frequency determined by Ω. The scattering matrix is more conveniently computed by going to the object's reference frame.

We start with the field equations in the laboratory (static) frame. The wave

[4]There are however mixed terms between the two polarizations which vanish in this limit, see Ref. [22].

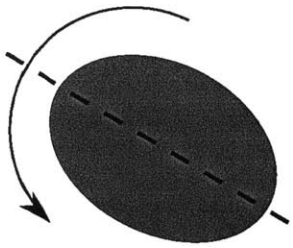

Figure 3-2: An (asymmetric) spinning object. The object slows down as it emits "photons".

equation, $\Box\Phi = 0$, in polar coordinates is

$$\left[\frac{1}{c^2}\partial_t^2 - \frac{1}{r}\partial_r r\partial_r - \frac{1}{r^2}\partial_\phi^2\right]\Phi(t,r,\phi) = 0. \tag{3.57}$$

The incoming and outgoing waves are defined as

$$\Phi_{\omega m}^{\text{in/out}}(t,r,\phi) = e^{-i\omega t}e^{im\phi}H_m^{(1,2)}\left(\frac{\omega r}{c}\right), \tag{3.58}$$

where H is the Hankel function. (We have dropped an irrelevant constant in the definition of the these functions.) The rotating frame is described by

$$t' = t, \quad r' = r, \quad \phi' = \phi - \Omega t. \tag{3.59}$$

The field equation in the latter frame takes the form

$$\left[\frac{1}{c^2}(\partial_t - \Omega\partial_{\phi'})^2 - \frac{1}{r}\partial_r r\partial_r - \frac{1}{r^2}\partial_{\phi'}^2\right]\Phi'(t,r,\phi') = 0. \tag{3.60}$$

Note that $\Phi'(t,r,\phi') = \Phi(t,r,\phi)$. Specifically, in the new coordinate system, the functions $\Phi_{\omega m}$ as defined in Eq. (3.58) become

$$\Phi'_{\omega-\Omega m\, m}(t,r,\phi') = e^{-i(\omega-\Omega m)t}e^{im\phi'}H_m^{(1,2)}\left(\frac{\omega r}{c}\right). \tag{3.61}$$

The rotating frame is more convenient to write the scattering ansatz as the object does not move in this frame, and thus the time dependence drops out as a phase

factor. In the latter frame, the boundary conditions take the form

$$\left[e^{im\phi'}H_m^{(2)}\left(\frac{\omega r}{c}\right)+\sum_{m'}S_{m',m}e^{im'\phi'}H_{m'}^{(1)}\left(\frac{(\omega-\Omega(m-m'))r}{c}\right)\right]_\Sigma=0, \tag{3.62}$$

where Σ denotes the boundary. One can see that this equation indeed satisfies Eq. (3.60) once the time dependence, $e^{-i(\omega-\Omega m)t}$, is restored. The scattering matrix sends the frequency ω to $\omega-\Omega(m-m')$ from the point of view of an observer in the lab frame. To obtain an analytical expression for the scattering matrix, we consider the non-relativistic limit where the object's (linear) velocity is small compared to c. It then suffices to compute the scattering matrix for the lowest partial waves. As a specific example we consider an ellipse close to a circle of radius R with δ being the difference of the two semiaxes, i.e., in polar coordinates, defined as $r(\phi)=R+\cos(2\phi)\delta/2$. The scattering matrix to the lowest order in δ is then obtained as

$$\begin{aligned} S_{\omega+2\Omega\,2,\omega\,0}&=\frac{i\pi(\omega+2\Omega)^2R\delta}{8c^2\log(|\omega|R/c)}\,,\\ S_{\omega+2\Omega\,0,\omega\,-2}&=\frac{i\pi\omega^2R\delta}{8c^2\log((\omega+2\Omega)R/c)}\,. \end{aligned} \tag{3.63}$$

The energy radiation per unit time, according to Eq. (3.10), is

$$\mathcal{P}\approx\frac{\pi\hbar R^2\delta^2\Omega^6}{10c^4\log(\Omega R/c)^2}\,. \tag{3.64}$$

Therefore, an (asymmetric) object which is spinning, even at a constant rate, slows down due to quantum dissipation. Note that the torque (due to the back-reaction) is simply the radiation rate divided by the frequency Ω.

3.2.9 A Dirichlet disk in 2+1 dimensions: linear vs angular motion

Now consider a circular disk of radius R subject to Dirichlet boundary conditions in two spatial dimensions. Below we contrast two different types of motion, see Fig. 3-3.

First we consider a linear oscillation, $q(t) = \delta \cos \Omega t$ (with δ being the amplitude

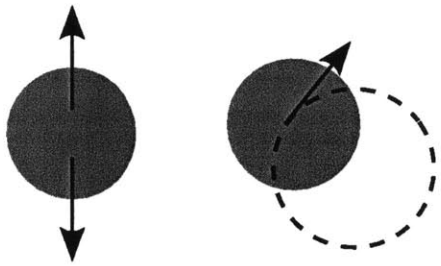

Figure 3-3: Linear *vs* angular motion; the radiated energy is comparable in the two cases.

of the oscillation) along the x-axis. The scattering from an oscillating disk can be obtained by using Green's theorem; see Appendix B.3 for more details. We obtain the scattering matrix as

$$S_{\omega+\Omega\, m\pm1,\omega\, m} = \frac{2i\,\delta}{\pi R} M_m\left(\frac{\omega R}{c}\right) M_{m\pm1}\left(\frac{(\omega+\Omega)R}{c}\right), \tag{3.65}$$

where the function M is

$$M_m(x) = \frac{1}{H_m^{(1)}(x)}\,. \tag{3.66}$$

At low frequency, $\Omega R/c \ll 1$, the scattering matrix for the lowest partial waves is obtained as

$$S_{\omega+\Omega\,\pm1,\omega\,0} = \mp\frac{i\pi(\omega+\Omega)\delta}{4c\log(\omega R/c)}\,. \tag{3.67}$$

The energy radiation (per unit time) can be computed from Eq. (3.10); for a linearly oscillating disk, we find

$$\mathcal{P}_{\updownarrow} = \frac{\pi\hbar\,\delta^2\Omega^4}{64c^2\log(\Omega R/c)^2}\,. \tag{3.68}$$

Next we consider the same disk undergoing orbital motion. The latter can be thought as a rotation around a point off the center of the disk. Specifically, we assume that the disk's center undergoes a trajectory $(r,\phi) = (\delta, \Omega t)$ in polar coordinates, i.e. the center is at a fixed radius δ while orbiting around the origin at frequency Ω. The scattering process can be examined by techniques similar to the previous

(sub)section where we considered a spinning object. We must assume $\Omega R/c \ll 1$ as well as $\delta \ll R$—similar to the linear motion. The latter allows us to compute the scattering matrix only for the lowest partial waves, as

$$S_{\omega+\Omega 1,\omega 0} = -\frac{i\pi(\omega+\Omega)\delta}{2c\log(|\omega|R/c)}\,,$$
$$S_{\omega+\Omega 0,\omega -1} = \frac{i\pi\omega\delta}{2c\log((\omega+\Omega)R/c)}\,. \tag{3.69}$$

Note the similarity between Eqs. (3.67) and (3.69). The radiated energy by a revolving disk can then be computed according to Eq. (3.10), as

$$\mathcal{P}_\circ = \frac{\pi\hbar\delta^2\Omega^4}{24c^2\log(\Omega R/c)^2}\,. \tag{3.70}$$

It is interesting to compare Eqs. (3.68) and (3.70) where linear and angular motion have been considered, respectively. We notice that, apart form a proportionality constant, the analytical form of the dissipated energy is identical in the two cases.

The above results can be compared with the previous (sub)section. In the former case, the setup is symmetric under inversion with respect to the origin while the latter is not. Thus, in the lowest order, scattering of waves changes the angular momentum by two units for a spinning ellipse and by one unit for a disk in (linear or circular) motion; cf. Eqs. (3.63), (3.67) and (3.69). Consequently, the energy radiation in the former case, Eq. (3.64), is suppressed by two orders of magnitude in comparison with Eqs. (3.68) and (3.70) for a disk.

3.3 Stationary motion of lossy objects

In this section, we consider lossy objects but limit ourselves to constant (linear or angular) speed. Among other results, we reproduce existing formulas in the literature with significantly less labor. Our starting point is Eq. (3.20) in application to rotating objects. We then generalize to the case of multiple objects in relative motion.

3.3.1 Rotating object

Let us consider a solid of revolution spinning around its axis of symmetry at frequency Ω. We choose polar coordinates (r, ϕ, z) where the z direction is along the axis of symmetry. The latter coordinates describe the lab frame in which the object is rotating. The rotating (or comoving) frame is defined by the coordinate transformation

$$t' = t, \quad r' = r, \quad \phi' = \phi - \Omega t, \quad z' = z. \tag{3.71}$$

A partial wave defined by frequency ω and azimuthal index m in the lab frame is characterized by the frequency

$$\tilde{\omega}_m = \omega - \Omega m \tag{3.72}$$

from the perspective of the rotating frame; see Ref. [65] for a detailed discussion. In harmony with the discussion in Sec. 3.1, the object spontaneously emits energy when $\omega > 0$ and $\tilde{\omega}_m < 0$, i.e. in the frequency window

$$0 < \omega < \Omega m, \tag{3.73}$$

or the so-called superradiating regime first introduced by Zel'dovich [58]. Therefore, the energy radiation per unit time from a rotating object to the environment at zero temperature is given by

$$\mathcal{P} = \int_0^\infty \frac{\mathrm{d}\omega}{2\pi} \hbar\omega \,\mathrm{Tr}\left[\Theta(\Omega\,\hat{l}_z - \omega)\left(\mathbb{S}(\omega)\,\mathbb{S}(\omega)^\dagger - \mathbb{I}\right)\right], \tag{3.74}$$

where $\hat{l}_z$ is the z-component of the angular momentum operator in units of $\hbar$. Note that the scattering matrix is diagonal in frequency, ω, since the object is undergoing a stationary motion with its shape and orientation fixed in time. Equation (3.74) indeed gives the spontaneous emission by a rotating object consistent with Ref. [65] where the Rytov formalism is used through an involved analysis. For a small object,

only the lowest partial waves contribute to the radiation, and we recover the results of Ref. [56]. Note that in deriving Eq. (3.74) we did not use any approximations regarding the velocity of the rotating object.

For the sake of generalization to multiple objects, we point out that Eq. (3.1) can be interpreted in a simple way to arrive at the same results. According to this equation, the probability amplitude for spontaneous emission is given by

$$\mathcal{A}_m(\omega) = U_m(\omega), \tag{3.75}$$

where we have suppressed all quantum numbers other than ω and m, and used the fact that the amplitude is diagonal in m due to the rotational symmetry of the object. The rate of this process is

$$\mathcal{N}_m(\omega) = |U_m(\omega)|^2 = |S_m(\omega)|^2 - 1, \tag{3.76}$$

where, in the last equality, we have used Eq. (3.15) in the superradiating regime, i.e. for $0 < \omega < \Omega m$. Note that, in this regime, $|S_m(\omega)| > 1$, hence superradiance. The integral of $\mathcal{N}$ multiplied by $\hbar\omega$ (over superradiating frequencies) reproduces the energy radiation as given by Eq. (3.74).

3.3.2 Moving plates

A system comprising two lossy parallel plates undergoing relative lateral motion is the canonical example of non-contact friction. In the following, we sketch a simple derivation of this friction based on Eqs. (3.1) and (3.17).[5] We first note that Eq. (3.17) can be interpreted via a classical argument. One can denote the RHS of this equation as the rate of "photon" absorption in a dispersive medium. Current conservation implies that the latter should be equal to the influx of the field quanta outside the

[5]For a uniform translational motion, one can Lorentz-transform Eq. (3.17) to the moving frame.

body. Let us consider a classical wave scattered from the object as

$$\Phi = \Phi_\alpha^{\text{in}} + \sum_\beta S_{\beta\alpha}\Phi_\beta^{\text{out}}, \tag{3.77}$$

where we have suppressed the frequency, ω. The current density going into the body is given by $\frac{-1}{2i}[\Phi^* \nabla\Phi - \nabla\Phi^* \Phi]$. Since Φ_α and Φ_β are properly normalized (see Eqs. (3.3) and (3.4) and the explanation thereafter), the total influx of field quanta is

$$\frac{i}{2}\oint \mathrm{d}\boldsymbol{\Sigma}\cdot[\Phi^* \nabla\Phi - \nabla\Phi^* \Phi] = 1 - \sum_\beta |S_{\beta\alpha}|^2. \tag{3.78}$$

But this is exactly the LHS of Eq. (3.17).

To study moving plates we need to extend Eq. (3.17) to evanescent waves which arise in non-compact geometries (plates, cylinders, etc.), but are absent for a compact geometry. Since such waves are not propagating, "incoming" and "outgoing" wave functions lose their straightforward interpretation. In other words, they do not carry currents

$$\oint \mathrm{d}\boldsymbol{\Sigma}\cdot\left[\Phi_\alpha^{\text{out/in}*} \nabla\Phi_\beta^{\text{out/in}} - \nabla\Phi_\alpha^{\text{out/in}*} \Phi_\beta^{\text{out/in}}\right] = 0, \tag{3.79}$$

but satisfy a different relation (after proper normalization)

$$\frac{1}{2}\oint \mathrm{d}\boldsymbol{\Sigma}\cdot\left[\Phi_\alpha^{\text{in}*} \nabla\Phi_\beta^{\text{out}} - \nabla\Phi_\alpha^{\text{in}*} \Phi_\beta^{\text{out}}\right] = \delta_{\alpha\beta}. \tag{3.80}$$

Therefore an incoming wave scattered from the object, $\Phi = \Phi_\alpha^{\text{in}} + \sum_\beta S_{\beta\alpha}\Phi_\beta^{\text{out}}$, carries an influx of "photons" given by

$$\frac{i}{2}\oint \mathrm{d}\boldsymbol{\Sigma}\cdot[\Phi^* \nabla\Phi - \nabla\Phi^* \Phi] = 2\,\mathrm{Im}\, S_{\alpha\alpha}, \tag{3.81}$$

where Eqs. (3.79) and (3.80) are used. Then the conservation of current dictates

$$(\mathbb{U}\mathbb{U}^\dagger)_{\alpha\alpha} = 2\,\mathrm{Im}\,(\mathbb{S})_{\alpha\alpha}\,. \tag{3.82}$$

Equations (3.17) and (3.82) define the matrix $\mathbb{U}$ in terms of the scattering (or reflection) matrix for propagating and evanescent waves, respectively.

We can now compute the friction between two "dielectric" plates moving in parallel. We assume that the first plate is at rest while the other plate, separated from the first by a distance d, moves at a constant velocity v along the x axis. Because of translational symmetry, all matrices are diagonal in the frequency ω and the wavevector $\mathbf{k}_\parallel$ parallel to the surface. Here, Eq. (3.1) finds a two-fold application. On one hand, it allows for spontaneous emission from an object, while on the other hand, it describes the reflection and absorption of waves by a second object.

1) Spontaneous emission: the source fluctuations in the first plate give rise to outgoing wave fluctuations. The amplitude of the spontaneous emission is given by

$$\mathcal{A}_1 = U_1, \tag{3.83}$$

where the dependence of the matrix U on ω and $\mathbf{k}_\parallel$ is implicit. Note that incoming waves do not contribute to spontaneous emission.

2) Reflection: These outgoing waves propagate to the second plate and get a factor of $e^{ik_\perp d}$ with $k_\perp = \sqrt{\omega^2/c^2 - \mathbf{k}_\parallel^2}$; a phase factor for propagating waves while exponentially decaying for evanescent waves. There they are partly reflected and partly absorbed by the second plate. The amplitude for "photons" spontaneously emitted by the first plate and then absorbed by the second one is

$$\mathcal{A}_{2\leftarrow 1} = e^{ik_\perp d} U_2 U_1. \tag{3.84}$$

Equivalently, the rate of the latter process is given by

$$\mathcal{N}^{1^{\text{st}}}_{2\leftarrow 1} = |\mathcal{A}_{2\leftarrow 1}|^2 \, n_1 = \left|e^{ik_\perp d}\right|^2 |U_2|^2 |U_1|^2 \, n_1, \tag{3.85}$$

where $n_1 = n(\omega, T_1)$ is the Bose-Einstein occupation number defined at temperature T_1. The superscript 1^{st} indicates that Eq. (3.85) is computed within the first reflection. One can similarly compute $\mathcal{N}_{1\leftarrow 2}$, the current from the second to the first plate. But

in the latter case, $n_2(\omega, \mathbf{k}_\parallel)$ is centered at $\omega - vk_x$, i.e. $n_2 = n(\omega - vk_x, T_2)$, because the thermal fluctuations are defined with respect to the comoving frame.[6] The total flux from the first to the second plate, within the first reflection, is then

$$\mathcal{N}^{1^{st}}_{2\leftarrow 1} - \mathcal{N}^{1^{st}}_{1\leftarrow 2} = \left|e^{ik_\perp d}\right|^2 |U_2|^2 |U_1|^2 \, (n_1 - n_2). \tag{3.86}$$

One can easily sum the contributions from multiple reflections,

$$\begin{aligned} \mathcal{A}^{\text{tot}}_{2\leftarrow 1} &= \sum_{n=0}^{\infty} e^{ik_\perp d} U_2 \left(e^{2ik_\perp d} R_1 R_2\right)^n U_1 \\ &= \frac{e^{ik_\perp d} U_2 U_1}{1 - e^{2ik_\perp d} R_1 R_2}, \end{aligned} \tag{3.87}$$

where R_1 and R_2 are the reflection matrices. Note that the n-th term in the last equation is the amplitude for a "photon" spontaneously emitted by the first plate (U_1), reflected n times from the two plates ($(e^{2ik_\perp d} R_1 R_2)^n$) before finally getting absorbed by the second plate (U_2). The amplitude $\mathcal{A}^{\text{tot}}_{1\leftarrow 2}$ is obtained similarly. The total rate then becomes

$$\mathcal{N}_{2\leftarrow 1} - \mathcal{N}_{1\leftarrow 2} = \frac{\left|e^{ik_\perp d}\right|^2 |U_2|^2 |U_1|^2}{\left|1 - e^{2ik_\perp d} R_1 R_2\right|^2} \, (n_1 - n_2). \tag{3.88}$$

Also note that, from Eqs. (3.17) and (3.82), we have

$$|U_i|^2 = \begin{cases} 1 - |R_i|^2, & \text{for propagating waves,} \\ 2 \operatorname{Im} R_i \,, & \text{for evanescent waves.} \end{cases} \tag{3.89}$$

Finally friction is the rate of (lateral-)momentum transfer integrated over all partial waves,

$$f = \int_0^\infty \frac{\mathrm{d}\omega}{2\pi} \int \frac{L^2 \mathrm{d}\mathbf{k}_\parallel}{(2\pi)^2} \, \hbar k_x \frac{\left|e^{ik_\perp d}\right|^2 |U_2|^2 |U_1|^2}{\left|1 - e^{2ik_\perp d} R_1 R_2\right|^2} \, (n_1 - n_2). \tag{3.90}$$

We should emphasize that the reflection matrix for the second plate should be computed in its rest-frame, and then transformed to the lab frame according to Lorentz

[6] For relativistic velocities, one should also include the Lorentz factor $\gamma(v) = 1/\sqrt{1 - v^2/c^2}$.

transformations. The last equation is the analog of the results in Refs. [52, 53] for the scalar field.

To be more concrete, we consider a scalar model that is described by a free field equation in empty space while inside the object a "dielectric" (or, a response) function ϵ is assumed which characterizes the object's dispersive properties. The field equation for this model reads

$$\left(\epsilon(\omega,\mathbf{x})\omega^2+\nabla^2\right)\Phi(\omega,\mathbf{x})=0, \tag{3.91}$$

with ϵ being 1 in the vacuum, and a frequency-dependent constant inside the object.

For a semi-infinite plate, the reflection matrix R is given by

$$R_{\omega\mathbf{k}_\parallel}=-\frac{\sqrt{\epsilon\,\omega^2/c^2-\mathbf{k}_\parallel^2}-\sqrt{\omega^2/c^2-\mathbf{k}_\parallel^2}}{\sqrt{\epsilon\,\omega^2/c^2-\mathbf{k}_\parallel^2}+\sqrt{\omega^2/c^2-\mathbf{k}_\parallel^2}}. \tag{3.92}$$

This is easily obtained by solving the field equations inside and outside the plate and demanding the continuity of the field and its first derivative along the boundary. In a moving frame, the frequency and the wavevector should be properly Lorentz-transformed.

These reflection matrices can then be inserted in Eq. (3.90) to compute the frictional force.

3.3.3 An *atom* moving parallel to a plate

In this section, we consider a small spherical object, an *atom*, moving parallel to a plate. In the non-retarded limit, an electrostatic computation is done in Ref. [88] for a similar setup. For our purposes, it is more convenient to consider the rest frame of the "atom" in which the plate moves laterally. This is another example of stationary motion where the geometrical configuration does not change even though the objects are undergoing relative motion. We assume a small spherical object of radius a (much smaller than the separation distance d), such that the first-reflection approximation suffices. Similar to the previous (sub)section, we first consider spontaneous emission by each object. The plate (denoted by sub-index 2) emits "photons" of frequency ω

and wavevector $\mathbf{k}_\parallel$ with a probability amplitude

$$\mathcal{A}_2(\omega, \mathbf{k}_\parallel) = U_2(\omega, \mathbf{k}_\parallel). \tag{3.93}$$

Then, these waves propagate to and reflect from the "atom." Planar waves pick up a factor $e^{ik_\perp d}$ upon traveling a distance d. To find the scattering off of the spherical object, we must change to a basis of spherical waves. A planar wave can be expressed as a superposition of spherical waves as

$$e^{i\mathbf{k}\cdot\mathbf{x}} = 4\pi \sum_{lm} i^l j_l(\omega r/c) Y_{lm}(\hat{\mathbf{x}})\, Y^*_{lm}(\hat{\mathbf{k}}), \tag{3.94}$$

where $\hat{\mathbf{x}}$ and $\hat{\mathbf{k}}$ are the unit vectors parallel to the vectors $\mathbf{x}$ and $\mathbf{k}$, respectively. A planar wave, $\Phi_{\omega\mathbf{k}_\parallel}$, defined with respect to a reference point on the plate's surface below the sphere's center is related to spherical waves, $\Phi_{\omega lm}$, centered around the "atom" as

$$\Phi^{\text{out}}_{\omega\mathbf{k}_\parallel} = \sum_{lm} \frac{2\pi i^l e^{ik_\perp d} Y^*_{lm}(\hat{\mathbf{k}})}{\sqrt{k_\perp \omega/c}} \left(\Phi^{\text{in}}_{\omega lm} + \Phi^{\text{out}}_{\omega lm}\right); \tag{3.95}$$

see Appendix B for the definition of planar and spherical waves. Then the amplitude for "photons" spontaneously emitted by the plate and then absorbed by the sphere is

$$\mathcal{A}_{1\leftarrow 2} = \frac{2\pi i^l e^{ik_\perp d} Y^*_{lm}(\hat{\mathbf{k}})}{\sqrt{k_\perp \omega/c}}\, U_{1\,lm}(\omega) U_2(\omega, \mathbf{k}_\parallel), \tag{3.96}$$

where U_1 characterizes the loss due to the "atom." Similarly, we can compute the amplitude $\mathcal{A}_{2\leftarrow 1}$ for the inverse process where the spontaneous emission due to the "atom" is absorbed by the plate. One can then obtain the rate of energy or momentum transfer between the objects. An analysis similar to the previous (sub)section gives the force within the first reflection,

$$f = \int_0^\infty \frac{\mathrm{d}\omega}{2\pi} \int \frac{\mathrm{d}\mathbf{k}_\parallel}{(2\pi)^2} \hbar k_x \left(n_1 - n_2\right) \sum_{l,m} \frac{\left|e^{ik_\perp d}\right|^2 |Y_{lm}(\hat{\mathbf{k}})|^2 |U_{1\,lm}(\omega)|^2 |U_2(\omega, \mathbf{k}_\parallel)|^2}{|k_\perp|\omega/4\pi^2 c}, \tag{3.97}$$

where $n_1(\omega) = n(\omega, T_1)$ and $n_2(\omega, \mathbf{k}) = n(\omega - vk_x, T_2)$ are the Bose-Einstein factors for the "atom" at temperature T_1 and the plate at temperature T_2, respectively. Note that we have only considered the first reflection as the "atom" is small compared to the separation distance. The matrix U_2 is given as in Eq. (3.89) while, for the spherical object, there is no evanescent wave and thus the matrix U_1 is constrained by

$$|U_{1\,lm}(\omega)|^2 = 1 - |S_{lm}(\omega)|^2, \tag{3.98}$$

with $S_{lm}(\omega)$ being the scattering matrix of the "atom." This equation indicates that a frictional force (or energy transfer) arises only if the "atom" is lossy, i.e. $|S_{lm}(\omega)| < 1$. For the scalar model introduced in the previous (sub)section, the sphere's scattering matrix is

$$S_{lm}(\omega) = -\frac{h_l^{(2)}(\omega a/c)\partial_a j_l(n\omega a/c) - \partial_a h_l^{(2)}(\omega a/c)\, j_l(n\omega a/c)}{h_l^{(1)}(\omega a/c)\partial_a j_l(n\omega a/c) - \partial_a h_l^{(1)}(\omega a/c)\, j_l(n\omega a/c)}, \tag{3.99}$$

where a is the sphere's radius, and $n(\omega) = \sqrt{\epsilon_S(\omega)}$ with ϵ_S being the "dielectric" function of the spherical object. To the lowest order in a/d, we shall limit ourselves to the low-frequency scattering of the partial wave $l = m = 0$.[7] Within this approximation, the friction at zero temperature takes the form

$$f \approx \frac{4\hbar a^3}{3\pi^2 c^2} \int_{k_x>0} \mathrm{d}\mathbf{k}_\parallel \int_0^{vk_x} \mathrm{d}\omega \frac{e^{-2|\mathbf{k}_\parallel| d} k_x \omega^2 \,\mathrm{Im}\,\epsilon_S(\omega)\,\mathrm{Im}\,R_{\omega'\mathbf{k}'_\parallel}}{|\mathbf{k}_\parallel|}. \tag{3.100}$$

The reflection matrix R can be obtained from Eq. (4.2) via Lorentz transformation. Similarly, one can consider the frictional force between a rotating sphere and a stationary plate [89]. With our scalar model, the scattering matrix for a rotating sphere is obtained from Eq. (3.99) by changing the argument of the Bessel functions to $n(\tilde{\omega}_m)\tilde{\omega}_m a/c$ where $\tilde{\omega}_m = \omega - \Omega m$. Having the scattering matrices of a moving plate and a rotating sphere, one can compute the friction when both objects are set in motion.

[7] One should note that in the case of electrodynamics there are no monopole fluctuations and thus the leading contribution to the friction comes from $l = 1$ [88].

Chapter 4

Quantum Cherenkov Radiation and Non-contact Friction

An intriguing manifestation of quantum theory in macroscopic bodies is the non-contact friction between objects in relative motion. For example, two surfaces (or semi-infinite plates) moving in parallel experience a frictional force if the objects' material is lossy [52, 53, 54]. The origin of this force is the quantum fluctuations of electromagnetic field, within and between the objects; the same fluctuations also give rise to Casimir/van der Waals forces. In brief, quantum fluctuations induce currents in each object, which then couple to result in the interaction between them. For moving objects, a phase lag between currents leads to a frictional force between them.

For parallel plates, the friction force is related to amplitude of the reflected wave upon scattering of an incident wave from each surface (formalized into a reflection matrix below) [52, 53]. Due to its quantum origin, friction persists even at zero temperature, where it is related to the imaginary part of the reflection matrix corresponding to evanescent waves. It is usually assumed that the dielectric (or response) function itself has an imaginary part due to dissipative properties of the material; this then leads to an imaginary reflection matrix and hence friction [34]. However, this is not necessary as, even for a vanishingly small loss, evanescent waves lead to an imaginary reflection matrix.

We consider a constant dielectric function, which fixes the speed of light within the medium[1]. We show that when the velocity of moving plates, in their *center-of-mass* frame, is larger than the phase speed of light in the medium, a frictional force arises between them. This is, in fact, a quantum analog of the well-known *classical Cherenkov* radiation. We elaborate on the relation between the friction, and radiation in the gap as well as within the plates.

Quantum Cherenkov radiation was first discovered by Ginzburg and Frank [90] in a rather different setup. They argued that when an object (an atom, for example) moves inertially and superluminally, i.e. larger than the phase speed of light in a medium, it spontaneously emits photons; see Refs. [91, 92] for subsequent reviews by Ginzburg. This phenomenon is intimately related to *superradiance*, first discovered by Zel'dovich [58] in the context of rotating objects and black holes: A rotating body amplifies certain incident waves even if it is lossy. The underlying physics is that a moving object (atom) can lose energy by getting excited. This is because, at superluminal velocities, an excitation in the rest-frame of the object corresponds to a loss of energy in the *lab* frame. Ginzburg and Frank refer to this eventuality as the *anomalous* Doppler effect [90]; see also Ref. [69].

Since these unusual observations span several subfields of physics, we find it useful to demonstrate the results by a number of different formalisms. We first generalize the arguments by Ginzburg and Frank to prove dissipation effects associated with the relative motion of two parallel plates. We then use the input–output formalism of quantum optics to derive and compute the friction force based on the scattering matrices. An alternative proof follows approaches introduced in the context of quantum field theory in curved space-time, making use of an inner product to identify the wavefunctions and their (quantum) character. Finally we employ the Rytov formalism [55] which is grounded in the fluctuation-dissipation theorem for electrodynamics and well-known to practitioners of non-contact friction.

To ease computations, however, we consider a scalar field theory as a simpler

[1]The frequency-independence of the dielectric function follows from a vanishing imaginary part, due to Kramers-Kronig relations.

substitute for electromagnetism. The former shares the same conceptual complexity while being more tractable analytically. This is particularly useful in expressing complicated Green's functions with points both inside and outside each plate, or within the gap between them. The generalization to vector and dyadic electromagnetic expressions should be straightforward but laborious. Finally to avoid complications of the full Lorentz transformations, we limit ourselves to small velocities—both the relative velocity of the objects and the speed of light in their media.

In the following, we explicitly consider semi-infinite plates described by a constant and real dielectric function. However, the underlying physics is rather general, and does not depend on the idealizations that made for the sake of convenience. For example, rather than a semi-infinite plate, we can consider a thick slab of a material with a complex dielectric function ϵ. The slab will act like an infinite medium provided that the imaginary part of ϵ while small, is sufficiently large to absorb the emitted energy within the slab, with almost no radiation escaping the far end. Such conditions can be met for a broad range of the thickness and lossy-ness.

The techniques that we develop here are applicable to a variety of other setups: An interesting situation, closer in spirit to Cherenkov radiation, is when a particle passes through a small channel drilled into a dielectric. Another closely related problem is a particle moving parallel to a surface [88, 89, 93]. Our approach of utilizing scattering theory in conjunction with a host of other methods, including input-output and Rytov formalism, should be useful in analyzing such situations.

The remainder of the paper is organized as follows. In Sec. 4.1, existing formulas are used without proof to compute friction, and to discuss the similarities with the classical Cherenkov effect. In this section, we elaborate on friction in a specific example. In Sec. 4.2, we consider a general setup, argue for and derive the friction force, as well as emitted radiation, in great detail. This section comprises 4 subsections each devoted to one particular method. Specifically, we discuss how the radiation within the plates, and in the gap, depend on the reference frame.

4.1 Friction

We start with a scalar model that is described by a free field theory in empty space, while inside the object a "dielectric" (or, a response) function ϵ is assumed which characterizes the object's dispersive properties. The field equation for this model reads

$$\left(\nabla^2 + \epsilon(\omega, \mathbf{x})\frac{\omega^2}{c^2}\right)\Phi(\omega, \mathbf{x}) = 0, \tag{4.1}$$

with $\epsilon = 1$ in the vacuum, and a frequency-dependent constant inside an object.

We consider the configuration of two parallel semi-infinite dielectric media ('plates') in D spatial dimensions, separated by a vacuum gap of size d. For each plate in its rest frame, a plane wave of frequency ω and wavevector $\mathbf{k}$ is reflected with amplitude ('reflection matrix')

$$R_{\omega\mathbf{k}_\parallel} = -\frac{\sqrt{\epsilon\,\omega^2/c^2 - \mathbf{k}_\parallel^2} - \sqrt{\omega^2/c^2 - \mathbf{k}_\parallel^2}}{\sqrt{\epsilon\,\omega^2/c^2 - \mathbf{k}_\parallel^2} + \sqrt{\omega^2/c^2 - \mathbf{k}_\parallel^2}}, \tag{4.2}$$

where $\mathbf{k}_\parallel$ is the component of the wavevector parallel to the surface. This result is easily obtained by solving the field equations inside and outside the plate, and matching the reflection amplitude to satisfy the continuity of the field and its first derivative along the boundary. We are particularly interested in friction at zero temperature which is mediated solely by evanescent waves. Such waves contribute to friction through the imaginary part of the reflection matrices [52, 53, 54]. If one plate moves laterally with velocity v along the x axis, while the other is at rest, the friction force is given by (introducing the notation $đx = dx/2\pi$)

$$f = \int_0^\infty đ\omega\, L^{D-1} \int đ\mathbf{k}_\parallel\ \hbar k_x \frac{e^{-2|k_\perp|d}\,(2\,\mathrm{Im}\,R_1)\,(2\,\mathrm{Im}\,R_2)}{|1 - e^{-2|k_\perp|d} R_1 R_2|^2}\,\Theta(-\omega + v k_x)\,, \tag{4.3}$$

where Θ is the Heaviside step function, $k_\perp = \sqrt{\omega^2/c^2 - \mathbf{k}_\parallel^2}$, and L^{D-1} is the area. Note that the reflection matrix of the static plate is given by Eq. (4.2), but that of the moving plate is obtained after Lorentz transforming to the lab frame. We leave the

derivation of Eq. (4.3) to the next section, but discuss its implications here. While this equation has been studied extensively in the literature, it is usually assumed that the dielectric medium is lossy, with a nonzero imaginary part of ϵ. However, even when $\mathrm{Im}\,\epsilon$ is vanishingly small, a frictional force can be obtained as follows. With $\mathrm{Im}\,\epsilon \approx 0$, the medium can be characterized by the modified speed of light $v_0 = c/\sqrt{\epsilon}$. The only relevant length scale in the problem (aside from the overall area L^{D-1}) is the separation d. We can then construct the frictional force on purely dimensional grounds as

$$f = \frac{\hbar\, v_0 L^{D-1}}{d^{D+2}}\, \tilde{g}\left(\frac{v}{v_0}, \frac{v}{c}\right) ,$$

where $\tilde{g}$ is a function of two dimensionless velocity ratios. Any velocity could have appeared as prefactor (with a correspondingly modified function $\tilde{g}$); we have chosen v_0 for convenience. For small velocities, the dependence on vacuum light velocity c drops out, and

$$f \approx \frac{\hbar\, v_0 L^{D-1}}{d^{D+2}}\, g\left(\frac{v}{v_0}\right) , \tag{4.4}$$

with g depending only on the ratio of the velocity v to the light speed in the medium v_0. Interestingly, at small v, only the modified speed within the media is relevant.

Now note that the Heaviside function in Eq. (4.3) restricts to frequencies

$$(0 <)\, \omega < v k_x\, . \tag{4.5}$$

Furthermore, the imaginary part of the reflection matrix R_1, given by Eq. (4.2), is only nonzero when $\omega^2/c^2 - \mathbf{k}_\parallel^2 < 0$ and $\epsilon\,\omega^2/c^2 - \mathbf{k}_\parallel^2 > 0$, which, in turn, imply

$$|\omega| > v_0 |\mathbf{k}_\parallel| > v_0 |k_x| . \tag{4.6}$$

A similar condition holds for the second plate: $|\omega'| > v_0 |k'_x|$ with primed values defined in the moving reference-frame. For simplicity, we assume that $v, v_0 \ll c$, and

thus neglect the complications of a full Lorentz transformation. Hence, $\omega' \approx \omega - vk_x$ and $k'_x \approx k_x - v\omega/c^2 \approx k_x$. Then the analog of Eq. (4.6) for the second plate reads

$$|\omega - vk_x| \gtrapprox v_0|k_x|. \tag{4.7}$$

The above conditions limit the range of integration to

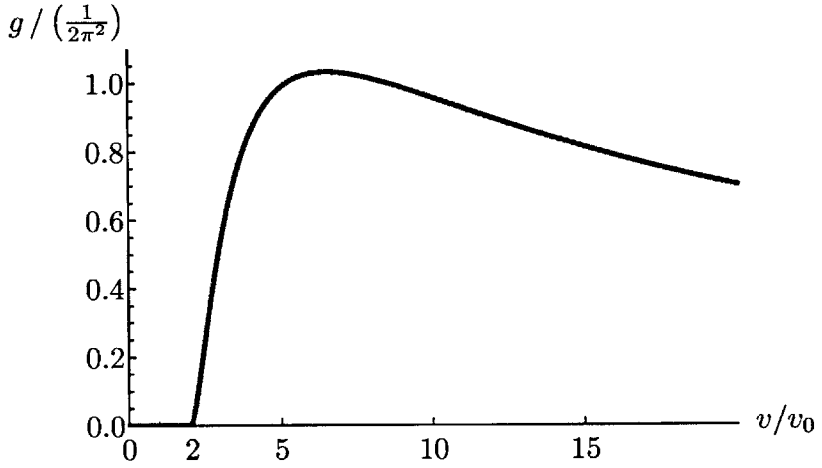

Figure 4-1: Friction depends on velocity v through the function g. Below a certain velocity, $v_{\min} = 2v_0 = 2c/\sqrt{\epsilon}$, the friction force is zero; it starts to rise linearly at $v_{\min}$, achieves a maximum and then falls off.

$$k_x > 0, \qquad \text{and} \qquad v_0 k_x < \omega < (v - v_0)k_x. \tag{4.8}$$

One then finds the minimum velocity where a frictional force arises as

$$v_{\min} = 2v_0 = 2\frac{c}{\sqrt{\epsilon}}. \tag{4.9}$$

This threshold velocity is reminiscent of the classical Cherenkov effect, although larger by a factor of two. However, in the *center-of-mass* frame where the two plates move at the same velocity but in opposite directions, we find the same condition as that of the Cherenkov effect: A frictional force arises when, in the center-of-mass frame, the plates' velocity exceeds that of light in the medium. As a specific example, we

consider a two dimensional space, i.e. surfaces represented by straight lines. The dependence of friction force on relative velocity is then plotted in Fig. 4-1.

4.2 Formalism and derivation

In the previous section we argued for the appearance of friction between moving parallel plates which is reminiscent of the Cherenkov effect. Establishing a complete correspondence requires a full analysis of the radiation within each object. In this section, we provide several arguments to demonstrate why and how a fluctuation-induced friction arises in the context of macroscopic objects in relative motion. We start with a heuristic argument, making a connection with the Frank-Ginzburg condition. We then present three distinct derivations of the friction force using techniques developed in different fields: The first method relies on the input-output formalism in a second-quantized picture; the second one appeals to quantum field theory in curved space-time. The last, and the longest, derivation is based on fluctuation-dissipation theorem, or the closely related Rytov formalism. The advantage of the latter approach is in finding correlation functions inside and outside the two plates which can be used to compute the radiation within each plate and in the gap between them.

4.2.1 Why is there any friction/radiation?

To start with, let us consider a space-filling dielectric medium described by a constant real ϵ. A wave described by wavevector $\mathbf{k}$ satisfies the dispersion relation $\omega = v_0|\mathbf{k}|$, with $v_0 = c/\sqrt{\epsilon}$ being the speed of light in the medium. This relation describes the spectrum of quantum field excitations. If the medium is set in motion, the new spectrum can be deduced simply by a Lorentz transformation from the static to the moving frame. Assuming again that the speed of light in medium is small (or ϵ is large), we find

$$\omega = v_0|\mathbf{k}| + vk_x\,, \tag{4.10}$$

with the medium moving with speed v parallel to the x axis.

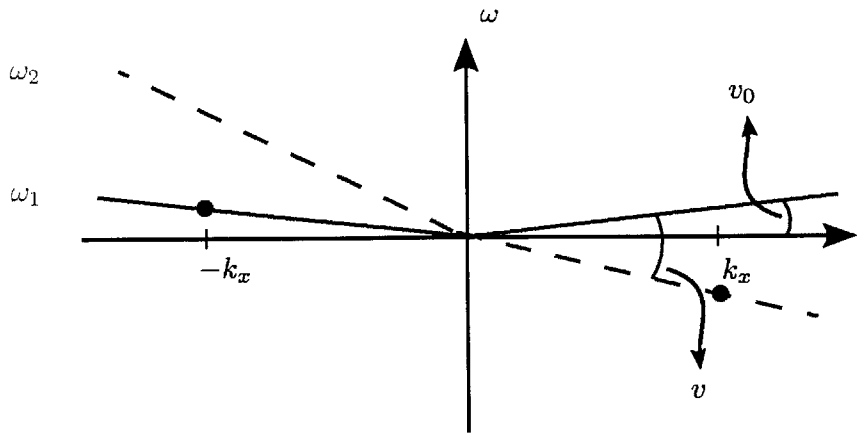

Figure 4-2: The energy spectra for a medium at rest (solid curve denoted by ω_1), and a moving medium (dashed curve denoted by ω_2), in the (ω, k_x) plane. The spectrum for the moving medium is merely tilted. The production of a pair of excitations, indicated by solid circles at opposite momenta, is energetically possible for $v > 2v_0$.

Next consider two (semi-infinite) media one of which moves laterally with velocity v, whereas the other is at rest. Although the boundaries modify the dispersion relation, we may assume that Eq. (4.10) *approximately* describes each medium (with $v = 0$ for the stationary body). This is justified by considering wavepackets away from boundaries. We thus have two distinct spectra: The spectrum for the plate at rest is akin to a cone while that of the moving plate is *tilted* towards the positive x axis, as in Fig. 4-2. For the sake of simplicity, we limit ourselves to $\mathbf{k} = k_x\hat{\mathbf{x}}$. Let us consider the (spontaneous) production of two particles, one in each medium. Since linear momentum is conserved the two particles must have opposite momenta (k_x and $-k_x$). This process is energetically favored if the sum of the energy of the two particles is negative, that is, spontaneous pair production occurs if it lowers the energy of the composite system. This condition is satisfied when

$$\omega_1 + \omega_2 = 2v_0|k_x| + vk_x < 0\,, \tag{4.11}$$

which is possible only if $v > 2v_0$. We stress that our argument is not specific to a particular reference frame. If both plates are moving with velocities v_1 and v_2, the

velocity v in Eq. (4.11) is replaced by $v_2 - v_1$, thus this equation puts a bound on the relative velocity.

The above argument is similar to the Landau criterion for obtaining the critical velocity of a superfluid flowing past a wall [94]. The instability of the quantum state against spontaneous production of elementary excitations (and vortices) breaks the superfluid order beyond a certain velocity. Quantum friction provides a close analog to Landau's argument in the context of macroscopic bodies. The same line of reasoning is adopted in the work of Frank and Ginzburg [90, 91, 92]. While this argument correctly predicts the threshold velocity for the onset of friction, it does not quantify the magnitude of friction and its dependence on system parameters.

4.2.2 The input-output formalism

The input-output formalism deals with the second quantized operators corresponding to incoming and outgoing wave functions, relating them through the classical scattering matrix [76, 77, 78, 66]. From the (known) distribution of the incoming modes, one can then determine the out-flux of the outgoing quanta. The input-output formalism has been used to study the dynamical Casimir effect in theoretical [42, 43] as well as experimental [31] contexts, and is recently generalized in application to lossy objects by utilizing scattering techniques [93]. In the present context of parallel plates, we consider incoming waves as originated well within each plate, far away from the gap between them (asymptotic infinity). These waves propagate towards the gap, and then scatter (backwards or forwards) to asymptotic infinities. The incoming and outgoing wave-functions for each plate are normalized such that the current density perpendicular to the surface of the plate is unity up to a sign.

The second-quantized field $\hat{\Phi}_i$ is now indexed by $i = 1, 2$ designating the two objects. This operator (with implicit index i) is now decomposed into modes

$$\hat{\Phi} = \sqrt{\frac{\hbar}{2}} \sum_{\omega \mathbf{k}_\parallel} e^{-i\omega t} (\varphi^{\text{in}}_{\omega \mathbf{k}_\parallel} \hat{a}^{\text{in}}_{\omega \mathbf{k}_\parallel} + \varphi^{\text{out}}_{\omega \mathbf{k}_\parallel} \hat{a}^{\text{out}}_{\omega \mathbf{k}_\parallel}) + \text{h.c.}\,, \tag{4.12}$$

with two copies of this equation, one for each plate. The wavefunction $\varphi_{\omega\mathbf{k}_\parallel}$, in the object's rest frame, is defined as

$$\varphi^{\text{out/in}}_{\omega\mathbf{k}_\parallel} = \begin{cases} \frac{1}{\sqrt{\tilde{k}_\perp}} e^{i\mathbf{k}_\parallel\cdot\mathbf{x}_\parallel \pm i\tilde{k}_\perp z}, & \omega > 0, \\ \frac{1}{\sqrt{\tilde{k}_\perp}} e^{i\mathbf{k}_\parallel\cdot\mathbf{x}_\parallel \mp i\tilde{k}_\perp z}, & \omega < 0, \end{cases} \tag{4.13}$$

with the prefactor being chosen to ensure the normalization, z measuring the distance from the surface, and $\tilde{k}_\perp = \sqrt{\epsilon\omega^2/c^2 - \mathbf{k}_\parallel^2}$. Note that the designation of incoming or outgoing for propagating waves depends on the relative signs of ω and $\tilde{k}_\perp$, as indicated in the above equation. For the moving plate, the corresponding wavefunctions are obtained by a Lorentz transformation of ω and k_x, while $\tilde{k}_\perp$ (being perpendicular to the velocity) remains invariant.

With the operators defined above, the input-output relation takes the form

$$\begin{pmatrix} \hat{a}_1^{\text{out}} \\ \hat{a}_2^{\text{out}} \end{pmatrix} = \mathbb{S} \begin{pmatrix} \hat{a}_1^{\text{in}} \\ \hat{a}_2^{\text{in}} \end{pmatrix}, \tag{4.14}$$

where $\mathbb{S}$ is the 2×2 scattering matrix, and the dependence on ω and $\mathbf{k}_\parallel$ is implicit. The scattering matrix can be straightforwardly computed by matching the wavefunction and its first derivatives along the boundaries. Note that a scattering channel relates a wavefunction labeled by $(\omega, \mathbf{k}_\parallel)$ on one plate to $(\omega', \mathbf{k}'_\parallel)$, the frequency and wavevector as seen from the moving frame, on the second plate. At small velocities, we have $\omega' \approx \omega - vk_x$ and $\mathbf{k}'_\parallel \approx \mathbf{k}_\parallel$. Therefore, a positive-frequency mode on one plate can be coupled to a mode with negative frequency on the other plate. However, when the frequency becomes negative, the corresponding operator changes character, i.e. an operator $a_{\omega\mathbf{k}_\parallel}$ with negative ω is, in fact, a creation operator. We can make this more explicit by writing $\hat{a}_{\omega\ \mathbf{k}_\parallel} = \hat{a}^\dagger_{-\omega\ -\mathbf{k}_\parallel}$[2]. This mixing between positive and negative frequencies is at the heart of the dynamical Casimir effect [34, 93]. In a frequency window where this mixing occurs, i.e. for $0 < \omega < vk_x$, the input-output relation is

[2]The sign of the wavevector is reversed due to complex conjugation.

recast as

$$\hat{a}^{\rm out}_{1\,\omega\mathbf{k}_\parallel} = S_{11}\,\hat{a}^{\rm in}_{1\,\omega\mathbf{k}_\parallel} + S_{21}\,\hat{a}^{\rm in\,\dagger}_{2\,vk_x-\omega\,-\mathbf{k}_\parallel}\,. \tag{4.15}$$

One can then compute the expected flux of the outgoing modes, $\langle \hat{a}_1^{\rm out\,\dagger}\hat{a}_1^{\rm out}\rangle$. At zero temperature, $\langle \hat{a}_1^{\rm in\,\dagger}\hat{a}_1^{\rm in}\rangle = 0$, and the only contribution to the outflux is due to the second term in the RHS of Eq. (4.15), resulting in

$$\langle \hat{a}^{\rm out\,\dagger}_{1\,\omega\mathbf{k}_\parallel}\,\hat{a}^{\rm out}_{1\,\omega\mathbf{k}_\parallel}\rangle = \Theta(vk_x-\omega)\;|S_{21}|^2, \tag{4.16}$$

with Θ being the Heaviside step function. The radiated energy (per unit time) is then

$$\mathcal{P} = \int_0^\infty \text{đ}\omega\, L^{D-1}\int \text{đ}\mathbf{k}_\parallel\;\hbar\omega\,\Theta(vk_x-\omega)\;|S_{21}|^2\,. \tag{4.17}$$

Similarly, since friction is the transfer of the lateral momentum, it can be computed by replacing $\hbar\omega$ by $\hbar k_x$ in the last equation. It is a simple exercise to compute the scattering matrix. One can then see that Eq. (4.17), or, more precisely, its counterpart for friction, is indeed in agreement with Eq. (4.3). The input-output formalism makes the derivation almost trivial.

Equations (4.14) and (4.15) relate annihilation and creation operators which satisfy canonical commutation relations,

$$[\hat{a}^{\rm out/in}_{i\,\omega\mathbf{k}_\parallel}, \hat{a}^{\rm out/in\,\dagger}_{j\,\omega\mathbf{k}_\parallel}] = \mathrm{sgn}(\omega)\,\delta_{ij}\,. \tag{4.18}$$

The function $\mathrm{sgn}(\omega)$ merely indicates that, for negative frequencies, the creation and annihilation operators should be identified correctly. The above canonical relations applied to Eq. (4.15) yield

$$1-|S_{11}|^2 = \mathrm{sgn}(\omega-vk_x)|S_{21}|^2\,, \tag{4.19}$$

implying that the scattering amplitude corresponding to the backscattering in the first medium is larger than unity for $\omega < vk_x$. This is an example of the so-called *superscattering* due to Zel'dovich [58]: For certain modes, a moving (rotating) object

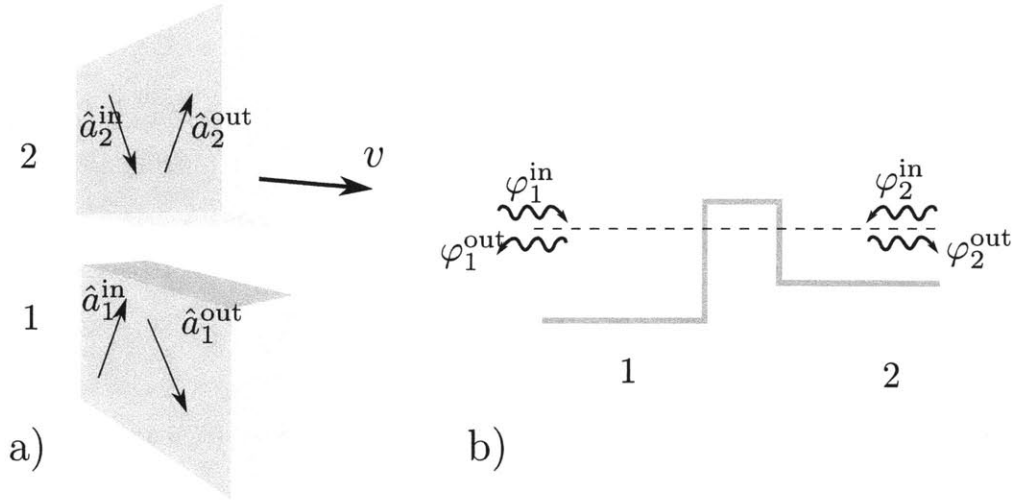

Figure 4-3: a) The operators within each object represent incoming and outgoing modes, related in the input-output formalism through the scattering matrix. b) The scattering problem is similar to the quantum tunneling over a barrier; friction resulting from transfer of momentum by the tunneling quanta.

amplifies incoming waves indicating that energy is extracted from motion. A closely related phenomenon occurs for rotating black holes and is known as the Penrose process [60]. Superradiance signals quantum instability of the moving object resulting in energy and momentum radiation, and a corresponding exertion of frictional force [58, 69, 65].[3] Equations (4.17) and (4.19) can be combined to yield

$$\mathcal{P} = \int_0^\infty \text{đ}\omega \, L^{D-1} \int \text{đ}\mathbf{k}_\parallel \, \hbar\omega \, \Theta(vk_x - \omega) \, (|S_{11}|^2 - 1) \, . \tag{4.20}$$

This expression is indeed very similar to quantum radiation from a rotating object (a rotating black hole in Ref. [61] or a rotating cylinder in Ref. [65]) with the following substitutions: $v \to \Omega$ (linear to angular velocity), $k_x \to m$ (linear to angular momentum), and S_{11} to be replaced by the scattering matrix of the rotating body.

It is worth noting that the only contribution to the radiation is from modes with $k_x > \omega/v > \omega/c$, corresponding to evanescent waves in the gap between the two plates. In this respect, the radiation is a quantum tunneling process across a barrier

[3] An alternative approach to the rotational friction is given in Ref. [56].

(in this case, the gap). We can recast the wave equation in a fashion similar to the Schröinger equation as

$$(-\partial_z^2 + V)\varphi = 0\,, \tag{4.21}$$

with $V_1 = -(\epsilon\,\omega^2/c^2 - \mathbf{k}_\parallel^2)$, $V_2 = -(\epsilon\,(\omega - vk_x)^2/c^2 - \mathbf{k}_\parallel^2)$, and $V_{\rm gap} = |\omega^2/c^2 - \mathbf{k}_\parallel^2|$; see Fig. 4-3. The relative motion of the two media results in a steady tunneling of particles of opposite momenta from one plate to another, thus leading to the slowdown of the motion.

4.2.3 Inner-product method

To quantize a field theory, a first step is to decompose the quadratic part of the Hamiltonian into a collection of (infinite) harmonic oscillators; define the corresponding annihilation and creation operators, and impose canonical commutation relations. One can then construct the Fock space with the vacuum state of no particles, and excited single- and multi-particle states obtained by applying creation operators. In high energy physics, the usual starting point is empty space, but the above procedure works equally well in the presence of background matter, as is the case for the Casimir effect. The reason is that canonical quantization only relies upon time translation and time reversal symmetry. The former allows construction of eigenmodes of a definite frequency, which is the basis of the notion of modes/quanta/particles. Time reversal symmetry, on the other hand, is used to identify creation and annihilation operators: The coefficient of a positive (negative) frequency mode is understood as an annihilation (creation) operator. To make this correspondence explicit, consider a quantum field $\hat{\Phi}(t, \mathbf{x})$, possibly in the presence of a background *object* which is static. One can find a basis of eigenmodes $\phi_{\omega\alpha}(\mathbf{x})$ labeled by frequency ω and quantum number α to expand the field as

$$\hat{\Phi}(t, \mathbf{x}) = \sqrt{\frac{\hbar}{2}} \sum_{\omega>0,\,\alpha} e^{-i\omega t}\phi_{\omega\alpha}(\mathbf{x})\,\hat{a}_{\omega\alpha} + e^{i\omega t}\phi^*_{\omega\alpha}(\mathbf{x})\,\hat{a}^\dagger_{\omega\alpha}\,, \tag{4.22}$$

with (defining $\delta(x) = 2\pi\delta(x)$)

$$[a_{\omega_1\alpha}, a^\dagger_{\omega_2\beta}] = \delta(\omega_1 - \omega_2)\,\delta_{\alpha\beta}\,. \tag{4.23}$$

The latter follows from the canonical commutation relations between the field $\hat{\Phi}(t, \mathbf{x})$ and its conjugate momentum $\hat{\Pi}(t, \mathbf{y})$,

$$[\hat{\Phi}(t, \mathbf{x}), \hat{\Pi}(t, \mathbf{y})] = i\hbar\,\delta(\mathbf{x} - \mathbf{y}). \tag{4.24}$$

When the object is moving, we lose one or both symmetries in time. The case of two parallel plates in lateral motion respects time translation symmetry as the relative position does not change. Time reversal symmetry, on the other hand, is broken; in the backward direction of time the plate moves in the opposite direction. In the absence of time reversal symmetry, the above correspondence between positive (negative) frequency and the annihilation (creation) operators breaks down. There is, however, a more general way to identify operators as follows. Let us consider two functions ϕ_1 and ϕ_2, which are solutions to the classical field equation, and define an inner product as [95, 96]

$$\langle \phi_1, \phi_2 \rangle = \frac{i}{2} \int \mathrm{d}\mathbf{x}\, (\phi_1^* \pi_2 - \pi_1^* \phi_2), \tag{4.25}$$

where π_i is the corresponding conjugate momentum, and the integral is over the whole space. One can easily see that the inner product defined in Eq. (4.25) is independent of the choice of the reference frame or the (space-like) hypersurface as the integration domain. Furthermore, we can always find a set of functions $\phi_{\omega\alpha}$ which solve the classical field equation and form an orthonormal basis,[4]

$$\langle \phi_{\omega_1\alpha}, \phi_{\omega_2\beta} \rangle = \delta(\omega_1 - \omega_2)\delta_{\alpha\beta}, \tag{4.26}$$

[4]Note that ω is still a good quantum number because of the translation symmetry in time.

while their conjugate modes are orthonormal up to a negative sign,

$$\langle \phi^*_{\omega_1\alpha}, \phi^*_{\omega_2\beta} \rangle = -\delta(\omega_1 - \omega_2)\delta_{\alpha\beta}. \tag{4.27}$$

These modes form a complete basis, such that the field $\hat{\Phi}$ can be expanded as

$$\hat{\Phi}(t, \mathbf{x}) = \sqrt{\frac{\hbar}{2}} \sum_{\omega\alpha:\, \text{positive-norm}} e^{-i\omega t}\phi_{\omega\alpha}(\mathbf{x})\, \hat{a}_{\omega\alpha} + e^{i\omega t}\phi^*_{\omega\alpha}(\mathbf{x})\, \hat{a}^\dagger_{\omega\alpha}\,. \tag{4.28}$$

Note that unlike Eq. (4.22), an annihilation (creation) mode is identified with a positive (negative) norm and not frequency; the latter depends on the reference frame while the former does not. The above relations become obvious for a field theory in a static background where the conjugate momentum is proportional to $\partial_t\Phi$; Eq. (4.25) then implies that a positive (negative) ω corresponds to positive (negative) norm.

The inner-product method is used in application to quantum field theory in curved space-time. For example, it has been employed to show that a rotating black hole is unstable due to spontaneous emission [61]. For two parallel plates in motion, we first introduce a complete basis. Due to the translation symmetry in time and space (parallel to the plates' surface), wavefunctions can be labelled by frequency ω and tangential wavevector $\mathbf{k}_\parallel$ defined in the lab frame where the first plate is at rest and the second one is moving. There are two independent solutions defined as

$$\phi^{\mathrm{I}}_{\omega\mathbf{k}_\parallel} = \begin{cases} \varphi^{\mathrm{in}}_{1\,\omega\mathbf{k}_\parallel} + S_{11}\, \varphi^{\mathrm{out}}_{1\,\omega\mathbf{k}_\parallel}, & \text{plate 1,} \\ S_{21}\, \varphi^{\mathrm{out}}_{2\,\omega\mathbf{k}_\parallel}, & \text{plate 2,} \end{cases} \tag{4.29}$$

and

$$\phi^{\mathrm{II}}_{\omega\mathbf{k}_\parallel} = \begin{cases} S_{12}\, \varphi^{\mathrm{out}}_{1\,\omega\mathbf{k}_\parallel}, & \text{plate 1,} \\ \varphi^{\mathrm{in}}_{2\,\omega\mathbf{k}_\parallel} + S_{22}\, \varphi^{\mathrm{out}}_{2\,\omega\mathbf{k}_\parallel}, & \text{plate 2.} \end{cases} \tag{4.30}$$

The incoming and outgoing functions are defined in Eq. (4.13), with the functions in the second plate properly Lorentz-transformed; see the explanation below Eq. (4.13). To find the conjugate momentum, note that Eq. (4.1) can be schematically derived

from a Lagrangian $\mathcal{L} = \frac{1}{2}[\frac{1}{v_0^2}(\partial_t\Phi)^2 - (\nabla\Phi)^2]$ with $v_0 = c/\sqrt{\epsilon}$, hence $\Pi = \partial L/\partial\dot{\Phi} = \frac{1}{v_0^2}\,\partial_t\Phi$. Similarly for a moving object $\mathcal{L} \approx \frac{1}{2}[\frac{1}{v_0^2}(\partial_t\Phi + v\partial_x\Phi)^2 - (\nabla\Phi)^2]$ and $\Pi = \frac{1}{v_0^2}(\partial_t\Phi + v\partial_x\Phi)$. In terms of partial waves, $\pi_{\omega\mathbf{k}} = -i\frac{\omega - vk_x}{v_0^2}\,\phi_{\omega\mathbf{k}}$ within the moving plate and similarly for the static plate with $v = 0$.[5] One can then see that

$$\langle \phi^{\rm I}_{\omega_1\mathbf{k}_\parallel}, \phi^{\rm I}_{\omega_2\mathbf{l}_\parallel}\rangle = \bar{\delta}(\omega_1 - \omega_2)\,\bar{\delta}(\mathbf{k}_\parallel - \mathbf{l}_\parallel), \qquad \omega_1 > 0, \tag{4.31}$$

and

$$\langle \phi^{\rm II}_{\omega_1\mathbf{k}_\parallel}, \phi^{\rm II}_{\omega_2\mathbf{l}_\parallel}\rangle = \mathrm{sgn}(\omega_1 - vk_x)\,\bar{\delta}(\omega_1 - \omega_2)\,\bar{\delta}(\mathbf{k}_\parallel - \mathbf{l}_\parallel), \quad \omega_1 > 0. \tag{4.32}$$

(We have exploited the fact that the norms are diagonal in frequency to obtain the delta functions in $\tilde{k}_\perp$ which are then converted to those of ω.[6]) Note that the (super)unitary relation in Eq. (4.19) is essential in deriving the norms. Functions of type I have positive norm so they serve as the coefficients of annihilation operators. However, type II functions include negative-norm modes for $0 < \omega < vk_x$. Therefore, despite the positive sign of frequency, the latter should be identified as creation operators. We thus expand the field as

$$\frac{\hat{\Phi}(t,\mathbf{x})}{\sqrt{\hbar/2}} = \sum_{\omega>0,\,\mathbf{k}_\parallel} e^{-i\omega t}\phi^{\rm I}_{\omega\mathbf{k}_\parallel}(\mathbf{x})\,\hat{a}^{\rm I}_{\omega\mathbf{k}_\parallel} + \sum_{0<\omega\,,vk_x<\omega\,,\mathbf{k}_\parallel} e^{-i\omega t}\phi^{\rm II}_{\omega\mathbf{k}_\parallel}(\mathbf{x})\,\hat{a}^{\rm II}_{\omega\mathbf{k}_\parallel} + \sum_{0<\omega<vk_x,\,\mathbf{k}_\parallel} e^{-i\omega t}\phi^{\rm II}_{\omega\mathbf{k}_\parallel}(\mathbf{x})\,\hat{a}^{\rm II\,\dagger}_{\omega\mathbf{k}_\parallel} + \text{h.c.}, \tag{4.33}$$

where the summation is a shorthand for multiple integrals, and $\hat{a}$ and $\hat{a}^\dagger$ satisfy the usual commutation relations. The radiation within the first plate is given by

$$\begin{aligned}\frac{\mathcal{P}}{L^{D-1}} &= \langle \partial_t\Phi\,\partial_z\Phi\rangle \\ &= \int_0^\infty \mathrm{d}\omega \int \mathrm{d}\mathbf{k}_\parallel \frac{\hbar\omega}{2}\Big\{-(1 - |S_{11}|^2) + |S_{12}|^2\Big\} \\ &= \int_0^\infty \mathrm{d}\omega \int \mathrm{d}\mathbf{k}_\parallel\, \hbar\omega\,\Theta(vk_x - \omega)\,|S_{12}|^2\,,\end{aligned} \tag{4.34}$$

[5] An alternative is to define the integration hypersurface to consist of each object's rest frame.

[6] The integral over the gap does not contribute to the frequency delta functions and thus is neglected.

where we have again exploited Eq. (4.19), arriving at the same results as in the previous sections. Notice that only *superradiating modes* contribute to the radiation while other modes cancel out in the second line of the last equation.

4.2.4 Radiated energy: The Rytov formalism

In this section, we employ the *Rytov* formalism [55] to study the correspondence between friction and radiation in some detail. This formalism is based on the fluctuation-dissipation theorem, and has been extensively used in the context of non-contact friction [53]; see also Ref. [54] and references therein. This section goes beyond the existing literature by computing various correlation functions and the energy radiation within the plates (as well as in the gap between them) and discuss their dependence on the reference frame.

We start by relating fluctuations of the field to those of "sources" within each medium by

$$-\left(\triangle+\frac{\omega^2}{c^2}\,\epsilon(\omega,\mathbf{x})\right)\Phi(\omega,\mathbf{x})=-\frac{i\omega}{c}\,\rho_\omega(\mathbf{x})\,. \tag{4.35}$$

The "charge" ρ fluctuates around zero mean with correlations (co-variance)

$$\langle\rho_\omega(\mathbf{x})\rho^*_\omega(\mathbf{y})\rangle=a(\omega)\,\mathrm{Im}\,\epsilon(\omega,\mathbf{x})\,\delta(\mathbf{x}-\mathbf{y}), \tag{4.36}$$

where

$$a(\omega)=2\hbar\left[n(\omega,T)+\frac{1}{2}\right]=\hbar\,\coth\left(\frac{\hbar\omega}{2k_BT}\right)\,. \tag{4.37}$$

The field is related to the sources via the Green's function, G, defined by

$$-\left(\triangle+\frac{\omega^2}{c^2}\epsilon(\omega,\mathbf{x})\right)G(\omega,\mathbf{x},\mathbf{z})=\delta(\mathbf{x}-\mathbf{z}). \tag{4.38}$$

In equilibrium (uniform temperature and static), this results in the field correlations

$$\langle\Phi(\omega,\mathbf{x})\Phi^*(\omega,\mathbf{y})\rangle=$$

$$= \frac{\omega^2}{c^2} \int_{\text{All space}} \mathrm{d}\mathbf{z}\, G(\omega,\mathbf{x},\mathbf{z}) G^*(\omega,\mathbf{y},\mathbf{z})\, \langle \rho_\omega(\mathbf{z}) \rho_\omega^*(\mathbf{z}) \rangle$$
$$= \frac{\omega^2}{c^2} a(\omega) \int_{\text{All space}} \mathrm{d}\mathbf{z}\, G(\omega,\mathbf{x},\mathbf{z})\, \mathrm{Im}\, \epsilon(\omega,\mathbf{z})\, G^*(\omega,\mathbf{y},\mathbf{z})$$
$$= a(\omega)\, \mathrm{Im}\, G(\omega,\mathbf{x},\mathbf{y}), \tag{4.39}$$

in agreement with the fluctuation-dissipation condition which relates correlation functions to dissipation through the imaginary part of the response function. Note that the second line in Eq. (4.39) follows from $\frac{\omega^2}{c^2}\,\mathrm{Im}\,\epsilon = -\,\mathrm{Im}\,G^{-1}$ according to Eq. (4.38).

For the case of two plates, we first compute the correlation function for two points in the gap. The source fluctuations in each plate will be treated separately; starting with those in the static plate (indicated by subindex 1 on the integral)

$$\langle \Phi(\omega,\mathbf{x}) \Phi^*(\omega,\mathbf{y}) \rangle_1 = \frac{\omega^2}{c^2} a_1(\omega) \int_1 \mathrm{d}\mathbf{z}\, G(\omega,\mathbf{x},\mathbf{z})\, \mathrm{Im}\, \epsilon(\omega,\mathbf{z})\, G^*(\omega,\mathbf{y},\mathbf{z})$$
$$= \frac{\omega^2}{2ic^2} a_1(\omega) \int_1 \mathrm{d}\mathbf{z}\, \left[\epsilon(\omega,\mathbf{z}) G(\omega,\mathbf{x},\mathbf{z})\right]\, G^*(\omega,\mathbf{y},\mathbf{z}) - G(\omega,\mathbf{x},\mathbf{z})\, \left[\epsilon(\omega,\mathbf{z}) G(\omega,\mathbf{y},\mathbf{z})\right]^*$$
$$= \frac{i}{2} a_1(\omega) \int_1 \mathrm{d}\mathbf{z}\, \left[\triangle_{\mathbf{z}} G(\omega,\mathbf{x},\mathbf{z})\right]\, G^*(\omega,\mathbf{y},\mathbf{z}) - G(\omega,\mathbf{x},\mathbf{z})\, \triangle_{\mathbf{z}} G^*(\omega,\mathbf{y},\mathbf{z})$$
$$= \frac{i}{2} a_1(\omega) \int_1 \mathrm{d}\mathbf{\Sigma} \cdot \left[\left(\nabla_{\mathbf{z}} G(\omega,\mathbf{x},\mathbf{z})\right) G^*(\omega,\mathbf{y},\mathbf{z}) - G(\omega,\mathbf{x},\mathbf{z})\, \nabla_{\mathbf{z}} G^*(\omega,\mathbf{y},\mathbf{z})\right]. \tag{4.40}$$

Note that we used Eq. (4.38) in going from the second to the third line above, and then integrated by parts to obtain an integral over the surface adjacent to the gap. The contribution due to the other surface at infinity vanishes since ϵ is assumed to have a small but finite imaginary part.

To compute the surface integral in Eq. (4.40), one needs the (out-out) Green's function with both points in the gap. The latter is given by Eq. (C.1), and leads to

$$\langle \Phi(\omega,\mathbf{x}) \Phi^*(\omega,\mathbf{y}) \rangle_1 = -\sum_\alpha \frac{a_1(\omega)}{4p_\alpha^*} \frac{|e^{ip_\alpha d}|^2}{|1 - e^{2ip_\alpha d} R_\alpha \tilde{R}_\alpha|^2} |U(R_\alpha)|^2 \times$$
$$\left(\Phi_{\tilde{\alpha}}^{\mathrm{reg}}(\omega,\tilde{\mathbf{x}}) + \tilde{R}_{\tilde{\alpha}} \Phi_{\tilde{\alpha}}^{\mathrm{out}}(\omega,\tilde{\mathbf{x}})\right) \overline{\left(\Phi_{\tilde{\alpha}}^{\mathrm{reg}}(\omega,\tilde{\mathbf{y}}) + \tilde{R}_{\tilde{\alpha}} \Phi_{\tilde{\alpha}}^{\mathrm{out}}(\omega,\tilde{\mathbf{y}})\right)}. \tag{4.41}$$

In this equation, R_α ($\tilde{R}_\alpha$) is the reflection coefficient from the first (second) object with

α being a shorthand for both the frequency and wavevector. Also $\mathbf{x}/\mathbf{y}$ ($\tilde{\mathbf{x}}/\tilde{\mathbf{y}}$) is the distance from a reference point on the surface of the first (second) plate—the reference points on two surfaces have identical parallel components, $\mathbf{x}_\parallel = \tilde{\mathbf{x}}_\parallel$, but differ in their z-component as $z_{\tilde{\mathbf{x}}} = d - z_{\mathbf{x}}$. The regular and outgoing functions are defined with respect to the corresponding plate; see Appendix A for more details. Furthermore, the overbar notation implies complex conjugation, and $|U(R_\alpha)|^2$ is defined as

$$|U(R_\alpha)|^2 = \frac{\int \mathrm{d}\boldsymbol{\Sigma} \cdot \left[\Phi_\alpha^* \nabla\Phi_\alpha - (\nabla\Phi_\alpha^*)\,\Phi_\alpha\right]}{\int \mathrm{d}\boldsymbol{\Sigma} \cdot \left[\Phi_\alpha^{\mathrm{reg}*} \nabla\Phi_\alpha^{\mathrm{reg}} - (\nabla\Phi_\alpha^{\mathrm{reg}*})\,\Phi_\alpha^{\mathrm{reg}}\right]}\,, \tag{4.42}$$

with $\Phi_\alpha = \Phi_\alpha^{\mathrm{reg}}(\omega,\mathbf{z}) + R_\alpha \Phi_\alpha^{\mathrm{out}}(\omega,\mathbf{z})$, such that

$$\begin{aligned} |U(R_\alpha)|^2 &= 1 - |R_\alpha|^2, \qquad \alpha \in \text{propagating waves,} \\ &= 2\,\mathrm{Im}\, R_\alpha, \qquad \alpha \in \text{evanescent waves.} \end{aligned} \tag{4.43}$$

One can similarly find the correlation function due to source fluctuations in the second plate

$$\begin{aligned} \langle \Phi(\omega,\mathbf{x})\Phi^*(\omega,\mathbf{y})\rangle_2 = -\sum_\alpha \frac{a_1(\omega - \mathbf{v}\cdot\mathbf{k}_\alpha)}{4p_\alpha^*} \frac{|e^{ip_\alpha d}|^2}{|1 - e^{2ip_\alpha d} R_\alpha \tilde{R}_\alpha|^2} |U(\tilde{R}_\alpha)|^2 \times \\ \left(\Phi_{\tilde{\alpha}}^{\mathrm{reg}}(\omega,\mathbf{x}) + R_{\tilde{\alpha}}\Phi_{\tilde{\alpha}}^{\mathrm{out}}(\omega,\mathbf{x})\right) \overline{\left(\Phi_{\tilde{\alpha}}^{\mathrm{reg}}(\omega,\mathbf{y}) + R_{\tilde{\alpha}}\Phi_{\tilde{\alpha}}^{\mathrm{out}}(\omega,\mathbf{y})\right)}\,. \end{aligned} \tag{4.44}$$

The total correlation function is the sum of the contributions due to each plate,

$$\langle \Phi(\omega,\mathbf{x})\Phi^*(\omega,\mathbf{y})\rangle = \langle \Phi(\omega,\mathbf{x})\Phi^*(\omega,\mathbf{y})\rangle_1 + \langle \Phi(\omega,\mathbf{x})\Phi^*(\omega,\mathbf{y})\rangle_2.$$

The frictional force is then computed as the average of the appropriate component of the stress tensor as

$$f = \int_{-\infty}^{\infty} \mathrm{d}\omega \int \mathrm{d}\Sigma\, \langle \partial_x \Phi(\omega,\mathbf{x}) \partial_z \Phi^*(\omega,\mathbf{x})\rangle$$

$$= \int_0^\infty đ\omega\, L^{D-1} \int đ\mathbf{k}_\parallel\, \hbar k_x \frac{|e^{ik_\perp d}|^2\, |U(R_{\omega\mathbf{k}_\parallel})|^2 |U(\tilde{R}_{\omega\mathbf{k}_\parallel})|^2}{|1 - e^{2ik_\perp d} R_{\omega\mathbf{k}_\parallel} \tilde{R}_{\omega\mathbf{k}_\parallel}|^2} (n_1(\omega) - n_2(\omega - \mathbf{v}\cdot\mathbf{k})), \tag{4.45}$$

where we have restored $\mathbf{k}_\parallel$ in place of α. Further manipulations lead to Eq. (4.3). Similarly, the Rytov formalism allows us to calculate the energy flux from one object to the other as

$$\begin{aligned} P_{\text{gap}} &= \int_{-\infty}^\infty đ\omega \int \mathrm{d}\Sigma\, \langle \partial_t \Phi(\omega, \mathbf{x}) \partial_z \Phi^*(\omega, \mathbf{x}) \rangle \\ &= \int_0^\infty đ\omega\, L^{D-1} \int đ\mathbf{k}_\parallel\, \hbar\omega \frac{|e^{ik_\perp d}|^2\, |U(R_{\omega\mathbf{k}_\parallel})|^2 |U(\tilde{R}_{\omega\mathbf{k}_\parallel})|^2}{|1 - e^{2ik_\perp d} R_{\omega\mathbf{k}_\parallel} \tilde{R}_{\omega\mathbf{k}_\parallel}|^2} (n_1(\omega) - n_2(\omega - \mathbf{v}\cdot\mathbf{k})), \end{aligned} \tag{4.46}$$

i.e. by merely replacing $\hbar k_x$ with $\hbar\omega$ in Eq. (4.45).

Next we compute the energy flux *through each plate.* Since the dielectric function is assumed to be a real constant (albeit with a vanishingly small imaginary part), we can circumvent ambiguities in defining the Maxwell stress tensor in a lossy medium [79]. In the following, we find the field correlation function in the first (static) plate due to source fluctuations in the moving plate, by using an analog of Eq. (4.40) but evaluating a surface integral on the second plate. However, in this case, the appropriate Green's function is the (out-in) type given in Eq. (C.4). We then find the latter correlation function as

$$\begin{aligned} \langle \Phi(\omega, \mathbf{x}) \Phi^*(\omega, \mathbf{y}) \rangle_2 = \sum_\alpha \frac{a_2(\omega - \mathbf{v}\cdot\mathbf{k}_\alpha)}{4p_\alpha^*} \frac{|e^{ip_\alpha d}|^2}{|1 - e^{2ip_\alpha d} R_\alpha \tilde{R}_\alpha|^2} |U(\tilde{R}_\alpha)|^2 \times \\ \left(V_\alpha \psi_\alpha^+(\omega, \mathbf{x}) + W_\alpha \psi_\alpha^-(\omega, \mathbf{x})\right) \overline{\left(V_\alpha \psi_\alpha^+(\omega, \mathbf{y}) + W_\alpha \psi_\alpha^-(\omega, \mathbf{y})\right)}\,, \end{aligned} \tag{4.47}$$

where $\mathbf{x}$ and $\mathbf{y}$ are both inside the first plate, V and W are coefficients depending on α and system parameters, and the functions ψ are defined inside the medium; see Appendix A for more details. Henceforth, we assume that the objects are at zero temperature. Anticipating that only evanescent waves contribute, we obtain the

energy flux in the first plate due to the fluctuations in the second plate as [7]

$$P_2^{(1)} = \int đ\omega\, L^{D-1} \int đ\mathbf{k}_\parallel\ \hbar\omega\, \frac{e^{-2|k_\perp|d}}{|1 - e^{-2|k_\perp|d} R_{\omega\mathbf{k}_\parallel} \tilde{R}_{\omega\mathbf{k}_\parallel}|^2}\, 2\,\mathrm{Im}\, R_{\omega\mathbf{k}_\parallel}\, 2\,\mathrm{Im}\, \tilde{R}_{\omega\mathbf{k}_\parallel}\, \mathrm{sgn}(\omega - \mathbf{v}\cdot\mathbf{k}), \tag{4.48}$$

where we have used the fact that, for evanescent waves, $p_\alpha \equiv k_\perp = \sqrt{\omega^2/c^2 - \mathbf{k}_\parallel^2}$ is purely imaginary while $\tilde{p}_\alpha \equiv \tilde{k}_\perp = \sqrt{\epsilon\,\omega^2/c^2 - \mathbf{k}_\parallel^2}$ is real, leading to

$$|V_\alpha|^2 - |W_\alpha|^2 = \frac{|p_\alpha|}{\tilde{p}_\alpha}\, 2\,\mathrm{Im}\, R_\alpha\,. \tag{4.49}$$

In order to take into account the source fluctuations in the first plate (where we compute the field correlation function), we need the (in-in) Green's function in Eq. (C.8). The energy flux due to the latter fluctuations, $P_1^{(1)}$, is computed similarly but there is one subtlety. Unlike the previous cases, the correlation function is evaluated at points where there are also fluctuating sources. However, Eq. (4.40) contains, beyond the surface integral, a term proportional to $\mathrm{Im}\, G(\omega, \mathbf{x}, \mathbf{y})$ which does not contribute to the radiation. The remaining computation is similar to the previous case, and the overall energy flux is obtained as

$$\begin{aligned} P^{(1)} &= P_1^{(1)} + P_2^{(1)} \\ &= \int_0^\infty đ\omega\, L^{D-1} \int đ\mathbf{k}_\parallel\ \hbar\omega\, \frac{e^{-2|k_\perp|d}\, 2\,\mathrm{Im}\, R_{\omega\mathbf{k}_\parallel}\, 2\,\mathrm{Im}\, \tilde{R}_{\omega\mathbf{k}_\parallel}}{|1 - e^{2ik_\perp d} R_{\omega\mathbf{k}_\parallel} \tilde{R}_{\omega\mathbf{k}_\parallel}|^2}\, \Theta(\mathbf{v}\cdot\mathbf{k} - \omega). \end{aligned} \tag{4.50}$$

This is again in harmony with the results in the previous sections.

Comparing Eqs. (4.50) and (4.46), we observe that in the reference frame in which the first plate is at rest,

$$P^{(1)} = P_{\mathrm{gap}}. \tag{4.51}$$

However, P_{gap} must vanish in the *center of mass* (c.m.) frame from symmetry considerations. It can be obtained explicitly by a Lorentz transformation from the lab

[7] Inside the object, the "Poynting vector" is defined by the same tensor $\partial_t\Phi\partial_z\Phi$.

frame, which, to the lowest order in velocity, takes the form

$$0 = P_{\rm gap}^{\rm c.m.} = P_{\rm gap} - vf/2, \tag{4.52}$$

indicating $P^{(1)} = vf/2$. This conclusion can be verified directly as follows: First note that Eqs. (4.45) and (4.50) yield

$$P^{(1)} - \frac{vf}{2} = \int_{k_x>0} đ\mathbf{k}_\parallel \int_0^{vk_x} đ\omega\, \hbar \left(\omega - \frac{vk_x}{2}\right) \frac{e^{-2|k_\perp|d}\, 2\,\mathrm{Im}\, R_{\omega\mathbf{k}_\parallel}\, 2\,\mathrm{Im}\, \tilde{R}_{\omega\mathbf{k}_\parallel}}{|1 - e^{2ik_\perp d} R_{\omega\mathbf{k}_\parallel} \tilde{R}_{\omega\mathbf{k}_\parallel}|^2}, \tag{4.53}$$

where the x axis is chosen parallel to the velocity $\mathbf{v}$. Let us make the following change of variables

$$\begin{aligned} \omega' &= \omega - vk_x/2, \\ k_x' &= k_x - v\omega/2c^2 \approx k_x, \\ k_i' &= k_i, \quad i \neq x. \end{aligned} \tag{4.54}$$

It then follows that

$$P^{(1)} - \frac{vf}{2} = \int_{k_x'>0} đ\mathbf{k}_\parallel' \int_{-vk_x'/2}^{vk_x'/2} đ\omega' \hbar\omega' \frac{e^{-2|k_\perp|d}\, 2\,\mathrm{Im}\, R^-_{\omega',\mathbf{k}_\parallel'}\, 2\,\mathrm{Im}\, R^+_{\omega',\mathbf{k}_\parallel'}}{|1 - e^{2ik_\perp d} R^-_{\omega',\mathbf{k}_\parallel'} R^+_{\omega',\mathbf{k}_\parallel'}|^2}, \tag{4.55}$$

where R^+ and R^- are the reflection matrices from plates moving at velocities $v/2$ and $-v/2$, respectively, along the x axis. Since ϵ is real[8], we have

$$R^+_{-\omega',\mathbf{k}_\parallel'} = R^-_{\omega',\mathbf{k}_\parallel'}. \tag{4.56}$$

This implies that the integrand in Eq. (4.55) is antisymmetric with respect to ω' so that the integral vanishes.

When there is friction, work must be done to keep the moving plate in steady

[8]In general, the real part of the response function is even in frequency, i.e. $\mathrm{Re}\,\epsilon(\omega) = \mathrm{Re}\,\epsilon(-\omega)$.

motion. This work should be equal to the total energy dissipated in the plates,

$$vf = P_{\rm tot}, \tag{4.57}$$

where $P_{\rm tot}$ is the sum of energy flux through each plate. For Eq. (4.57) to hold, the energy flux through the second (moving) plate should also be equal to $P^{(1)} = vf/2$. In the *center-of-mass* frame too, we should have the same condition because of the energy conservation $vf = P^{(1)}_{\rm c.m.} + P^{(2)}_{\rm c.m.}$, and the symmetry $P^{(1)}_{\rm c.m.} = P^{(2)}_{\rm c.m.}$. (The force in the *center-of-mass* frame is almost identical to the lab frame since the velocity is small compared to the speed of light.) Therefore, we conjecture that $P^{(1)}_S = P^{(2)}_S = vf/2$ irrespective of the reference frame S, while $P^S_{\rm gap}$ sensitively depends on the reference frame S; it is $vf/2$ when the first plate is at rest, $-vf/2$ when the second plate is at rest, and zero in the *center of mass* frame.

Chapter 5

Outlook

In this thesis, we have developed a unified scattering approach to fluctuation-induced phenomena in moving systems. Extensions to other field theories should be of both theoretical and practical interest. A superfluid liquid, for example, presents a natural framework to study the effects of motion in a quantum vacuum. Indeed, similar effects such as radiation and spontaneous emission have been discussed in this context [63]. The theory of a superfluid condensate is more complicated due to the nonlinearity in the self-consistent field equations akin to the nonlinear Schrödinger equation, and the spectrum of the theory consists of both elementary excitations as well as vortices [97]. One can hope that scattering theory and input-output formalism would be useful in application to non-equilibrium situations.

Dynamical Casimir effect is widely considered to be related to Unruh effect [27] where an accelerating observer finds the quantum vacuum in a thermal bath with a temperature proportional to its acceleration [98]. The link, however, is not clear as the two effects correspond to two different reference frames: The dynamical Casimir effect makes predictions for an accelerating object in an *inertial* reference frame (which, by the way, implies no radiation by a constantly accelerated perfect mirror) while Unruh effect is pertinent to an *accelerating* frame. Nevertheless, these effects can be related by introducing a particle *detector*: According to Unruh, an accelerated detector beeps by absorbing photons in a thermal bath, while the inertial observer interprets the detector as a lossy object which heats up due to its motion similar to the rotating

body discussed in Section 2. The comparison between the two perspectives requires a generalization of the formalism presented in Sec. 3.1 to include both acceleration and lossy-ness where an expression solely in terms of the scattering matrix is desired.[1]

It is also worthwhile to consider configurations of multiple objects in arbitrary motion. We have partially tackled this problem in the context of stationary motion in Section 3.3 and non-contact friction in Section 4, while extensions to accelerating objects will present new challenges and provide further insights. Specifically, one can ask how the (inertial as well as dissipative) forces between two objects change as the result of their motion or acceleration.

The formulation of the dynamical Casimir effect in terms of the scattering matrix should also provide an efficient prescription for numerical computations. The scattering matrix is purely a classical quantity, and presumably can be numerically computed with high precision. This is particularly important if the motion cannot be treated perturbatively—when the speed, the amplitude of oscillations, or the corrugations of boundaries are not small. Even in these cases, the scattering formalism is applicable, and numerical methods should prove useful.

[1] A solid of revolution under rotation is an exception since its orientation and shape are constant and thus time translation symmetry is respected.

Appendix A

Green's theorem

The vector Green's theorem reads

$$E_i(\mathbf{x}) = \oint d\mathbf{\Sigma} \cdot \left[(\nabla \times \mathbf{G}_i(\mathbf{x}, \mathbf{z})) \times \mathbf{E}(\mathbf{z}) + \mathbf{G}_i(\mathbf{x}, \mathbf{z}) \times (\nabla \times \mathbf{E}(\mathbf{z})) \right], \tag{A.1}$$

where E_i is the i component of the electric field $\mathbf{E}$ which satisfies the vector Helmholtz equation, and $\mathbf{G}_i$ is a vector defined from the dyadic Green's function as $(\mathbf{G}_i)_j = \mathbb{G}_{ij}$. Also note that the point $\mathbf{x}$ is enclosed by the boundary of the integration. We choose $\mathbf{E} = \mathbf{E}_\beta^{\text{reg}}$, a partial wave indexed by β, and also employ the definition of the Green's function in Eq. (2.86) to find

$$[\mathbf{E}_\beta^{\text{reg}}(\mathbf{x})]_i = i \sum_\alpha (\mathbf{E}_\alpha^{\text{reg}}(\mathbf{x}))_i \oint d\mathbf{\Sigma} \cdot \left[(\nabla \times \mathbf{E}_{\bar{\alpha}}^{\text{out}}(\mathbf{z})) \times \mathbf{E}_\beta^{\text{reg}}(\mathbf{z}) + \mathbf{E}_{\bar{\alpha}}^{\text{out}}(\mathbf{z}) \times (\nabla \times \mathbf{E}_\beta^{\text{reg}}(\mathbf{z})) \right]. \tag{A.2}$$

The vector fields $\mathbf{E}_\alpha^{\text{reg}}$ constitute a complete set, hence

$$i \oint d\mathbf{\Sigma} \cdot \left[(\nabla \times \mathbf{E}_{\bar{\alpha}}^{\text{out}}(\mathbf{z})) \times \mathbf{E}_\beta^{\text{reg}}(\mathbf{z}) + \mathbf{E}_{\bar{\alpha}}^{\text{out}}(\mathbf{z}) \times (\nabla \times \mathbf{E}_\beta^{\text{reg}}(\mathbf{z})) \right] = \delta_{\alpha\beta}. \tag{A.3}$$

Using the definition of the regular wave-functions, we arrive at Eq. (2.91).

Appendix B

Scattering matrices

In this Appendix, we derive the scattering matrix for specific geometries. The Dirichlet boundary conditions are assumed throughout this section.

B.1 Plate

The perturbative scheme introduced in Sec. 3.2.1 can be generalized to d dimensions. We designate the coordinates spanning the surface by $\mathbf{x}_\parallel$ and the normal coordinate by z. The incoming and outgoing waves are identified as

$$\Phi^{\text{in/out}}_{\omega\mathbf{k}_\parallel}(t,\mathbf{x}) = \frac{1}{\sqrt{k_\perp}} \exp(-i\omega t + i\mathbf{k}_\parallel \cdot \mathbf{x}_\parallel \mp i k_\perp z)\,, \tag{B.1}$$

for $\omega > 0$ (and defined conversely for $\omega < 0$) where $\mathbf{k}_\parallel$ is a $(d-1)$-component wavevector parallel to the surface of the plate, and $k_\perp(\omega, \mathbf{k}_\parallel) = \sqrt{\omega^2/c^2 - \mathbf{k}_\parallel^2}$. Consider Φ_0 as the solution to the Dirichlet boundary problem for a static mirror,

$$\Phi_0(t,\mathbf{x}) = \Phi^{\text{in}}_{\omega\mathbf{k}_\parallel}(t,\mathbf{x}) - \Phi^{\text{out}}_{\omega\mathbf{k}_\parallel}(t,\mathbf{x})\,. \tag{B.2}$$

The scattering matrix can be computed perturbatively by organizing the field as $\Phi = \Phi_0 + \Phi_1 + \cdots$. The Dirichlet boundary condition, $\Phi(t, \mathbf{x}_\parallel, z + q(t,\mathbf{x}_\parallel)) = 0$, to

the first order is given by

$$\Phi_1(t, \mathbf{x}_\parallel, 0) = -q(t, \mathbf{x}_\parallel)\partial_z \Phi_0(t, \mathbf{x}_\parallel, 0), \tag{B.3}$$

where $q(t, \mathbf{x}_\parallel)$ is the boundary displacement as a function of time and position on the surface. Given the (time-dependent) value of the field Φ_1 on the boundary as given by Eq. (B.3), one can compute the latter field everywhere in the space by using Green's theorem,

$$\Phi(x) = \int_\Sigma \mathrm{d}\Sigma_\mu \Phi(x')\, \partial^\mu G_\mathrm{D}(x, x') \tag{B.4}$$

where x and x' are spacetime coordinates, and G_D is a Green's function satisfying Dirichlet boundary conditions on the plate. The integral in the last equation is over a closed surface including x in its interior. The Green's function, G_D, is, in Fourier space, given by

$$G_\mathrm{D}(\omega, \mathbf{k}_\parallel, z, z') = \frac{i}{2k_\perp} e^{ik_\perp z_>}(e^{-ik_\perp z_<} - e^{ik_\perp z_<}). \tag{B.5}$$

Using Eqs. (B.4) and (B.5), one obtains Φ_1, which in turn gives the scattering matrix as

$$S_{\omega+\Omega \mathbf{k}_\parallel+\mathbf{q},\, \omega \mathbf{k}_\parallel} = -2i\, \tilde{q}(\Omega, \mathbf{q}) \sqrt{k_\perp(\omega, \mathbf{k}_\parallel)\, k_\perp(\omega+\Omega, \mathbf{k}_\parallel + \mathbf{q})}\,. \tag{B.6}$$

B.2 Sphere

In spherical coordinates, the normalized incoming and outgoing waves are defined as

$$\Phi^{\mathrm{in/out}}_{\omega lm} = \sqrt{\frac{|\omega|}{c}} e^{-i\omega t}\, h_l^{(1,2)}\left(\frac{\omega r}{c}\right) Y_{lm}(\theta, \phi). \tag{B.7}$$

The Dirichlet boundary condition for a spherical object in motion is

$$\Phi(t, R\hat{r} + \vec{q}) = 0. \tag{B.8}$$

In this equation, R is the radius of the sphere, $\hat{r}$ is the unit vector along the radius, and $\vec{q}$ is the displacement as a function of time and position on the sphere's surface. For simplicity, we assume that the sphere undergoes a linear (but time-dependent) motion. Equation (B.8) can be expanded in powers of q. To the first order, we have

$$\Phi_1(t, R\hat{r}) = -q(t)\cos\theta\partial_r\Phi_0(t, r\hat{r})|_{r=R}, \tag{B.9}$$

where the zeroth-order solution is

$$\Phi_0(\omega, \mathbf{x}) = \Phi^{\text{in}}_{\omega lm} + S_l(\omega)\Phi^{\text{out}}_{\omega lm}, \tag{B.10}$$

with $S_l(\omega) = -\frac{h_l^{(2)}(\omega R/c)}{h_l^{(1)}(\omega R/c)}$ being the scattering matrix of a static sphere. The Green's function satisfying the Dirichlet boundary conditions on the sphere can be written as

$$\begin{aligned} &G_{\text{D}}(\omega, \mathbf{x}, \mathbf{x}') \\ &\quad = \frac{i\omega}{2c}\sum_{lm}\left(h_l^{(2)}(\omega r_</c) + S_l(\omega)h_l^{(1)}(\omega r_</c)\right)h_l^{(1)}(\omega r_>/c)Y_{lm}(\theta,\phi)Y^*_{lm}(\theta',\phi')\,. \end{aligned} \tag{B.11}$$

Green's theorem can then be applied to compute Φ_1, or equivalently the scattering matrix as

$$S_{\omega+\Omega l'm,\omega lm} = \frac{2i\tilde{q}(\Omega)}{c}\,d_{ll'm}\sqrt{(\omega+\Omega)\,\omega}\,F_l\left(\frac{\omega R}{c}\right)F_{l'}\left(\frac{(\omega+\Omega)R}{c}\right), \tag{B.12}$$

with F defined as

$$F_l(x) = \frac{1}{x\,h_l^{(1)}(x)}\,. \tag{B.13}$$

The constants $d_{l'lm}$ are nonzero only for $l' = l \pm 1$,

$$\begin{aligned} d_{l+1\,lm} &= \sqrt{\frac{(l+m+1)(l-m+1)}{(2l+1)(2l+3)}}\,, \\ d_{l-1\,lm} &= d_{l\,l-1\,m}\,. \end{aligned} \tag{B.14}$$

B.3 Disk (cylinder in 2d)

In polar coordinates, the normalized incoming and outgoing waves are defined as (up to an irrelevant constant)

$$\Phi_0^{\text{in/out}}(\omega, \mathbf{x}) = e^{-i\omega t} H^{(1,2)}(\omega r/c) e^{im\phi}. \tag{B.15}$$

The boundary condition for a circular disk in motion is described similarly to Eq. (B.8) with $\vec{r}$ being a two-dimensional radial vector. Again we make the assumption that the object undergoes a linear (but time-dependent) motion along the x-axis. Equation (B.8) can be expanded as

$$\Phi_1(t, R\hat{r}) = -q(t) \cos\phi \partial_r \Phi_0(t, r\hat{r})|_{r=R}, \tag{B.16}$$

with ϕ being the angle from the x axis. The zeroth order solution, Φ_0, is given by

$$\Phi_0(\omega, \mathbf{x}) = \Phi_{\omega m}^{\text{in}} + S_m(\omega) \Phi_{\omega m}^{\text{out}}, \tag{B.17}$$

where $S_m(\omega) = -\frac{H_m^{(2)}(\omega R/c)}{H_m^{(1)}(\omega R/c)}$ is the scattering matrix of a static disk. The Green's function subject to Dirichlet boundary conditions on the disk is

$$G_{\text{D}}(\omega, \mathbf{x}, \mathbf{x}') = \frac{i}{4} \sum_m \left(H_m^{(2)}(\omega r_</c) + S_m(\omega) H_m^{(1)}(\omega r_</c) \right) H_m^{(1)}(\omega r_>/c)\, e^{im(\phi - \phi')}. \tag{B.18}$$

With the knowledge of the field on the boundary, Eq. (B.16), one can apply Green's theorem to obtain the field elsewhere in space. One then finds the scattering matrix

$$S_{\omega+\Omega m \pm 1, \omega m} = \frac{2i\, \tilde{q}(\Omega)}{\pi R} M_m\left(\frac{\omega R}{c}\right) M_{m\pm1}\left(\frac{(\omega+\Omega)R}{c}\right), \tag{B.19}$$

where M is defined as

$$M_m(x) = \frac{1}{H_m^{(1)}(x)}. \tag{B.20}$$

Appendix C

Green's functions

In this appendix we compute a number of Green's functions where the two spatial arguments lie within or outside each plate. We take the first plate to be at rest while the second one is moving at a velocity $\mathbf{v}$ parallel to its surface. We further assume that $|\mathbf{v}| \ll c$ for simplicity.

• *Green's function with both points lying within the gap (outside both objects)*: In this case, the Green's function is given by (with $z_{\mathbf{x}} > z_{\mathbf{z}}$)

$$G_{\text{out-out}}(\omega, \mathbf{x}, \mathbf{z}) = \sum_{\alpha} \frac{1}{2ip_\alpha} \frac{e^{ip_\alpha d}}{1 - e^{2ip_\alpha d} R_\alpha \tilde{R}_\alpha} (\Phi_{\bar{\alpha}}^{\text{reg}}(\omega, \tilde{\mathbf{x}}) + \tilde{R}_{\bar{\alpha}} \Phi_{\bar{\alpha}}^{\text{out}}(\omega, \tilde{\mathbf{x}})) \times$$
$$(\Phi_\alpha^{\text{reg}}(\omega, \mathbf{z}) + R_\alpha \Phi_\alpha^{\text{out}}(\omega, \mathbf{z})), \tag{C.1}$$

where we used a compact notation defined as

$$\begin{aligned}
&\alpha = \mathbf{k}_\parallel\,, \quad \bar{\alpha} = -\mathbf{k}_\parallel\,, \quad p_\alpha = k_\perp = \sqrt{\omega^2 - \mathbf{k}_\parallel^2}\,, \\
&\Phi_\alpha^{\text{reg}} = e^{i\mathbf{k}_\parallel \cdot \mathbf{x}_\parallel + ik_\perp z}\,, \qquad \Phi_\alpha^{\text{out}} = e^{i\mathbf{k}_\parallel \cdot \mathbf{x}_\parallel - ik_\perp z}\,, \\
&R_\alpha \equiv R_1(\omega, \mathbf{k}_\parallel) = R_{\omega \mathbf{k}_\parallel}\,, \qquad \tilde{R}_\alpha \equiv R_2(\omega, \mathbf{k}_\parallel) = R_{\omega' \mathbf{k}'_\parallel}\,, \\
&z_{\tilde{\mathbf{x}}} = d - z_{\mathbf{x}}, \qquad \tilde{\mathbf{x}}_\parallel = \mathbf{x}_\parallel, \qquad \sum_\alpha = L^{D-1} \int \text{đ}\mathbf{k}_\parallel \equiv L^{D-1} \int \frac{d^{D-1}\mathbf{k}_\parallel}{(2\pi)^{D-1}}\,,
\end{aligned} \tag{C.2}$$

where ω' and $\mathbf{k}'_\parallel$ are the Lorentz transformation of ω and $\mathbf{k}_\parallel$, respectively. Also D is the number of (spatial) dimensions. According to these definitions, $\Phi_\alpha(\mathbf{z})$ is

defined with respect to an origin on the surface of the first plate, while $\Phi_\alpha(\tilde{\mathbf{x}})$ is the wavefunction defined with the origin on the surface of the second plate and the direction of the z-axis reversed. It is straightforward to check that the expression in Eq. (C.1) is indeed the Green's function. First note that, for $\mathbf{x} \neq \mathbf{z}$, it solves the homogenous version of Eq. (4.38). Furthermore, the coefficients are chosen to produce a delta function when $\mathbf{z} \to \mathbf{x}$ upon applying the Helmholtz operator.

• *Green's function with one point in the gap and the other inside the first plate*: This Green's function can be obtained from continuity conditions, i.e. by matching the Green's functions approaching a point on the boundary from inside and outside the object

$$G_{\text{out-out}}(\omega, \mathbf{x}, \mathbf{y})|_{\mathbf{y}\to\Sigma^+} = G_{\text{out-in}}(\omega, \mathbf{x}, \mathbf{y})|_{\mathbf{y}\to\Sigma^-}. \tag{C.3}$$

This leads to

$$G_{\text{out-in}}(\omega, \mathbf{x}, \mathbf{z}) = \sum_\alpha 1/(2ip_\alpha) \frac{e^{ip_\alpha d}}{1 - e^{2ip_\alpha d} R_\alpha \tilde{R}_\alpha} (\Phi^{\text{reg}}_{\tilde{\alpha}}(\omega, \tilde{\mathbf{x}}) + \tilde{R}_{\tilde{\alpha}} \Phi^{\text{out}}_{\tilde{\alpha}}(\omega, \tilde{\mathbf{x}})) \times (V_\alpha \psi^+_\alpha(\omega, \mathbf{z}) + W_\alpha \psi^-_\alpha(\omega, \mathbf{z})), \tag{C.4}$$

with

$$\psi^\pm_\alpha = e^{i\mathbf{k}_\parallel \cdot \mathbf{x}_\parallel \pm i\tilde{k}_\perp z}, \tag{C.5}$$

where $\tilde{k}_\perp \equiv \tilde{p}_\alpha = \sqrt{\epsilon\omega^2/c^2 - \mathbf{k}^2_\parallel}$. The (diagonal) matrices V and W are determined by imposing continuity equations, as

$$V_\alpha + W_\alpha = 1 + R_\alpha, \tag{C.6}$$

$$\tilde{p}_\alpha (V_\alpha - W_\alpha) = p_\alpha (1 - R_\alpha). \tag{C.7}$$

• *Green's function with both points inside the first plate*: This Green's function is

given by ($z_{\mathbf{x}} > z_{\mathbf{z}}$)

$$G_{\text{in-in}}(\omega, \mathbf{x}, \mathbf{z}) = \sum_{\alpha} 1/(2ip_{\alpha}) \frac{e^{ip_{\alpha}d}}{1 - e^{2ip_{\alpha}d} R_{\alpha} \tilde{R}_{\alpha}} \times (V_{\alpha}\psi_{\alpha}^{+}(\omega, \mathbf{x}) + W_{\alpha}\psi_{\alpha}^{-}(\omega, \mathbf{x})) \times$$
$$(\tilde{V}_{\bar{\alpha}}\psi_{\bar{\alpha}}^{+}(\omega, \mathbf{z}) + \tilde{W}_{\bar{\alpha}}\psi_{\bar{\alpha}}^{-}(\omega, \mathbf{z}))\,, \tag{C.8}$$

where, via continuity relations, we have

$$\tilde{V}_{\alpha} + \tilde{W}_{\alpha} = e^{ip_{\alpha}d}(1 + \tilde{R}_{\alpha})\,, \tag{C.9}$$

$$\tilde{p}_{\alpha}(\tilde{V}_{\alpha} - \tilde{W}_{\alpha}) = p_{\alpha}e^{ip_{\alpha}d}(1 - \tilde{R}_{\alpha}). \tag{C.10}$$

Bibliography

[1] H. B. G. Casimir, "On the attraction between two perfectly conducting plates," *Proc. K. Ned. Akad. Wet.*, vol. 51, pp. 793–795, 1948.

[2] E. M. Lifshitz, "The theory of molecular attractive forces between solids," *Sov. Phys. JETP*, vol. 2, p. 73, 1956.

[3] S. K. Lamoreaux, "Demonstration of the Casimir Force in the 0.6 to 6 μm Range," *Phys. Rev. Lett.*, vol. 78, pp. 5–8, 1997.

[4] U. Mohideen and A. Roy, "Precision measurement of the Casimir force from 0.1 to 0.9 μm," *Phys. Rev. Lett.*, vol. 81, pp. 4549–4552, 1998.

[5] H. Gies and K. Klingmüller, "Worldline algorithms for Casimir configurations," *Phys. Rev. D*, vol. 74, no. 4, p. 045002, 2006.

[6] A. Rodriguez, M. Ibanescu, D. Iannuzzi, J. D. Joannopoulos, and S. G. Johnson, "Virtual photons in imaginary time: Computing exact casimir forces via standard numerical-electromagnetism techniques," *Phys. Rev. A*, vol. 76, p. 032106, 2007.

[7] K. A. Milton, *The Casimir effect: Physical manifestations of zero-point energy.* Singapore: World Scientific, 2001.

[8] T. Emig, N. Graham, R. L. Jaffe, and M. Kardar, "Casimir forces between arbitrary compact objects," *Phys. Rev. Lett.*, vol. 99, p. 170403, 2007.

[9] O. Kenneth and I. Klich, "Casimir forces in a T-operator approach," *Phys. Rev. B*, vol. 78, no. 1, p. 014103, 2008.

[10] P. A. Maia Neto, A. Lambrecht, and S. Reynaud, "Casimir energy between a plane and a sphere in electromagnetic vacuum," *Phys. Rev. A*, vol. 78, no. 1, p. 012115, 2008.

[11] T. Emig, N. Graham, R. L. Jaffe, and M. Kardar, "Casimir forces between compact objects: The scalar case," *Phys. Rev. D*, vol. 77, p. 025005, 2008.

[12] S. J. Rahi, T. Emig, N. Graham, R. L. Jaffe, and M. Kardar, "Scattering theory approach to electrodynamic Casimir forces," *Phys. Rev. D*, vol. 80, no. 8, p. 085021, 2009.

[13] A. Canaguier-Durand, P. A. M. Neto, A. Lambrecht, and S. Reynaud, "Thermal Casimir effect in the plane-sphere geometry," *Phys. Rev. Lett.*, vol. 104, no. 4, pp. 040403–+, 2010.

[14] M. F. Maghrebi, S. J. Rahi, T. Emig, N. Graham, R. L. Jaffe, and M. Kardar, "Analytical results on Casimir forces for conductors with edges and tips," *Proc. Nat. Acad. Sci.*, vol. 108, pp. 6867–6871, 2011.

[15] M. F. Maghrebi, "Diagrammatic expansion of the casimir energy in multiple reflections: Theory and applications," *Phys. Rev. D*, vol. 83, no. 4, p. 045004, 2011.

[16] M. F. Maghrebi and N. Graham, "Electromagnetic Casimir energies of semi-infinite planes," *EPL (Europhysics Letters)*, vol. 95, p. 14001, 2011.

[17] M. F. Maghrebi, R. L. Jaffe, and R. Abravanel, "Implications of the Babinet principle for Casimir interactions," *Phys. Rev. D*, vol. 84, no. 6, p. 061701, 2011.

[18] G. T. Moore, "Quantum theory of the electromagnetic field in a variable-length one-dimensional cavity," *J. Math. Phys.*, vol. 11, pp. 2679–2691, 1970.

[19] S. A. Fulling and P. C. W. Davies, "Radiation from a moving mirror in two dimensional space-time - Conformal anomaly," *P. Roy. Soc. Lond. A Mat.*, vol. 348, pp. 393–414, 1976.

[20] M.-T. Jaekel and S. Reynaud, "Causality, stability and passivity for a mirror in vacuum," *Phys. Lett. A*, vol. 167, pp. 227–232, 1992.

[21] G. Calucci, "Casimir effect for moving bodies," *J. Phys. A-Math. Gen.*, vol. 25, no. 13, p. 3873, 1992.

[22] P. A. Maia Neto and S. Reynaud, "Dissipative force on a sphere moving in vacuum," *Phys. Rev. A*, vol. 47, pp. 1639–1646, 1993.

[23] C. K. Law, "Effective hamiltonian for the radiation in a cavity with a moving mirror and a time-varying dielectric medium," *Phys. Rev. A*, vol. 49, pp. 433–437, 1994.

[24] V. V. Dodonov, "Photon creation and excitation of a detector in a cavity with a resonantly vibrating wall," *Phys. Lett. A*, vol. 207, pp. 126–132, 1995.

[25] G. Barton and A. Calogeracos, "On the quantum electrodynamics of a dispersive mirror. I: Mass shifts, radiation, and radiative reaction," *Ann. Phys.-New York*, vol. 238, pp. 227–267, 1995.

[26] O. Méplan and C. Gignoux, "Exponential growth of the energy of a wave in a 1d vibrating cavity: application to the quantum vacuum," *Phys. Rev. Lett.*, vol. 76, pp. 408–410, 1996.

[27] M. Kardar and R. Golestanian, "The "friction" of vacuum, and other fluctuation-induced forces," *Rev. Mod. Phys.*, vol. 71, pp. 1233–1245, 1999.

[28] C. Braggio, G. Bressi, G. Carugno, C. D. Noce, G. Galeazzi, A. Lombardi, A. Palmieri, G. Ruoso, and D. Zanello, "A novel experimental approach for the detection of the dynamical casimir effect," *Europhys. Lett.*, vol. 70, no. 6, p. 754, 2005.

[29] A. Agnesi, C. Braggio, G. Carugno, F. D. Valle, G. Galeazzi, G. Messineo, F. Pirzio, G. Reali, and G. Ruoso, "A laser system for the parametric amplification of electromagnetic fields in a microwave cavity," *Rev. Sci. Instrum.*, vol. 82, p. 115107, 2011.

[30] P. Lähteenmäki, G. S. Paraoanu, J. Hassel, and P. J. Hakonen, "Dynamical Casimir effect in a Josephson metamaterial," 2011.

[31] C. M. Wilson, G. Johansson, A. Pourkabirian, M. Simoen, J. R. Johansson, T. Duty, F. Nori, and P. Delsing, "Observation of the dynamical Casimir effect in a superconducting circuit," *nature*, vol. 479, pp. 376–379, 2011.

[32] P. D. Nation, J. R. Johansson, M. P. Blencowe, and F. Nori, "Colloquium: Stimulating uncertainty: Amplifying the quantum vacuum with superconducting circuits," *Rev. Mod. Phys.*, vol. 84, pp. 1–24, 2012.

[33] V. V. Dodonov, "Current status of the dynamical casimir effect," *Phys. Scripta*, vol. 82, no. 3, p. 038105, 2010.

[34] D. A. R. Dalvit, P. A. Maia Neto, and F. D. Mazzitelli, "Fluctuations, dissipation and the dynamical Casimir effect," in *Lecture notes in physics*, vol. 834, p. 419, 2011.

[35] L. H. Ford and A. Vilenkin, "Quantum radiation by moving mirrors," *Phys. Rev. D*, vol. 25, pp. 2569–2575, 1982.

[36] V. B. Braginsky and F. Y. Khalili, "Friction and fluctuations produced by the quantum ground state," *Physics Letters A*, vol. 161, pp. 197–201, 1991.

[37] M.-T. Jackel and S. Reynaud, "Fluctuations and dissipation for a mirror in vacuum," *Quantum Optics*, vol. 4, pp. 39–53, 1992.

[38] M.-T. Jaekel and S. Reynaud, "Quantum fluctuations of position of a mirror in vacuum," *Journal de Physique I*, vol. 3, pp. 1–20, 1993.

[39] M. T. Jaekel and S. Reynaud, "Quantum limits in interferometric measurements," *EPL (Europhysics Letters)*, vol. 13, p. 301, 1990.

[40] G. Barton, "New aspects of the Casimir effect: Fluctuations and radiative reaction," in *Cavity quantum electrodyamics, Supplement: Advances in atomic, molecular and optical physics*, Academic Press, New York, 1993.

[41] R. Golestanian and M. Kardar, "Mechanical response of vacuum," *Phys. Rev. Lett.*, vol. 78, pp. 3421–3425, 1997.

[42] P. A. M. Neto and L. A. S. Machado, "Quantum radiation generated by a moving mirror in free space," *Phys. Rev. A*, vol. 54, pp. 3420–3427, 1996.

[43] A. Lambrecht, M.-T. Jaekel, and S. Reynaud, "Atomic wave diffraction and interference using temporal slits," *Phys. Rev. Lett.*, vol. 77, pp. 615–618, 1996.

[44] P. A. M. Neto and L. A. S. Machado, "Quantum radiation generated by a moving mirror in free space," *Phys. Rev. A*, vol. 54, pp. 3420–3427, 1996.

[45] M. Montazeri and M. Miri, "Radiation from a dynamically deforming mirror immersed in the electromagnetic vacuum," *Phys. Rev. A*, vol. 77, p. 053815, 2008.

[46] D. F. Mundarain and P. A. Maia Neto, "Quantum radiation in a plane cavity with moving mirrors," *Phys. Rev. A*, vol. 57, pp. 1379–1390, 1998.

[47] V. V. Dodonov and A. B. Klimov, "Generation and detection of photons in a cavity with a resonantly oscillating boundary," *Phys. Rev. A*, vol. 53, pp. 2664–2682, 1996.

[48] M. Crocce, D. A. R. Dalvit, and F. D. Mazzitelli, "Resonant photon creation in a three-dimensional oscillating cavity," *Phys. Rev. A*, vol. 64, p. 013808, 2001.

[49] G. Barton and C. Eberlein, "On 1uantum radiation from a moving body with finite refractive index," *Ann. Physics*, vol. 227, no. 2, pp. 222 – 274, 1993.

[50] J. Schwinger, "Brownian motion of a quantum oscillator," *Journal of Mathematical Physics*, vol. 2, pp. 407–432, 1961.

[51] L. Keldysh, "Diagram technique for nonequilibrium processes," *Zh.Eksp.Teor.Fiz.*, vol. 47, pp. 1515–1527, 1964.

[52] J. B. Pendry, "Shearing the vacuum - quantum friction," *J. Phys.-Condens. Mat.*, vol. 9, no. 47, p. 10301, 1997.

[53] A. I. Volokitin and B. N. J. Persson, "Theory of friction: The contribution from a fluctuating electromagnetic field," *J. Phys.-Condens. Mat.*, vol. 11, no. 2, p. 345, 1999.

[54] A. I. Volokitin and B. N. J. Persson, "Near-field radiative heat transfer and noncontact friction," *Rev. Mod. Phys.*, vol. 79, p. 1291, 2007.

[55] S. M. Rytov, Y. A. Kravtsov, and V. I. Tatarskii, *Priniciples of statistical radiophysics. 3. Elements of random fields.*, vol. 3. Berlin: Springer, 1989.

[56] A. Manjavacas and F. J. García de Abajo, "Vacuum friction in rotating particles," *Phys. Rev. Lett.*, vol. 105, p. 113601, 2010.

[57] A. Manjavacas and F. J. García de Abajo, "Thermal and vacuum friction acting on rotating particles," *Phys. Rev. A*, vol. 82, p. 063827, 2010.

[58] Y. B. Zel'dovich, "Generation of waves by a rotating body," *JETP Lett.*, vol. 14, p. 180, 1971.

[59] Y. B. Zel'Dovich, L. V. Rozhanskii, and A. A. Starobinskii, "Rotating bodies and electrodynamics in a rotating coordinate system," *Radiophys. and Quantum Electronics*, vol. 29, p. 761, 1986.

[60] R. Penrose, "Gravitational collapse: The role of general relativity," *Nuovo Cimento Rivista Serie*, vol. 1, p. 252, 1969.

[61] W. G. Unruh, "Second quantization in the kerr metric," *Phys. Rev. D*, vol. 10, pp. 3194–3205, 1974.

[62] S. W. Hawking, "Particle creation by black holes," *Commun. Math. Phys.*, vol. 43, pp. 199–220, 1975.

[63] A. Calogeracos and G. E. Volovik, "Rotational quantum friction in superfluids: Radiation from object rotating in superfluid vacuum," *JETP Lett.*, vol. 69, pp. 281–287, 1999.

[64] D. C. Roberts and Y. Pomeau, "Casimir-like force arising from quantum fluctuations in a slowly moving dilute Bose-Einstein condensate," *Phys. Rev. Lett.*, vol. 95, no. 14, p. 145303, 2005.

[65] M. F. Maghrebi, R. L. Jaffe, and M. Kardar, "Spontaneous emission by rotating objects: A scattering approach," *Phys. Rev. Lett.*, vol. 108, p. 230403, 2012.

[66] C. W. J. Beenakker, "Thermal radiation and amplified spontaneous emission from a random medium," *Phys. Rev. Lett.*, vol. 81, pp. 1829–1832, 1998.

[67] M. Krüger, T. Emig, and M. Kardar, "Nonequilibrium electromagnetic fluctuations: Heat transfer and interactions," *Phys. Rev. Lett.*, vol. 106, p. 210404, 2011.

[68] L. Boltzmann, "Ableitung des stefan'schen gesetzes, betreffend die abhngigkeit der wrmestrahlung von der temperatur aus der electromagnetischen lichttheorie," *Annalen der Physik*, vol. 258, no. 6, pp. 291–294, 1884.

[69] J. D. Bekenstein and M. Schiffer, "The many faces of superradiance," *Phys. Rev. D*, vol. 58, p. 064014, 1998.

[70] R. J. Glauber, "Time-dependent statistics of the Ising model," *Journal of Mathematical Physics*, vol. 4, pp. 294–307, 1963.

[71] P. L. Kelley and W. H. Kleiner, "Theory of electromagnetic field measurement and photoelectron counting," *Phys. Rev.*, vol. 136, pp. 316–334, 1964.

[72] J. D. Bekenstein and M. Schiffer, "Universality in grey-body radiance: Extending kirchoff's law to the statistics of quanta," *Phys. Rev. Lett.*, vol. 72, pp. 2512–2515, 1994.

[73] C. Beenakker, "Photon statistics of a random laser," *arXiv preprint quant-ph/9808066*, 1998.

[74] L. D. Landau and E. M. Lifshitz, *Statistical physics part 1*, vol. 5. Oxford: Pergamon Press, 1980.

[75] H. B. G. Casimir and D. Polder, "The influence of retardation on the london-van der waals forces," *Phys. Rev.*, vol. 73, p. 360, 1948.

[76] R. Matloob, R. Loudon, S. M. Barnett, and J. Jeffers, "Electromagnetic field quantization in absorbing dielectrics," *Phys. Rev. A*, vol. 52, pp. 4823–4838, 1995.

[77] T. Gruner and D.-G. Welsch, "Quantum-optical input-output relations for dispersive and lossy multilayer dielectric plates," *Phys. Rev. A*, vol. 54, pp. 1661–1677, 1996.

[78] M. Artoni and R. Loudon, "Quantum theory of optical pulse propagation through an absorbing and dispersive slab," *Phys. Rev. A*, vol. 55, pp. 1347–1357, 1997.

[79] J. D. Jackson, *Classical Electrodynamics*. New York: Wiley, 3 ed., 1998.

[80] J. van Bladel, "Electromagnetic fields in the presence of rotating bodies," *P. IEEE*, vol. 64, pp. 301–318, 1976.

[81] P. Král and H. R. Sadeghpour, "Laser spinning of nanotubes: A path to fast-rotating microdevices," *Phys. Rev. B*, vol. 65, p. 161401, 2002.

[82] M. T. H. Reid, A. W. Rodriguez, J. White, and S. G. Johnson, "Efficient computation of Casimir interactions between arbitrary 3D objects," *Phys. Rev. Lett.*, vol. 103, p. 040401, 2009.

[83] A. P. McCauley, A. W. Rodriguez, J. D. Joannopoulos, and S. G. Johnson, "Casimir forces in the time domain: Applications," *Phys. Rev. A*, vol. 81, p. 012119, 2010.

[84] M. O. Scully and M. S. Zubairy, *Quantum optics*. Cambridge University Press, 1997.

[85] V. Dodonov and A. Dodonov, "Quantum harmonic oscillator and nonstationary casimir effect," *J. Russ. Laser Res.*, vol. 26, pp. 445–483, 2005.

[86] C. D. Fosco, F. C. Lombardo, and F. D. Mazzitelli, "Quantum dissipative effects in moving mirrors: A functional approach," *Phys. Rev. D*, vol. 76, p. 085007, 2007.

[87] J. Sarabadani and M. Miri, "Mechanical response of the quantum vacuum to dynamic deformations of a cavity," *Phys. Rev. A*, vol. 74, p. 023801, 2006.

[88] G. Barton, "On van der waals friction. II: Between atom and half-space," *New J. Phys.*, vol. 12, no. 11, p. 113045, 2010.

[89] R. Zhao, A. Manjavacas, F. J. García de Abajo, and J. B. Pendry, "Rotational quantum friction," *Phys. Rev. Lett.*, vol. 109, p. 123604, 2012.

[90] I. M. Frank and V. L. Ginzburg, "Radiation of a uniform moving electron due to its transition from one medium into another," *J. Phys. (USSR)*, vol. 9, p. 353, 1945.

[91] V. L. Ginzburg, "Radiation by uniformly moving sources: Vavilovcherenkov effect," vol. 32 of *Progress in Optics*, pp. 267 – 312, Elsevier, 1993.

[92] V. L. Ginzburg, "Radiation by uniformly moving sources (vavilovcherenkov effect, transition radiation, and other phenomena)," *Physics-Uspekhi*, vol. 39, no. 10, p. 973, 1996.

[93] M. F. Maghrebi, R. Golestanian, and M. Kardar, "Scattering approach to the dynamical casimir effect," *Phys. Rev. D*, vol. 87, p. 025016, 2013.

[94] L. Landau, "The theory of superfluidity of Helium II," *Zh. Eksp. Teor. Fiz.*, vol. 11, p. 592, 1941.

[95] S. M. Carroll, *Spacetime and geometry. An introduction to general relativity.* Addison Wesley, 2004.

[96] N. D. Birrell and P. C. W. Davies, *Quantum fields in curved space.* No. 7, Cambridge University Press, 1984.

[97] E. P. Gross, "Hydrodynamics of a superfluid condensate," *Journal of Mathematical Physics*, vol. 4, pp. 195–207, 1963.

[98] W. G. Unruh, "Notes on black-hole evaporation," *Phys. Rev. D*, vol. 14, pp. 870–892, 1976.